Physics – Uspekhi **57** (6) 556 – 592 (2014)

REVIEWS OF TOPICAL PROBLEMS

PACS numbers: 42.65.Hw, **42.68. – w**, 42.68.Ay

Adaptive optics in the formation of optical beams and images

V P Lukin

DOI: 10.3367/UFNe.0184.201406b.0599

Contents

Abstract. In connection with the wide use of optoelectronic systems, we review the development of adaptive optics as an effective tool that allows using controllable optical elements to eliminate irregular distortions that occur as light propagates in an inhomogeneous medium. The subject matter of this rapidly developing field of science and technology is described. Of the ideas under development in recent years, many have been around for quite a long time, but it is only now, with the development of an up-to-date optoelectronic element base, that they have started being widely incorporated into science and engineering practice. We discuss the development of adaptive optics from mere ideas to their application in astronomy, high-power laser physics, and medicine. The current state of adaptive optics in stellar and solar astronomy is reviewed, and some results of its use in distortion correction systems of high-power laser systems and facilities are presented.

V P Lukin Zuev Institute of Atmospheric Optics, Siberian Branch, Russian Academy of Sciences,
pl. Akademika Zueva 1, 634021 Tomsk, Russian Federation
Tel. +7 (3822) 49 26 06. Fax +7 (3822) 49 20 86
E-mail: lukin@iao.ru

Received 19 April 2013, revised 17 December 2013
Uspekhi Fizicheskikh Nauk **184** (6) 599 – 640 (2014)
DOI: 10.3367/UFNr.0184.201406b.0599
Translated by M V Tsaplina; edited by A M Semikhatov

1. Introduction

Modern optoelectronic systems (OESs) fail to attain their maximum efficiency because of the technical imperfection of the constituent elements and random inhomogeneities on the paths of optical wave propagation. At the same time, because of the intense use of OESs for data transmission, targeted electromagnetic radiation energy transfer, and imaging in real conditions, it is relevant to develop correction methods and devices, including adaptive ones, which are the most radical means of combatting the decrease in efficiency. In systems operating in randomly inhomogeneous media, such as Earth's atmosphere, the dominant distorting factors are not only molecular absorption and aerosol light scattering but also large-scale random refractive index irregularities. They are first and foremost associated with atmospheric refraction and turbulent air mixing in the atmosphere and can also be due to molecular and aerosol absorption in the channel of high-power optical radiation propagation. Different methods can be used to minimize these distortions, for instance, by selecting the optimum wavelength, spatial parameters, and time regimes of radiation. But the most radical means are real-time adaptive optics (AO) systems that are currently being developed for real-time compensation of these distortions.

The term 'adaptive optics' generalizes a wide range of problems and optical devices proper that allow reducing the effect of atmospheric or other refractive index irregularities

on the efficiency of the optical system operation. The aim of the development of adaptive systems in application to atmospheric problems is to minimize distortions in the course of optical beaming and imaging. The adaptive system operation is based on control of the wavefront of received or transferred radiation. This control is realized by means of active elements, such as flexible or compound controllable mirrors and controllable phase transparencies.

Adaptive optics has now become a part of physical optics studying methods of using controllable optical elements to eliminate irregular distortions occurring upon light propagation in an inhomogeneous medium. The principal problems of AO are the heightening of the resolution limits of observation devices, optical radiation concentration on a receiver or a target, etc. Adaptive optics finds application in the design of ground-based astronomical telescopes, in optical communication systems, in industrial laser engineering, in ophthalmology, etc., where it allows compensating atmospheric distortions and optical system aberrations, in particular, optic elements of the human eye.

The relevance of the development of AO systems is confirmed by numerous international and Russian conferences, including those of the International Society for Optical Engineering (SPIE) and the AO sections in programs of various conferences related to laser physics, atmospheric optics, problems of remote sensing, and the application of lasers and optics in industry and medicine, especially in ophthalmology. Adaptive optics has passed the development phase and is now entering the stage of all-round inclusion in practice. The AO development was primarily stimulated by practical problems in the creation of optical systems whose successful operation necessitates elimination of the wavefront perturbation caused by uncontrolled random effects. The best-known systems of this type are ground-based telescopes for astronomical studies, systems of formation and focusing of laser radiation, laser high-frequency measuring systems working in the atmosphere, and optical systems of high-power laser radiation formation. The tasks of AO systems are quite diverse, but they are united by the general idea of using controllable optical elements to eliminate irregular distortions occurring in light propagation in an inhomogeneous medium.

2. First years of the development of adaptive optics

What are the AO systems and what was the starting point of their development? The first studies of AO systems are considered to have been carried out in the late 1950s. The ideas that gave start to the development of AO systems capable of real-time compensation of atmospheric wavefront distortions were almost simultaneously suggested in the USA (Babcock) [1] and in the USSR (Linnik) [2]. We emphasize that we are talking about the contemporary epoch of AO progress, because it was Archimedes, Leonardo da Vinci, and others (mentioned in monograph [3]) who paid attention to the problems of control optics wave parameters. In paper [1], Babcock proposed correcting distortions via controllable feedback optical elements. In [2], Linnik suggested the idea of the possibility, in principle, of compensating active atmospheric distortions in astronomical observations using mirror devices with a compound or continuous deformable surface.

Without a doubt, the first ideas of AO creation were expressed earlier than the first possibilities of their realization appeared. Special elements were needed to construct AO systems. They only appeared in the 1970s, and hence the first relatively significant progress in the evolution and application of AO refers to precisely that time. In this connection, the review work by Hardy [4] on the use of AO systems for correction of dynamic distortion in optical waves is noteworthy. We note that Hardy proposed designing the first adaptive optical system for atmospheric distortion correction [5] called RTAC (real-time atmospheric compensation), which was elaborated under his guidance by the Jtek firm (USA).

The RTAC system contained a telescope with a 30 cm aperture and an active corrector based on a massive piezoelectric mirror with 21 control channels. A schematic of this system is demonstrated in Fig. 1. The figure shows that it was a system of distortion correction of the received optical signal. Unfortunately, we have poor knowledge of the actual operation of such a system.

We note that the truly successful pioneering work on the use of AO systems was conducted precisely in astronomy; the first AO systems were quite expensive, and it was only within major scientific projects, which have always been and still are large astronomical telescopes, that the construction of such objects was possible. The many-year studies [6] conducted at the European Southern Observatory should be mentioned especially.

Theoretical and experimental studies on the application of optical systems in the atmosphere, based on advances in the theory of wave propagation in randomly inhomogeneous media [7–15], developed rapidly in the 1970s. A special place among the first theoretical studies is taken by Fried's work [10, 12], in which the optical systems were parameterized from the standpoint of the level of phase fluctuations in the optical wave, the so-called atmosphere coherence radius was first introduced, and the notions of short and long exposition in recording random optical signals were introduced. The studies of Greenwood [13, 14], in which the concept of Greenwood frequency was introduced that determined the minimum requirement on the speed of response of the AO system feedback loop, became important. These studies, first of all, allowed formulating the necessary requirements on AO system elements. This was done for the problems of both imaging and coherent laser beaming in the atmosphere [15–17]. A summary of the development of early studies became topical issues [18, 19] of the journal of the American Optical Society devoted to the problems of adaptive corrections of atmospheric distortions. In the preface to one of these issues [18], Fried noted that many had customarily discoursed on Earth's atmosphere turbulence, just as on the weather, but nobody had tried to strive against it. However, the situation was changing rapidly. The optical engineering had reached such a level that it was becoming possible to somehow stand against the harmful effect of turbulence on optical signal propagation. This 'somehow' was called 'adaptive optics'. It should be added that the means of AO permit not only decreasing the distorting effect of atmospheric turbulence but also compensating distortions due to other reasons, for example, thermal mirror deformations or inaccuracy in their fabrication [17, 20–23].

The results of investigations on the construction of AO systems in the USSR were discussed at the first All-Union Scientific Conference on the Application of AO Systems, held in 1986 in the Crimean astrophysical observatory [24]. We note that several topical issues on atmospheric adaptive

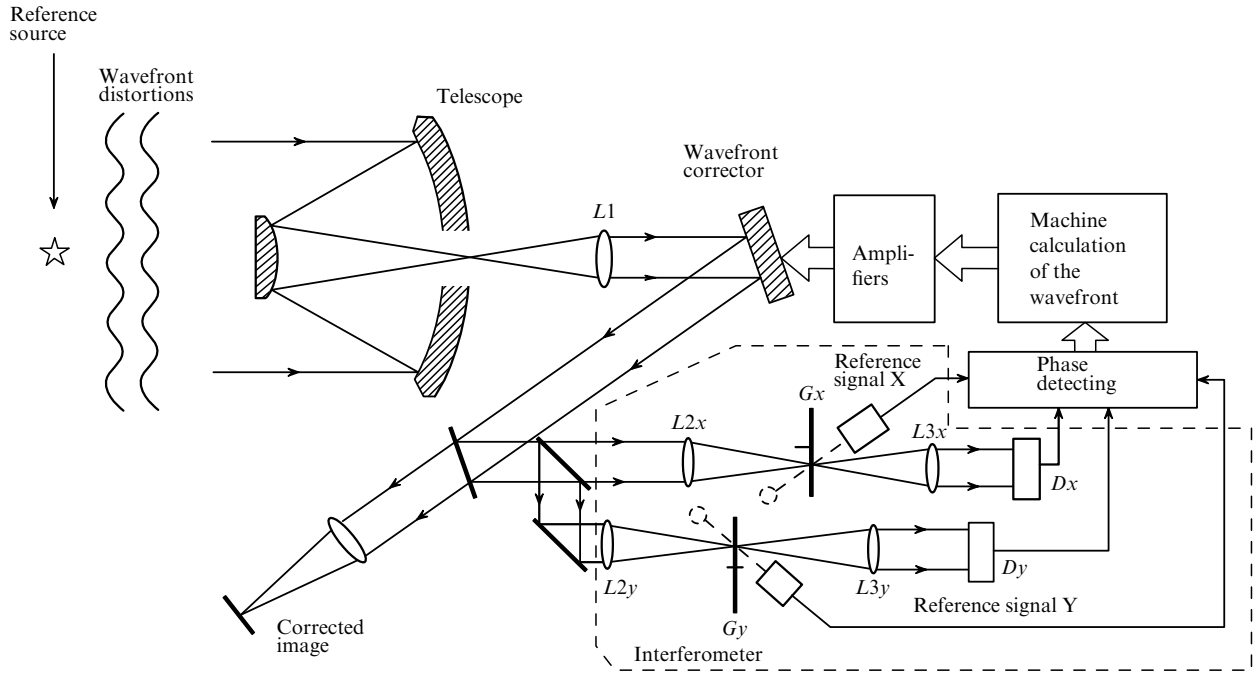

Figure 1. Schematic of the RTAC system for real-time compensation of atmospheric distortions.

optics in journals, *Izv. vuzov. Fizika* (*Sov. Phys. J.*) [25] and *Optika atmosfery i okeana* (*Atmospheric Opt.*) [26–30], appeared in the late 1980s and early 1990s. In 1993–1996, original domestic projects of adaptive telescopes were worked out rather intensely [31–34].

3. Basic principles of adaptive optics system operation

In this section, principles of AO system operation are briefly formulated. We first note that the operation of such systems is based on the principles of linearity, reciprocity, and quasi-stationarity of the optical wave propagation medium itself, the Helmholtz reciprocity principle being the main one. This essentially corresponds to the principle of information reversibility, according to which fluctuations of an elementary spherical wave that has passed through a random medium in forward and backward directions are absolutely identical [7–9, 16, 17, 35]. This principle is fulfilled for both a free space and an inhomogeneous turbulent and refractive medium, which allows fully eliminating the effect of the medium.

3.1 General properties of direct and conjugate waves in a randomly inhomogeneous medium

In what follows, we proceed from the assumption that an optical wave propagates in a randomly inhomogeneous medium with a permittivity $1+\varepsilon(\mathbf{r})$. In this case, the optical wave propagation can be described by the scalar Helmholtz equation [7, 8, 35]

$$\Delta U(\mathbf{r}) + k^2\left[1+\varepsilon(\mathbf{r})\right] U(\mathbf{r}) = 0\,. \tag{1}$$

For radiation with a wavelength λ ($k=2\pi/\lambda$) much smaller than the characteristic scales of inhomogeneities l_ε of the randomly inhomogeneous medium, the solution of (1) can be sought [35] in the form $v(\mathbf{r}) = U(x,\boldsymbol{\rho})\exp(\mathrm{i}k|x-x_0|)$. The wave is assumed to propagate along the x axis of a Cartesian coordinate system and the boundary conditions are specified in the original plane x_0. Under the conditions $\lambda \ll l_\varepsilon$ and $\lambda|x-x_0|/l_\varepsilon^2 \ll l_\varepsilon^2/\lambda^2$, the complex field amplitude $U(x,\boldsymbol{\rho})$ in (1) satisfies two equations describing the leftward and rightward propagation from the radiation source:

$$2\mathrm{i}k\,\frac{\mathrm{d}U}{\mathrm{d}x} + \Delta_\rho U + k^2\varepsilon(x,\boldsymbol{\rho})\,U(x,\boldsymbol{\rho}) = 0\,, \quad x > x_0\,, \tag{2}$$

$$-2\mathrm{i}k\,\frac{\mathrm{d}U}{\mathrm{d}x} + \Delta_\rho U + k^2\varepsilon(x,\boldsymbol{\rho})\,U(x,\boldsymbol{\rho}) = 0\,, \quad x < x_0\,, \tag{3}$$

with the boundary condition $U(x_0,\boldsymbol{\rho}) = U_0(\boldsymbol{\rho})$. For Eqn (1), we can introduce the Green's function $G(x_0,\boldsymbol{\rho}_0,x,\boldsymbol{\rho})$ of the problem, which has the meaning of the field generated at the point $(x,\boldsymbol{\rho})$ by the point source of the unit amplitude located at the point $(x_0,\boldsymbol{\rho}_0)$. By virtue of linearity, the solution of Eqns (2) and (3) can be written as

$$U(x,\boldsymbol{\rho}) = \iint \mathrm{d}^2\rho_0 U_0(\boldsymbol{\rho}_0)\,G(x_0,\boldsymbol{\rho}_0,x,\boldsymbol{\rho})\,. \tag{4}$$

Formula (4) expresses the Huygens–Fresnel principle. For a homogeneous medium (for $\varepsilon(\mathbf{r})=0$), the Green's function $G^0(x_0,\boldsymbol{\rho}_0,x,\boldsymbol{\rho})$ in the Kirchhoff approximation is given by [7, 8, 35]

$$G^0(x_0,\boldsymbol{\rho}_0,x,\boldsymbol{\rho}) = \frac{1}{2\pi\mathrm{i}|x-x_0|}\exp\left\{\mathrm{i}k|x-x_0| + \frac{\mathrm{i}k}{2|x-x_0|}\,(\boldsymbol{\rho}-\boldsymbol{\rho}_0)^2\right\}. \tag{5}$$

Analyzing the Green's function properties, we can show that for $x_0 < x < x_1$ or $x_0 > x > x_1$, we have

$$G(x_0,\boldsymbol{\rho}_0,x_1,\boldsymbol{\rho}_1) = \iint \mathrm{d}^2\rho\, G(x_0,\boldsymbol{\rho}_0,x,\boldsymbol{\rho})\,G(x,\boldsymbol{\rho},x_1,\boldsymbol{\rho}_1)\,, \tag{6}$$

that is, the so-called Green's function superposition rule holds, which allows composing the two Green's functions defined on adjacent intervals into the Green's function defined on the union of these two intervals.

Another property of Green's functions, which is very important for substantiation of AO system operation, is the reciprocity principle [35], which means that the field generated at a point $(x_1, \boldsymbol{\rho}_1)$ by the source located at a point $(x_0, \boldsymbol{\rho}_0)$ is equal to the field generated at $(x_0, \boldsymbol{\rho}_0)$ by the source located at $(x_1, \boldsymbol{\rho}_1)$:

$$G(x_0, \boldsymbol{\rho}_0, x_1, \boldsymbol{\rho}_1) = G(x_1, \boldsymbol{\rho}_1, x_0, \boldsymbol{\rho}_0)\,. \tag{7}$$

We note that the reciprocity principle is valid for any functions $\varepsilon(x, \boldsymbol{\rho})$, in particular, for discontinuous and complex ones. For media in which $\varepsilon(x, \boldsymbol{\rho}) = \varepsilon^*(x, \boldsymbol{\rho})$, i.e., in the absence of absorption and amplification, direct (G) and conjugate (G^*) waves propagate in the same medium. Using reciprocity principle (6), we can then show that

$$\iint \mathrm{d}^2\rho G^*(x_0, \boldsymbol{\rho}_0, x, \boldsymbol{\rho})\, G(x_0, \boldsymbol{\rho}_0, x, \boldsymbol{\rho}) = \delta(\boldsymbol{\rho}_0 - \boldsymbol{\rho})\,. \tag{8}$$

This expression can be considered the Green's function orthogonality property. We note that in contrast to the reciprocity principle, orthogonality only takes place for a medium with a real permittivity.

The property of the Green's function orthogonality is associated with the energy conservation law. Using the properties of the Green's function, we can write the total radiation power $P(x)$ in any plane x in the form [16, 17]

$$\begin{aligned} P(x) &= \iint \mathrm{d}^2\rho U(x, \boldsymbol{\rho})\, U^*(x, \boldsymbol{\rho}) \\ &= \iint \mathrm{d}^2\rho U(x_0, \boldsymbol{\rho})\, U^*(x_0, \boldsymbol{\rho}) = P(x_0)\,. \end{aligned} \tag{9}$$

Expression (8) admits the following physical interpretation. Multiplying its left- and right-hand sides by the original field $U^*(x_0, \boldsymbol{\rho}_0)$ and integrating, we arrive at

$$\iint \mathrm{d}^2\rho_1 U^*(x_1, \boldsymbol{\rho}_1)\, G(x_1, \boldsymbol{\rho}_1, x_0, \boldsymbol{\rho}_0) = U^*(\boldsymbol{\rho})\,. \tag{10}$$

This means that the optical wave that has covered the optical path in the forward direction and has been reflected from the element performing the wavefront reversal operation (such that complex conjugation of the reflected wave occurs), after going back over the same path, reconstructs the field conjugate to the original one, which means that the amplitude and phase field distributions coincide with the initial ones. Expression (10) is in fact a theoretical substantiation of the applicability of the algorithm (operation) of wavefront reversal (WFR) for correction of distributed wavefront distortions. It is then necessary to ensure that the optical wave pass twice — forward and backward — through the same random inhomogeneities. The authors of [36–41] showed that upon wave reflection from a finite-size WFR element, the energy fraction that in the reflected wave falls to the conjugate component remains unchanged during wave propagation in an inhomogeneous medium and is equal to the incident energy fraction within the WFR element aperture. Proceeding from these general properties of the wave equation, it was established that the wavefront reversal operation performed on the entire plane allows reconstruction, using (10), of the initial distribution of the field that has passed through a randomly inhomogeneous medium.

3.2 Methods of inverse wave formation

The authors of [39] noticed that in linear (both geometrical and wave) optics of transparent media, the time reversibility principle holds because the Maxwell equations or the corresponding wave equations remain invariant under time reversal. Therefore, for any solution of the equation, e.g., in the case of an optical field (laser beam) significantly distorted in an inhomogeneous medium, a 'reversed' solution of the same equation always exists. In particular, a reversed spherical wave that has passed through a layer of an inhomogeneous medium, after its total intercept and reverse propagation through the same medium, provides ideal wave focusing [see (8)]. This fact is essentially a substantiation of the possibility of adaptive WFR focusing of radiation beams onto a chosen point of the inhomogeneous medium.

Thus, as shown in [16, 17, 36–40], for receiving–transmitting optical systems, the most natural correction algorithm realizing the reversibility principle, and the WFR in particular, can be used. The wavefront reversal operation implies conjugation of the complete wave phase (such that the phase sign becomes opposite) and reconstruction of its amplitude distribution. For this reason, the wave reversal operation is called the wave-front conjugation in the English-language literature, and the term 'time reversal' is used. In the first years of studies, such an operation was called the 'WFR mirror' in the scientific literature [37–41]. This term stressed its peculiarities, namely, the reconstruction of the field amplitude (or power density) distribution and the phase sign reversal. In coherent optics, using the tools of nonlinear optics, positions and directions of the amplitude and phase of elementary beams can be arranged such that the reverse process of wave propagation could be further reproduced in detail. This works well, notably, because the coherent wave has (is characterized by) a relatively small number of degrees of freedom of the elements whose generalized velocities are to be reversed. The following estimate was obtained in monograph [39]: to form an optical field in a volume of approximately 1 cm^3, it is necessary to control the number of the degrees of freedom of the order of 10^4 on average. We show below (see Section 4) how such estimates of the degrees of freedom are obtained for an optical system at the modern level.

We note that the WFR phenomenon, observed in nonlinear optical processes, can be used for laser beam formation. When the WFR is used, elements such as a wavefront corrector, an analyzer of the field scattered by the object, and a control system can be absent from the system, because all these functions are jointly present in one nonlinear optical WFR device. To obtain high-efficiency real-time correction of the radiation front, the reversal should occur before the wave surface shape is distorted [36, 39–42]. The existing systems with WFR and those now being developed actually have a rather high spatial resolution, which permits compensating small-scale phase fluctuations, and a rather short reaction time, inaccessible for other types of adaptive devices.

In the 1970s–1980s, many methods of 'reversed' wave formation were proposed and actually worked out [37–41, 43]. The following methods can be singled out: WFR formation in static and dynamic holography, parametric methods of WFR formation, and methods based on the use

of stimulated light scattering: stimulated Raman scattering, stimulated Mandelstam–Brillouin scattering, and a number of other mechanisms.

The formation of a WFR wave under reversal in a static hologram requires the presence of a reference wave in recording. This method has a shortcoming: for the reversal of each new wave, a new hologram should be recorded, which is difficult because WFR should be formed in real time. This deficiency is eliminated by using special media in which permittivity perturbations occur in the presence of interfering fields and vanish upon their removal. Holography in such media is called dynamic. The wave interaction processes in these media make up a subject of nonlinear optics, and the media themselves are referred to as nonlinear. In such media, the hologram recording and reading coincide in time. Great progress in dynamic holography was achieved in WFR formation with four-wave displacement, where two reference waves were used. At the same time, an absolute requirement for obtaining a high-quality reversed wave in these methods is the requirement that both the optically homogeneous working medium and reference waves homogeneous in the interaction volume be present. And to attain high WFR efficiency, the intensity of such reference waves must be sufficiently high. These requirements are mutually contradictory, because smooth high-intensity waves in nonlinear reactive media are unstable. In conditions of developing instability, the perturbations irregularly distort the structure of reference waves, decreasing the efficiency and quality of WFR. This, in turn, imposes restrictions on the applicability of the WFR formation method itself.

The parametric methods of WFR formation are based on the fact that optical media exist in which, under the interaction of strong optical fields E_0, the permittivity changes by a quantity proportional to the local value of this field, $\delta\varepsilon \propto \chi^{(2)} E_0$. Here, $\chi^{(2)}$ is the coefficient characterizing quadratic nonlinearity of the medium. The idea is to form a strong reference wave at the doubled frequency of the signal, and if the signal wave E_s from which the reversed-front wave should be formed propagates in the same direction as the reference wave E_0, then a wave $\chi^{(2)} E_0 E_s^*$ in the opposite direction is formed. Although very attractive from the principal standpoint, the parametric methods of WFR formation have not been widespread in optics, because it is difficult to provide synchronous modulation at a doubled frequency in a large volume.

To realize the stimulated light scattering methods, it is necessary that at least two monochromatic waves of different frequencies propagate in the medium. And to realize stimulated scattering, the difference between the frequencies of these waves should be close to the frequency of some eigenmodes of the medium. Furthermore, a mechanism should exist allowing the running interference pattern of fields to build up these eigenmodes and allowing the eigenmodes to modulate the permittivity of the medium. For example, for stimulated Mandelshtam–Brillouin scattering, the eigenmodes of the medium correspond to sound waves of a very high frequency (of the order of 10^9 Hz, which is the so-called hypersound), and the build-up mechanism is due to electrostriction forces drawing matter into regions with a high local value of the field strength. In turn, density perturbations in the medium change its permittivity. The propagating waves are scattered by the appearing inhomogeneities. It is very important here that the spatial structure of the excited oscillations of the medium is strictly consistent with the interference pattern of the exciting light fields. Among other shortcomings of WFR based on stimulated light scattering is the threshold character of the latter process, necessitating a relatively high power of the reversed wave. The general deficiency of the above-mentioned methods of WFR field formation consists in stringent requirements on the optical quality of the nonlinear medium, the spatial structure of reference waves, and the monochromaticity of the fields. All this limits the accuracy of reversed wave reconstruction and makes the correction inefficient. On the other hand, the requirements on the accuracy of WFR reconstruction naturally depend on the conditions of optical wave propagation along the path. The main condition providing the reversibility of fluctuations means in fact that a random medium should be 'frozen', and propagation in the medium proceeds practically instantaneously. This is precisely what guarantees the full correspondence between forward and backward propagation. In expression (7), the forward and backward waves pass through the same inhomogeneities of the medium and hence experience the same distortions. This is only possible if the time lag in the system associated with the time of light propagation along the path, and also with the time of the 'response' of the active medium forming the reversed wavefront, can be neglected. This imposes restrictions on the pathlength, on the choice of the substance for WFR-mirror formation, and on the value of the fluctuation level on the path of wave propagation.

We note that devices based on WFS elements are limited in size both from above and from below, because it is difficult to make homogeneous large active media, while on small scales in liquids and gases (which are the substances of active media for WFR formation), effects associated with substance viscosity and thermal conductivity show up. At the same time, an increase in the radiation power leads to irretrievable destruction of the active substance that ensures the mechanism of the reversed wavefront formation. Moreover, for instance, for astronomical applications, the WFR methods can hardly be used when the received signal is a flux of separate photons, and in many cases it is necessary to ensure the formation in OES of a WFR wave for nonmonochromatic radiation, which can hardly be done. All this lowers the precision of reversed wave reproduction and restricts the applicability of such systems.

Along with the application of nonlinear optics for distortion correction in optical waves on the basis of the WFR algorithm, so-called linear adaptive optics is being extensively developed. In the scientific literature on adaptive optics, in the first years of its development [4, 18, 19, 43], the adaptive correction was customarily divided according to the type of applied methods, namely, the methods of reversed wave formation and the methods based on direct phase correction of wavefront distortions. For this purpose, fairly efficient technical means (optical elements) of optical wave phase control have been developed and are already successfully being applied. These are deformable optical elements, including mirrors, lenses, and phase transparencies. In the case of linear phase correction, the correction quality is restricted because of the loss of information on the amplitude and also of the effect of spatial boundedness of the correction area. These restrictions were studied in numerous papers, including those by Soviet (Russian) scientists [36–42], which, in particular, permitted formulating a highly efficient theory of the application of wavefront phase correction methods.

3.3 Substantiation of the 'phase conjugation' algorithm

Optical field correction methods using the reversed wavefront formation have actually been developed rather intensely; but for a number of applications, the use of this technique in optical systems is complicated. The technical realization of the WFR algorithm has turned out to be not always practically possible, and as an alternative to WFR, the phase conjugation (PC) or adaptive phase correction algorithm has been widely used in AO systems [43–45]. The linear adaptive optics borrows the fundamental reversibility principle from the wave propagation theory, but uses it somewhat differently. Reference radiation or a reference source of light is used in WFR systems to create WFR elements themselves, while linear AO systems are based on the application of reference sources for phase distortion measurements.

We consider classical WFR in which optical radiation is formed through a layer of a randomly inhomogeneous medium, for example, atmospheric turbulence. The goal set for the system itself is to transmit radiation through the layer with minimum light scattering loss. The WFR capabilities can be improved by an adaptive system involving adaptive phase correction with measurements of phase fluctuations in reference radiation taken into account. It is assumed that in addition to the main radiation, which is to be subjected to correction, so-called reference radiation exists. Depending on the purpose of the OES, the reference radiation is singled out in different ways. For example, in astronomy, the radiation from the investigated object (star) can itself be regarded as reference; if the object is weak, a neighboring object (some stronger star) is used, and if no such objects are closely located in the sky, the technique of laser reference star formation is used [17, 44, 45]. In any case, the radiation of a reference source covers practically the same path through a layer of a randomly inhomogeneous medium as the radiation to be transmitted to another object.

In AO problems, for laser radiation beams, a reference source can be formed as a special (additional) source; for this, one can also use the radiation reflected from the object onto which the radiation is focused or from some other nearby objects. Anyway, a source located at a certain distance can be regarded as a reference one. If possible, it is a source with a sufficiently smooth field distribution. It can be readily shown that the optical wave phase control is more efficient than the control over its intensity [4, 43–45], and this is why phase systems of linear adaptive correction are being developed. In the case of adaptive phase correction, only the fluctuating part of the wave phase measured in the field of the reference source that has passed through a random medium is to be controlled, while the distribution of the optical wave radiation intensity remains invariable. As a result, phase conjugation reduces to control over the phase distribution of the radiation field (upon transmission or reception of radiation) based on information about the instantaneous distribution of inhomogeneities of the medium in which radiation propagates.

In this connection, AO systems can be characterized as those with an optical feedback closed through a layer of a randomly inhomogeneous medium, and they can be described by introducing the so-called reference source. Being the main element of the system, such a reference source can be either real (a purposefully formed or a natural source) or imaginary, for example, formed by radiation reflection. The main correction algorithm for most AO systems amounts to phase conjugation first of all because the amplitude (or radiation intensity) control in optics is obstructed, and correction based on the PC algorithm is essentially a realization of the method of reflected wave formation with the loss of information about the optical wave amplitude.

We assume that as a result of propagation through a random medium, a reference source has a field $E_0(x_0, \boldsymbol{\rho}_0)$ and the phase of the reference-source field is measured by a wavefront sensor. The phase $\varphi(x_0, \boldsymbol{\rho}) = \arg[E_0(x_0, \boldsymbol{\rho}_0)]$ measured by the PC algorithm, i.e., with the minus sign, is introduced into the initial distribution of the main beam at its entrance into the random medium, and then the corrected field of the beam formed in the x plane of the object is given by

$$U(x, \boldsymbol{\rho}) = \iint \mathrm{d}^2\rho_0 U_0(\boldsymbol{\rho}_0)\, G(x_0, \boldsymbol{\rho}_0, x, \boldsymbol{\rho}) \times \exp\left(-\mathrm{i}\arg\left[E_0(x_0, \boldsymbol{\rho}_0)\right]\right). \quad (11)$$

The information on the amplitude (intensity) distribution in the reference source is here lost, while the WFR algorithm assumes conjugation of the total wave phase (diffraction and fluctuation) and the amplitude (intensity) reconstruction. The PC algorithm is based on the fact that before being sent to a random medium, the original beam experiences 'predistortions' that are inverse in sign to the phase of the received reference wave that has passed through the same medium in the opposite direction. If we used the WFR algorithm in expression (11), then, for a sufficiently large aperture, a transformation of type (11) would reconstruct the original distribution, i.e., the initial radiation would be transferred as in the case of propagation in a vacuum. In [17–20, 37, 38, 44], from the reciprocity principle and its corollaries, the possibility was substantiated of describing AO feedback systems on the basis of the use of a 'reference' source introduced into the loop of current control over the parameters of the randomly inhomogeneous medium in which radiation propagates. This led to a clear demonstration of the extreme possibilities of adaptive correction based on the formation of a wave with a reversed wavefront and of the PC algorithm only correcting the fluctuation-induced phase increment, which is supplementary to the diffraction-induced one and is due to the action of the randomly inhomogeneous medium. The PC algorithm can be applied for both receiving and transmitting OESs.

Regarding the task of laser beam formation on remote objects, the situation is as follows. Phase fluctuations are here measured in the field generated by the reference source, and phase correction (adaptive control) is applied to another optical field, for example, the field of a certain laser beam transmitted to a remote object; the effect of correction must show up precisely in the region of formation of this main radiation. This effect occurs owing to the field fluctuation reciprocity, because the main and the reference fields have passed through the same inhomogeneities of the random medium. Because the PC algorithm compensates only fluctuation-induced random phase distortions, its applicability is associated first and foremost with the creation of adaptive systems of laser beam formation with the divergence in the atmosphere decreased to the diffraction limit. The potentialities of the PC algorithm have been investigated in a number of studies [16, 17, 36, 42], including in the most general setup, when both the reference and corrected fields were represented in the form of restricted Gaussian beams of radiation. In the analysis of correction efficiency, the

corrected and reference fields diffracted in a random medium were expanded with respect to a system of elementary plane and spherical waves. It was shown that if a point-like source placed in the reception plane x at a point $\boldsymbol{\rho}_\mathrm{b}$ is used as a reference source, then Eqn (11) yields the radiation field corrected by the PC algorithm in the form

$$U_\mathrm{PC}(x,\boldsymbol{\rho}) = \iint \mathrm{d}^2\rho_1 U_0(\boldsymbol{\rho}_1)\, G(x_0,\boldsymbol{\rho}_1,x,\boldsymbol{\rho}) \frac{G^*(x_0,\boldsymbol{\rho}_1,x,\boldsymbol{\rho}_\mathrm{b})}{G_0^*(x_0,\boldsymbol{\rho}_1,x,\boldsymbol{\rho}_\mathrm{b})}\,. \tag{12}$$

Here, the position of the point-like source is determined by the vector $\boldsymbol{\rho}_\mathrm{b}$, and $G_0^*(x_0,\boldsymbol{\rho}_1,x,\boldsymbol{\rho}_\mathrm{b})$ is the Green's function characterizing the optical wave propagation in a vacuum. If we assume that the contribution of the random medium to the phase of the point-like reference source is additive with respect to the diffraction phase, then the ratio $G^*(x_0,\boldsymbol{\rho}_1,x,\boldsymbol{\rho}_\mathrm{b})/G_0^*(x_0,\boldsymbol{\rho}_1,x,\boldsymbol{\rho}_\mathrm{b})$ actually represents the distortions due to the action of the random medium, corrected by the PC algorithm, i.e., the reference wave phase becomes

$$\exp\left(-\mathrm{i}\arg\left[E_0(x_0,\boldsymbol{\rho}_1)\right]\right) = \frac{G^*(x_0,\boldsymbol{\rho}_1,x,\boldsymbol{\rho}_\mathrm{b})}{G_0^*(x_0,\boldsymbol{\rho}_1,x,\boldsymbol{\rho}_\mathrm{b})}\,. \tag{13}$$

In the analysis of the quality of correction [17, 26–29] based on the PC algorithm, not the corrected field $U_\mathrm{PC}(x,\boldsymbol{\rho})$ itself but its statistical moments were analyzed, for example, the distribution of the mean intensity $\langle I_\mathrm{PC}(x,\boldsymbol{\rho})\rangle = \langle U_\mathrm{PC}(x,\boldsymbol{\rho})\, U_\mathrm{PC}^*(x,\boldsymbol{\rho})\rangle$ or higher moments. It turned out that in contrast to WFR, the PC algorithm (11) naturally reconstructs the corrected beam diffracted in a vacuum, and with an appropriate choice of the reference source, this algorithm provides diffraction-restricted characteristics for the corrected beam of an arbitrary shape. It is of interest to note that for wide laser beams with an effective size a such that the wave parameter $\Omega = ka^2/(x-x_0) \gg 1$, the most efficient is a reference beam that is narrow in the diffraction sense (in the limit, a spherical reference wave). At the same time, WFR actually forms a reference radiation beam and depends crucially on the shape of the reference signal. However, it was also revealed in [17, 27–29] that the PC algorithm efficiency for distortion correction in laser beaming on long paths decreases sharply with increasing the turbulence level or the path length. When the intensity fluctuations are 'strong' [7, 9, 15, 35], the PC algorithm loses efficiency, and the amplitude–phase correction [33], to which WFR belongs, again becomes relevant.

3.4 Schemes for construction of adaptive optics systems

We now consider the classical scheme of AO system construction. To operate properly, an AO system must typically contain the following basic components:

(1) a device affecting the wavefront (an active corrector), which can be reflective or refractive;

(2) a measuring device (a wavefront sensor) receiving light and generating a signal connected with the property to be optimized;

(3) an information processor receiving the results of measurements and converting them to signals for control over the device affecting the wavefront;

(4) a reference source providing information about fluctuations of the optical wave upon its propagation in a random medium.

These are the additional elements that must be part of an optoelectronic system that ensures correction. Some reviews and monographs [17–23, 46, 47] contain rather comprehensive information on them. We note that all elements in the composition of AO systems are rather traditional except for the essentially new optical controllable (active) element. The position of these main components in an AO system is determined, first of all, by the purpose of the optical system itself.

All the varieties of AO systems intended for correction of random wavefront distortions can be reduced to several basic types. The correction systems are typically classified on the basis of expansion of phase distortions occurring in an optical wave propagating in a random medium with respect to some system of orthogonal polynomials, e.g., Zernike polynomials [48–55]. This is of course related to the fact that the main aberrations of optical systems have typically been described using expansion in orthogonal polynomials [48–54].

In the simplest systems of active optics, so-called zero-order systems, the wavefront propagates along the axis without any changes. A typical example is given by relocatable mirrors for optical resonator length variation [4]. A first-order system provides adjustment of wavefront tilts. Active second-order systems vary the wavefront curvature, thus controlling the effective focal length. All these systems can use rigid optical elements, for instance, traditional lenses and mirrors.

Active optics underwent further development owing to the creation of modern deformable mirrors and lenses. These systems have a large number of degrees of freedom (consequently, their surface is described by higher-order polynomials) and realize the phase wavefront variation via phase expansion in a system of orthogonal polynomials (mode expansion) or via a zonal discrete representation; these are flexible continuous mirrors [23, 46] in the former case and a compound coherent aperture in the latter. Coherent systems of wavefront variation above the second order have appeared quite recently. They are being intensely developed for mirror surface (profile) shape control in large telescopes [46] and for real-time correction of atmospheric turbulence effects and compensation of thermal distortions.

Several classifications of AO systems themselves based on different approaches are proposed in some studies [4, 17, 46]. The systems were classified according to the purpose of the OES itself, the form of information in the feedback loop, the chosen algorithm of correction, etc.

In the classification according to the purpose of the optical system itself, two classes can be distinguished: emitted-wave systems and received-wave systems. The former are coupled systems, laser radars, laser beaming systems with a prescribed phase front profile, and target designation systems; the latter class systems are imaging systems or systems determining the parameters (coordinates, velocity, etc.) of the motion of a self-luminous (or indirectly illuminated) object source. Systems pertaining to the former class are characterized by the fact that during operation of the whole system, both the signal reception point (a reflected wave) and the radiation transmission point are accessible. Such systems serve to focus the original radiation distribution and are based on measurements in a scattered wave; to provide correction, predistortions are introduced that optimize the radiation characteristics both on the scattering object and in the location signal itself [4, 17, 20, 43–45]. We can distinguish systems of the second class, which are capable of manipulating only the received radiation itself formed

through a randomly inhomogeneous medium. To provide adaptive correction, knowledge of a priori information about the object (at least, whether the object is resolved by the optical system) is generally needed. Furthermore, if imaging is based on optimization of some image criterion, a logical element comparing the corrected image with an ideal one should be present in the system.

An alternative classification is by the form of the exploited reference information in the feedback loop of the adaptive system. The following classes are distinguished here: (a) systems working with data on phase front distortions from real sources; (b) systems using reflected waves (in some cases, they can be regarded as systems working with 'imaginary' reference sources); and (c) systems that do not use reference-wave measurements. If a randomly inhomogeneous medium is such that fluctuations are reciprocal in the forward and backward passage of an elementary spherical wave, the correction system can be constructed in which the data of measurements of the phase front from the reference source (real or imaginary) are used as predistortions of the initial field distribution.

We discuss the classification of adaptive systems according to the form of the relevant algorithm of introducing adaptive correction. Among the presently known methods of wavefront distortion compensation, we single out the most important ones. They contain adaptive correction systems based on the phase conjugation algorithm [17, 43–45] working with both reception and transmission of radiation; the aperture probing system [47] maximizing the performance criterion by the method of successive approximations; multiconjugate correction systems; and systems using WFR realized by nonlinear optics methods [37–41].

It is known that the main problems solved by optical systems can be reduced to two: energy transfer and imaging. In the former case, adaptive system control is realized at the entrance into a distorting medium, i.e., predistortions are introduced into the wavefront, after which the beam covers the atmospheric path, and at the same time, for receiving systems, both imaging and correction are realized at the same location, at the signal reception. The working element in the WFR algorithm can be given by a special device (a WFR mirror). In optical beam phase control, when the adaptive system works by the phase conjugation algorithm, a deformable mirror is normally used as an active element. The highest precision is reached if the paths of 'direct' and reference beams coincide and the time lag is absent. In phase conjugation, the wavefront of a reference signal is recorded by a wavefront sensor. Therefore, the sensor is here the key element, which largely affects the distortion compensation efficiency.

Thus, several structure schemes of the most typical AO systems can be proposed that are intended for correction of random wave-front distortions (Fig. 2). The source of distortions in these systems can be aberrations in an optical system, turbulence, the presence of discrete inhomogeneities on the propagation path, and thermal self-action of optical radiation.

The systems presented in Fig. 2a, b are radiating, and therefore AO must provide maximization of the radiation flux density on the target or the power density of the location signal itself. In a phase conjugation system (Fig. 2a), the light beam that has reached the target is reflected from its small regions and produces flare spots emitting spherical waves. These reflected waves propagate backward, and, under the condition of linear propagation of the inhomogeneity, exert the same influence on their spatial properties as on the emitted beam. In the wavefront sensor, the received wave is compared with the standard one, and the data processing device calculates the necessary correction, which is phase-conjugate with the measured wavefront distortion. Next, the correcting device introduces predistortion into the emitted front. The predistortion superposed on the emitting wave exactly compensates the distortions occurring when the emitted wave is propagating along the path. Owing to this, a wavefront with the needed shape maximizing the light flux density comes onto the target (object).

The second wave-radiating system is constructed according to the aperture probing principle. Here, perturbations of

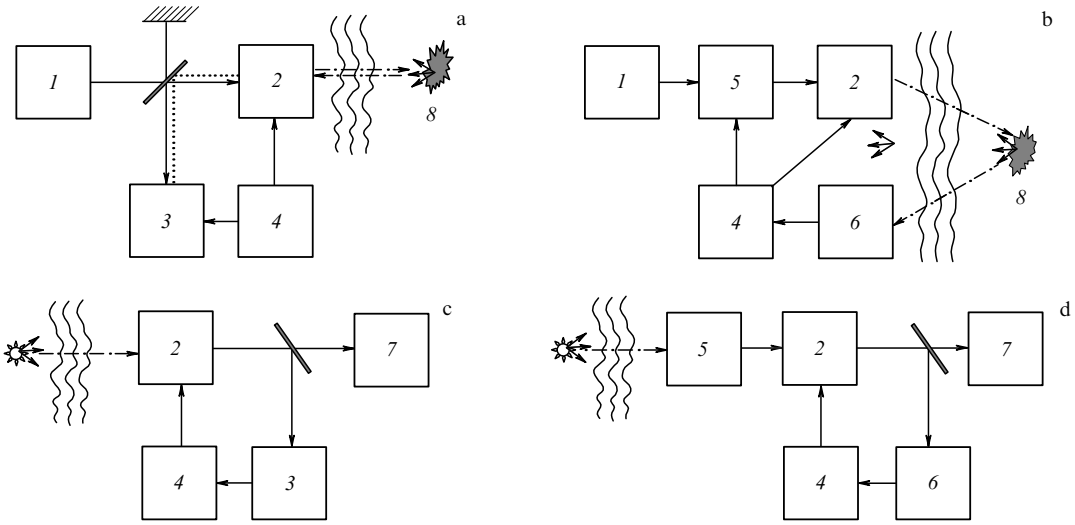

Figure 2. Main types of AO systems: (a) a phase conjugation system; (b) an aperture probing system; (c) a system operating by the method of wavefront compensation; (d) a system operating by the principle of increasing the image sharpness. *1* is the source of optical radiation; *2* is the device affecting the wavefront, the controlled active optical element; *3* is the wavefront sensor; *4* is the data processing device; *5* is the aperture probing system; *6* is the optical receiver (of intensity); *7* is the image receiver-analyzer; *8* is the target.

the emitted wavefront are tested, and the power of light that returns from the flare spot on the target is analyzed; on this basis, the perturbations that increase the light flux are determined [46, 47]. The iteration process lasts until the flux density becomes optimal (maximal). Several methods have been proposed for the creation of trial perturbations: multi-frequency vibrations and successive or multi-step vibrations. In the first case, the perturbations consist of an ensemble of sinusoidal vibrations with different frequencies, and in the second case, within the successive method, the vibrations proceed in successive steps in a definite time order.

Both these algorithms use information on the state of the medium between the radiation source and the target (object); this information is transferred by the reflected waves. In the literature, these algorithms are called 'returned wave algorithms' [4, 43, 46].

The systems shown in Fig. 2c, d are receiving systems intended to obtain the best possible image (or the maximum energy) of a remote light source or a radiation-exposed object when its radiation passes through an inhomogeneous medium. The optical receiving part of a locator or a telescope used for observations through the atmospheric depth can serve as an obvious example. In that case, luminous objects are observed that radiate incoherent light in a wide spectral range.

The method of wavefront compensation resembles the phase conjugation method for laser radiating systems. The observed object can be regarded as an ensemble of unresolvable point-like sources, each of which emits a spherical wave distorted when passing through the atmosphere. A beam with a distorted wavefront is captured by the locator aperture after passing through the device affecting the wavefront and is then separated depending on the intensity. Part of it is sent onto the wavefront sensor, which determines the local deviations and the local tilt of the entire wavefront relative to an ideal wave. Thus, the wavefront sensor performs phase measurements and creates a complete error pattern of the received wavefront, and then the required distortion correction is calculated in the data processing device, and control signals corresponding to each aperture region are fed to the device affecting the wavefront. The wavefront error at the sensor input becomes equal to zero, and hence the image formed on the receiver is in fact limited by the diffraction limits only. A device involving the described approach was first proposed by Linnik [2].

The sharpness increase principle is similar to the aperture probing method. In this case, trial perturbations of a received wavefront are also generated, and then, using a receiver located in the image plane, their effect is estimated by the maximum sharpness criterion. For this, a certain quantity is used related to the image sharpness, for example, the integral of the field strength squared over the entire image area. The increase in sharpness is an indirect method, because it requires a reliable way of distinguishing separate perturbations on the aperture.

Phase conjugation systems measure and correct the wavefront by the optical reversibility principle [43–46], according to which the light-beam phase distortion equals the complex conjugate distortion of the backward beam.

The operation quality of all the AO systems considered here depends on factors such as the wavefront measurement error, the quick action of the feedback loop compared to the perturbation time constant, and the spatial resolution of the front corrector.

4. Key components of adaptive optics systems and the requirements imposed on them

Adaptive correction schemes must include the basic elements of the optical feedback loop, namely, a reference wave carrying information on irregularities of the refractive index of the medium, a wavefront sensor extracting this information, and a wavefront corrector. In a system operating by the phase conjugation algorithm, the corrector introduces correcting predistortions into the emitted wave, and in a compensation system, corrects the received-radiation aberrations. In the simplest (zero-order) AO systems and in first-order systems, hard optical surfaces, i.e., traditional mirrors and lenses, are used. The appearance of modern deformable mirrors has stimulated further development of AO. To study the efficiency of the adaptive correction of atmospheric distortions, account should be taken of the finite space–time resolution of the adaptive system, i.e., its ability to form and take control over a corrected wavefront (or wave phase) at a definite speed and at a definite finite spatial-scale range. The time resolution of an adaptive system is determined, on the one hand, by the correction algorithm and, on the other hand, by the operating frequency band of the electronic, mechanical, and optical elements of the system. The spatial resolution is largely determined by the geometry of key elements of the system, such as the wavefront sensor and the corrector.

4.1 Wavefront sensors and methods of wavefront reconstruction

The wavefront sensor (WFS) is one of the main elements in an AO system because the information gained through it is primary for the functioning of all the elements of the system. Typically, a wavefront sensor may be needed long before the creation of the whole adaptive system because it can be used at the system design stage, in determining the parameters of the whole AO system. Also, sensor operation errors determine the operative errors of the system as a whole. The WFS work amounts to determining the deformation structure of the wavefront arriving at the sensor input. The wavefront shape deviation from the prescribed (or required) one is typically referred to as wave aberration. As far back as the 1970s, wavefront aberrations due to atmospheric turbulence were described in some papers [48–50] by a system of orthogonal polynomials (Zernike, Karhunen–Loève et al.) The most widespread now is the expansion of wavefront aberrations in Zernike polynomials, which is frequently used to estimate both the level of phase distortions and the capacity of the adaptive corrector [48–52].

Direct measurements of phase fluctuations of electromagnetic oscillations in the optical range are known to be practically impossible. Therefore, the operation of any optical WFS is based on the wavefront phase reconstruction in accordance with the results of intensity measurements. The wave is preliminarily subjected to a certain transformation, diffractional or interferential, after which the measured intensity distribution pattern experiences the corresponding processing yielding the required estimate of the two-dimensional phase distribution. Two main approaches to phase front measuring exist [43, 46, 53, 54]. One of them is based on the measurement of phase differences, and the other is based on the measurement of local tilts. The phase differences are measured using the interferential transformation, and the optical part of the sensor is, accordingly, an interferometer. In

adaptive systems, transverse shearing interferometers are mainly used [4, 5]. The shear interferometer measurements yield estimates of the phase differences between two small areas, and in the ideal case, of phase differences between two spatially separated points.

Currently, WFS based on the Hartmann method is used most generally in AO [5, 43, 53–57]. The well-known Hartmann test, initially invented for telescopic optics control, was adapted for AO problems. This method is implemented by different types of devices in which the image of the input pupil of the optical system is projected on a lens array, i.e., a set of small identical lenses. Each lens occupies a small part of the aperture (and is referred to as a subaperture), and, as a result, in the plane close to the focal plane, the source image is formed as an ordered system of focal spots. All these focal spots/images are formed on one photoreceiver. When an incoming wavefront remains, say, planar, as is the case with a remote star, all the focal images are located on a regular grid determined by the original geometry of the lens array. As soon as the wavefront is distorted, the focal images are displaced from their nominal positions. The displacements of the centers of gravity (centroids) of images in two orthogonal directions turn out to be proportional to the mean wave front tilts in these directions to subapertures. Thus, the WFS gives a matrix of measured values of mean wavefront tilts within the subapertures. Next, by matrix transformations, the wavefront is reconstructed from the array of measured tilts. The resolution of such a sensor is determined by the size of an individual subaperture. The lenses (subapertures) entering in the sensor raster are typically arranged in a certain order, in rows forming a square or other rectangular structures. Sometimes, other configurations are used, for instance, in the form of a hexagonal packing. For detection, a multipixel video camera is used. Video cameras with a matrix having a rather large number of photosensitive elements (pixels) are normally used, and the displacement of each focal spot is defined as the displacement of its center of gravity. This operation is usually performed by a computer connected to a video camera. Otherwise, energy redistribution between quadrants of a four-quadrant photoreceiver is registered (for each subaperture, its own quadrant sensor is used), and the displacement is determined by a direction-finding characteristic constructed beforehand.

Along with the Hartmann sensor, AO systems widely use the field curvature sensor proposed by Roddier [55] and the pyramid sensor of Ragazzoni [56] and others [57, 58], which are combinations of the abovementioned sensors. In view of the rapid growth of OES apertures and increased requirements on the correction precision, the further development of sensors is primarily connected with the reduced time of measurement and calculation of wavefront distortions.

Wavefront reconstruction using the WFS data can be carried out by different methods, among which two main approaches can be singled out. Within one approach, the measured local tilts are used to compute the phase differences, and then algorithms analogous to those applied in interferometric sensors are used [58–60]. According to the other approach, developed in [61–64], the wavefront is represented as a sum of some functions and then the values of local wavefront tilts are fitted to the measured tilt values. The measurement data (taken from the WFS) are represented as a vector $\mathbf{G}$ whose length is equal to the doubled number N of subapertures for Hartmann-type WFSs (the tilts are measured in two directions). The unknown wavefront is a certain vector $\boldsymbol{\varphi}$, which can be defined by phase values on the coordinate grid or by coefficients of the Zernike series expansion [48, 62]. The relations between measured and unknown values are assumed to be linear, at least in the first approximation. The most general form of the linear relation is given by the product of matrices of the form $\mathbf{G} = A\boldsymbol{\varphi}$, where A is called the interaction matrix. In real AO systems, the interaction matrix is found experimentally: signals are fed to each of the elements of a controlled deformable mirror, and the WFS response to these signals is recorded. The reconstructor matrix B performs the inverse operation of determining the wavefront vector from the measurements: $\boldsymbol{\varphi} = B\mathbf{G}$. The number of measurements is usually larger than the number of unknowns, and hence the solution based on the least-squares method is applicable. The reconstructor thus obtained has the form $B = (A^{\mathrm{T}}A)^{-1}A^{\mathrm{T}}$. Here, the superscript T means the transposed matrix, and '-1' is the inverse matrix. In almost all cases, matrix inversion encounters difficulties because $A^{\mathrm{T}}A$ is a singular matrix. This means that the measured data do not impose restrictions on some parameters (or a combination of parameters). For this reason, a reconstructor involving the least-square technique is not the best one.

It is known that the best reconstruction can be attained by using a priori information on the signal properties. In AO, such information is the statistics of wavefront perturbations and the statistics of WFS noise. For a modal wavefront reconstruction on the sensor aperture by the estimates of local tilts, the method in [61] is typically used, according to which the unknown distribution of the phase φ is represented as an expansion in a certain basis of polynomials $Z_l(\boldsymbol{\rho})$ with the expansion coefficients a_l,

$$\varphi(\boldsymbol{\rho}) = \sum_{l=1}^{N} a_l Z_l(\boldsymbol{\rho}), \tag{14}$$

and then the local tilts of this expansion are fitted to the estimates obtained in WFS:

$$\sum_{m=1}^{M}\left[\sum_{l=1}^{N} a_l \mathbf{Z}_{lm} - \mathbf{g}_m\right]^2 \to \min . \tag{15}$$

Here, $\mathbf{Z}_{lm}$ is the local tilt of the lth basis function on the mth subaperture and $\mathbf{g}_m$ is the measured front tilt on the mth subaperture.

The local tilt $\mathbf{g}_m$ can be defined in different ways, for example, as the gradient at the center of a subaperture [61] or the gradient averaged over the subaperture area [62]. It is most simple to define the local tilt components as coefficients of an approximation by a linear function, i.e., as a solution of the problem of fitting to the nearest plane. The minimization problem in (15) is solved by the standard variational method, by equating the partial derivatives with respect to the expansion coefficients to zero,

$$\frac{\partial}{\partial a_k}\sum_{m=1}^{M}\left[\sum_{l=1}^{L} a_l \mathbf{Z}_{lm} - \mathbf{g}_m\right]^2 = 0, \quad M \leqslant N, \quad L \leqslant N, \tag{16}$$

which yields a system of linear equations that can be written in matrix form as

$$||A_{kl}||\,||a_l|| = ||B_k||, \tag{17}$$

where

$$A_{kl} = \sum_{m=1}^{M} \mathbf{Z}_{lm}\,\mathbf{Z}_{km}\,, \quad B_k = \sum_{m=1}^{M} \mathbf{s}_m\,\mathbf{Z}_{km}\,. \tag{18}$$

The solution of system (17) is written in terms of the inverse matrix:

$$||a_l|| = ||A_{kl}||^{-1}||B_k||\,. \tag{19}$$

The inversion of matrix (17) is performed numerically on initialization of the sensor data. Once calculated, the inverse matrix is then used in each exposition. The same occurs in a real adaptive system: the reconstruction matrix is written into the memory of a special processor, to which the measurement vector is fed. Different sets of functions are taken as the basis of expansion (12); the most frequently used are the Zernike polynomials and the Karhunen–Loève expansion, but the latter is worth using if the aberration statistics are known; but in the case of nonlinear distortions, the Karhunen–Loève representation becomes senseless [65].

Another well-known method of phase reconstruction customarily applied in the WFS software is based on the zonal ideology. The first step is the calculation (according to the data of measurements of the tilt $\mathbf{g}_k$) of the phase difference $\Delta_{km} = (\mathbf{g}_k + \mathbf{g}_m)(\boldsymbol{\rho}_k - \boldsymbol{\rho}_m)/2$ between the centers of neighboring subapertures, where $\boldsymbol{\rho}_k$ and $\boldsymbol{\rho}_m$ are coordinates of the centers of subapertures m and k, and $\mathbf{g}_k$ and $\mathbf{g}_m$ are estimates of the phase front tilts on these subapertures. The vector character of this notation allows extending the algorithm to an almost arbitrary geometry of subapertures. In particular, the cell configuration model can be realized (here, each subaperture borders on six neighboring ones). The minimization problem is solved by a usual variational method, leading to a system of linear equations whose number is equal to the number of subapertures N. For $N < 100$, the inversion of the corresponding matrix causes no problem. Because the phase is determined up to an arbitrary constant, an additional condition should be imposed to make the matrix well defined. The reconstruction algorithms are described in detail in [63–65] and realized using software [66–68] developed IAO SB RAS (Tomsk) in simulation of AO systems and the design of actually operating WFS models.

The corresponding solving device for WFS (calculating computer) must have sufficient speed of operation to allow real-time calculations of the matrix product of the measurement vector by the reconstruction matrix. The calculation of the map of aberrations can be combined with the calculation of controlling signals of the corrector. In this case, the matrix equal to the product of the reconstruction matrix and the control matrix is written in the solver memory. The size of the resulting matrix is the dimension of the WFS signal vector times the number of degrees of freedom of the wavefront corrector. We note that currently, in connection with a sharp increase in the measurement matrix dimensions, the requirements for the speed of computer operations are also increasing. This requires using the advances in technology of parallel calculations.

4.2 Active correctors of wavefront distortions

The wavefront corrector, which is most often an active reflecting optical element, is in a sense the concluding element of an AO system. It implements the capabilities inherent in the correction algorithm and guaranteed by all the other elements of the control loop. The efficiency of the system as a whole eventually depends on the space–time resolution of the wavefront corrector. In spite of great progress in the technology of corrector manufacturing, the creation of a high-quality corrector still remains a complicated and expensive problem. In designing an AO system, it is therefore important to impose requirements on its space–time resolution corresponding to the desired correction quality.

The first image correctors in history were wavefront tilt correctors providing object image stabilization on the optical system axis [3–5, 43, 46, 55]. These are so-called tilt correction mirrors, and they are still used now. However, for OESs with large apertures, the tilt correction alone is insufficient: higher-order optical correctors are needed. Controlled (active) deformable mirrors are the main type of present-day correctors used in AO systems.

Two main types of active mirrors exist: flexible and segmented (compound) [23]. The simplest active elements are compound correctors having the simplest, and therefore the most widespread, way of mirror surface control, namely, control using actuators. Such deformable mirrors are commonly described in terms of given response functions. Particular realizations of these devices differ in the number of the degrees of freedom, geometry of the actuator position, material, shape of the elements (segments), etc. The types of segmented correctors differ in two main parameters: the shape of the segment (element) and the number of its degrees of freedom. The general number of elements also varies. The element shape is typically square or hexagonal. The number of the degrees of freedom of each element varies from one to three and determines position control (an element with one degree of freedom), tilt control (with two degrees of freedom), and position and tilt control (with three degrees of freedom). Wavefront correctors are sometimes divided according to their response to the action, which can be local or integral. Some flexible adaptive mirrors are developed and supplied with an interface that enables reproducing a set of aberrations corresponding to several first Zernike polynomials. And, as is known, precisely these polynomials are used in optics to describe the main wavefront distortions [48–52].

Next in complexity after compound correctors are membrane-type correctors, whose reflecting surface is a flexible membrane with a shape varying under the action of the control signal. Several types of flexible mirror constructions exist, differing in both the actuator construction and the way they are fastened to the lower mirror plane surface. The most widespread are mirrors with discretely located points of application of force and, in some cases, moments of force.

There are presently numerous implemented active systems controlling the flexible mirror surface [19, 23, 67–70]. A review of such correction systems that have found wide application in astronomy is available in [68].

(1) These are so-called deformable actuator-based mirrors, in which the optical surface locally changes under the applied voltage or current with the help of a system of actuators fabricated of active ferroelectric or electrostriction materials. An active mirror of a virtually arbitrary size with an arbitrary geometry of the actuator position can be fabricated. Such mirrors employ a longitudinal piezoeffect and are controlled by a voltage of several hundred volts providing a local surface reconstruction of tens of microns [23, 69, 70].

(2) Next in practical capability are bimorph mirrors [68, 69], relying on the transverse piezoeffect. Such a mirror is an

optical surface glued onto a sandwich of two layers of piezoelectric elements, the first being continuous and the second a set of piezoelectric elements. The second layer of piezoelectric elements forms the distribution of controlling elements of the mirror. The control voltages are applied to the first and second piezoelectric layers with reversed phase, which guarantees local variations of the optical mirror surface curvature. Thus, control in a bimorph mirror is due to a local bend. The advantage of these mirrors is the simplicity of their fabrication. The drawback is the rather low resonance frequency, which lowers their capability of real-time AO operation.

To construct very large active mirrors, so-called 'voice-coil actuator' technology is beginning to be applied, in which control is realized by a thin optical film membrane 'suspended' with the help of a dense system of current coils. This technology will be able to provide high frequencies (up to 80 kHz) and extensive ranges (up to 50–70 μm) of control [68, 71].

Optical active elements (a micro electro–mechanical system, MEMS) whose fabrication is based on computer technologies have been actively developed [71] since the 1990s. They have allowed creating elements up to several centimeters in size and guaranteeing a precision reconstruction of the surface, with amplitudes up to 50 μm and frequencies up to 2 to 8 kHz.

The main manufacturers of these controllable elements are companies from the USA, France, Italy, and the Netherlands. In Russia, there is experience in the creation of compound optical elements and deformable actuator-based mirrors and also rather well-developed bimorph mirror production. We emphasize that in spite of constant advances, it is precisely the active optical elements that restrict the real frequency band of adaptive system correction.

4.3 Numerical simulation of adaptive optics systems

We note that the wide practical implementation of AO elements and systems that started in the 1970s revealed a number of problems that required the theory of optical wave propagation in the atmosphere to be developed further. Hence, the attention of AO system creators to numerical simulation is quite explicable. We stress that simulation of AO systems as dynamical should be carried out not only at the stage of design and determination of basic parameters but also in the course of creation of the mathematical apparatus providing a high-speed calculation of controlling signals.

The search for answers to the arising questions necessitates elaboration of a detailed and adequate mathematical model of AO and the use of a research method such as numerical experiment based on the solution of a system of differential equations describing optical wave propagation in the atmosphere. Numerical experiment allows taking the maximum number of factors into account for an adequate AO simulation and investigating, within a unified approach, practically any significant characteristic of radiation, namely, the efficient size of a light spot, the peak intensity, the receiving aperture power, and the statistic characteristics of radiation intensity and phase. With respect to AO systems, numerical experiment enables calculating and predicting the efficiency of different configurations of the system, while in a natural experiment, this would require great expenditure of time and money.

4.3.1. History of the development of the problem. Pioneering work devoted to numerical simulation of atmospheric distortions of beams and images and to the estimation of the capability of their adaptive correction goes back to the early 1970s [42, 72, 73]. We note that these problems appear to be closely related to each other. At the same time, under intense investigation were the problems of interaction between high-power laser radiation and an absorbing medium upon propagation at large distances, in particular, the problems of simulation of thermal blooming of high-power laser beams propagating in the atmosphere. They were carried out simultaneously in several large laboratories in the USA (Lincoln, Livermore, and others) [74] and in the USSR [72, 73, 75]. In particular, it is pertinent to mention here the first reports on the results of numerical simulation of thermal self-action obtained by Gebhardt and Smith [76–78], Bradley and Herrmann [79], and Ulrich et al. [80]. The first work in the USA on phase compensation of thermal blooming [81] and numerical studies of adaptive correction of turbulent image distortions [47] were published in 1974. In the USSR, the first work on adaptive correction theory appeared in 1977 [82]. In 1976, a paper by Fleck and Morris [83] appeared, which described methods for solving the nonstationary problem of thermal self-action in a turbulent atmosphere in detail. The 1977 issue of the *Journal of the Optical Society of America* [18] generalized the results of theoretical and experimental w*ork in the area of adaptive optics in the USA*.

In the USSR, the work on this subject began rather intensely in the late 1970s. Reports on numerical studies of AO systems are presented in publications by Vorobyev et al. [84] and Konyaev [85, 86].

At the same time, the first work by Vorontsov and Chesnokov [87] and by Vysloukh, Egorov, and Kandidov [88] on phase correction of nonlinear distortions was published. Papers of the first years devoted to this area were summarized in special topical issues of *Izvestiya vuzov. Fizika* (1983 and 1985) [25, 89] and in the monographs *Principles of Additive Optics* [20], *Atmospheric Adaptive Optics* [17], and *Controlled Optical Systems* [21].

It is known that the key point in numerical simulation of turbulent effects is always the generation of realizations of two-dimensional random phase screens imitating the wave-front distortion during propagation through the atmosphere. One of the first publications on numerical simulation of turbulent distortions of optical waves was the paper by Buckley [90], where the Fourier transform (spectral sampling) method was used to simulate one-dimensional random phase screens. In works by Fleck, Morris, and Feit [83], Kandidov and Ledenev [91], and Konyaev [86], the spectral sampling method was applied to generate two-dimensional random phase screens in the problem of coherent beam propagation in a randomly inhomogeneous medium and to estimate the efficiency of phase correction of atmospheric distortions. In [92], an analogous method was used in the analysis of the probability density function for intensity fluctuations.

The abovementioned Fourier transform method was primarily used for digital simulation in radio engineering [93]. However, a specific feature of a turbulent atmosphere as a randomly inhomogeneous medium is the exceedingly broad range (more than 1:1000) of the spatial scale of refractive index irregularities. For correct simulation of all scales (from inner to outer) of turbulent fluctuations, a mesh is needed with at least one thousand nodes along each coordinate,

which entails great computational expenditures. To overcome the difficulties due to the broadband spectrum of atmospheric turbulence, it is appropriate to apply a certain 'combined' method, first mentioned in the reports by Duncan and Collins [94, 95] and also in the paper by Tel'pukhovskii and Chesnokov [96]. The main idea consists of the joint use of the spectral (harmonic) and polynomial representations, each of them being applied for simulation of its own range of spatial scales: spectral expansion is used for simulation of small-scale inhomogeneities and polynomial expansion to represent scales exceeding the computational mesh size. This approach was further developed in [97, 98], where it was also extended to nonstationary (dynamic) problems. In propagation of high-power coherent (laser) beams through a transparent atmosphere, one of the main factors, along with turbulent fluctuations of the refractive index, is thermal self-action. This nonlinear effect has the lowest energy threshold and is due to absorption of part of the energy of optical radiation and the formation of thermal nonuniformity in the beam channel; therefore, the AO system designers consider these two distorting factors together [17, 72, 73].

The advances in studies of numerical simulation of atmospheric adaptive systems to the mid-1990s can be characterized as follows. First, basic numerical methods [56–68, 97–99] were developed to solve the problem of optical wave propagation in randomly inhomogeneous media, including the problem of thermal self-action of high-power beams. Work was started on creating numerical models of particular constituent elements of AO systems with their geometrical characteristics and space–time resolution taken into account and on the search for the most effective correction algorithms.

The computer programs worked out in the USSR at that time [85, 86, 98–101] made it possible to specify the scenario of laser beam propagation on an atmospheric path (horizontal, vertical, or slant), to estimate the amplitude–phase distortions of the beam occurring upon propagation in the atmosphere, and to determine the degree of efficiency of different ways of minimization of the occurring distortions by adaptive optics methods. Numerical realizations of the following three types of WFS were created: a phase sensor, a phase difference sensor, and a local tilt sensor (Hartmann sensor). To investigate the effect of specificities of different types of correctors, numerical models of the following devices were constructed: a modal corrector, a compound corrector, and a deformable mirror with given response functions. In all three cases, the original mathematical model was written using the concept of the actuator response functions.

The conditions of laser radiation propagation in the atmosphere included characteristics such as the laser source position and the position and properties of radiation receiver motions. The atmosphere was modeled as a multilayer structure. The variable parameters of the problem were the height of the laser transmitter, the initial beam radius, the radiation intensity on the optical axis, the distribution profile of the optical beam intensity, the receiver height, the zenith angle of the propagation path, the azimuth, and the scanning velocity of the laser transmitter.

We note that in the 1990s, one of the urgent problems was the description of thermal self-action during propagation of a high-power laser beam in an absorbing atmosphere. Both the USA and the USSR (and then Russia) were concerned with solving this problem [72, 73, 76–86]. The software created at IAO SB RAS [99] became the basic version for the numerical simulation of the thermal self-action of a paraxial wave beam. The simulation of laser beam propagation in an inhomogeneous medium is based on the numerical solution of the wave equation written in the parabolic approximation for the scalar complex amplitude U of the beam and the field of the refractive index n of the medium:

$$2\mathrm{i}k\,\frac{\partial U}{\partial z} = \left(\frac{\partial^2}{\partial x^2} + \frac{\partial^2}{\partial y^2} + 2k^2\delta n\right) U\,. \tag{20}$$

Here, k is the wave number, z is the coordinate in the propagation direction, x and y are transverse coordinates, and δn is the change in the refractive index. To obtain a particular solution, Eqn (20) is supplemented with boundary conditions for the complex amplitude of the field in the cross section of the radiating aperture and with initial conditions for the field of the refractive index. Simulation of dynamic and nonlinear problems requires a joint numerical solution of Eqn (20) and some material equation describing time variation of the state of the medium. Currently, the most effective and reliable method of numerical solution of evolution equations is splitting in combination with the fast Fourier transform (FFT) algorithm. The modified splitting method [89–92] and the FFT algorithm over the combined base [100] are customarily used, and in numerical simulations of optical wave propagation through a randomly inhomogeneous medium, the solution of the refraction part of the problem at each step of integration of the wave equation by the splitting method reduces to the generation of random phase screens satisfying the given statistics. The description of turbulent distortions is based on the formula for the distortion spectrum of the phase $F_\varphi(\kappa)$ for a plane wave that has passed through a layer of a randomly inhomogeneous medium of thickness Δz:

$$F_\varphi(\kappa) = 2\pi k^2 \Delta z \Phi_n(\kappa, L_0)\,, \tag{21}$$

where $\Phi_n(\kappa, L_0)$ is the turbulent spectrum of fluctuations of the refractive index of the atmosphere.

The known method of simulation of pseudorandom correlated sequences using the FFT algorithm was applied to the simulation of turbulent phase distortions considered as a stationary random process with a given spectral density (21). The random sequence is calculated as a sum of harmonics with random weights. The existing theory of random sequence generation imposes a restriction on the weight coefficient dispersion only. The distribution functions of the real and imaginary parts of these random coefficients are usually assumed to be Gaussian, based on the normality of the random process being simulated. In some cases, a uniform distribution is used because, by virtue of the central limit theorem, the statistics of the obtained sequence tends to normal. From this standpoint, all the distributions are equivalent. To substantiate the choice of the distribution function for Fourier coefficients, the simulation of a random process is considered from the standpoint of transition from a continuous to a discrete (line) spectrum. In this case, discretization leads to replacing the continuum of elementary harmonics in a band $\Delta\kappa$ with a single harmonic. It seems logical to require that the corresponding fluctuation energies be equal to each other. It was shown that this requirement implies the condition according to which the modulus of Fourier coefficients does not change from one realization to another. Randomness is guaranteed by the fact that the argument of these complex coefficients is a random quantity uniformly distributed in the interval $[0, 2\pi]$.

Two-dimensional randomly inhomogeneous phase distortions of the wavefront with the spectral density corresponding to the Kolmogorov turbulence spectrum model with finite inner and outer turbulence scales are simulated in order to account for the effect of turbulent fluctuations of the refractive index of the atmosphere on the laser radiation (laser beam) propagation. According to the Kolmogorov–Obukhov hypothesis, the structural function of fluctuations of temperature and the refractive index of the atmosphere obey a power law. In the inertial range, the spectrum of turbulent fluctuations is known to increase as $\kappa^{-11/3}$ as κ tends to zero. Finite values of the inner and outer scales of turbulence were taken into account in the calculations. The ratio of these scales is typically chosen equal to 1000. The structure function on which the intensity of turbulent distortions depends decreases in the surface layer ($h < 20$ m) with increasing the altitude, the character of this altitude dependence changing with varying meteorological conditions, which strongly hampers the construction of a single universal model. Therefore, several models are used, including a rather simple empirical model obtained from the experimental data (up to 20 km) in the worst, medium, and best viewing conditions [8, 17, 48, 51, 101].

The application of the Fourier method for simulation of the entire spectrum of inhomogeneities is uneconomical and leads to unreasonable computational expenditures. Special methods have been proposed in which large-scale inhomogeneities are considered to mainly affect the general wavefront tilt. Hence, the total wavefront aberration spectrum (12) can be obtained by combining the Fourier series and a truncated series of Zernike polynomials $Z_l(\boldsymbol{\rho})$ with random coefficients a_l. The first terms of the Zernike series correspond to linear and quadratic aberrations. It was shown that the Fourier and Zernike coefficients are not correlated, because they are determined by different ranges of the turbulence spectrum. For $a_l(t)$ realizations, the Fourier method is also used, but in the temporal region for which the corresponding time spectra are calculated, which are expressed through the spatial turbulence spectrum.

When the medium is heated by a powerful beam, owing to the absorption of a part of the optical radiation energy, an additional density variation occurs that leads to a decrease in the refractive index related to the density according to the Gladstone–Dale law. In the isobaric approximation, the density is uniquely related to the temperature by the equation of state of the gas, and the change in the refractive index can be expressed in terms of the temperature increment: $\delta n \approx (\partial n/\partial T)(T - T_0) = n'_T \delta T$, where n'_T is the derivative of the refractive index of the medium with respect to the temperature T. The isobaric approximation is valid for most atmospheric situations. Depending on the velocity v of mutual motion of the medium and the beam, induced thermal nonuniformity may develop in different hydrodynamic regimes. The developed software allows analyzing the following regimes: free convection ($v = 0$), beam scanning with a subsonic velocity ($M < 1$), beam scanning with a supersonic velocity ($M > 1$), and forced convection (isobaric approximation) ($M \ll 1$) (here, M is the Mach number). In adaptive correction problems, the last regime alone was considered. It corresponds to the equation of stimulated heat transfer for a temperature T:

$$\frac{\partial T}{\partial t} + \mathbf{v}_\perp \nabla T + \chi \Delta_\perp T = \frac{\alpha}{\rho C_p} I, \qquad (22)$$

where χ is the thermal conductivity coefficient, ρ is the density of the medium, α is the optical radiation absorption coefficient, and C_p is the heat capacity at constant pressure. For the solution of this equation, there is a monotonic conservative second-order approximation scheme with the scheme viscosity compensation (thermal conductivity) according to the Samarskii method. The scheme is constructed by the integro-interpolation method based on the difference approximation of the convective part of differential equation (22) with upstream differences and helps in solving a nonstationary problem of induced heat transfer with allowance for thermal conductivity, also with an arbitrary orientation of the wind velocity vector $\mathbf{v}$, and also when the vector $\mathbf{v}$ is a function of the transverse coordinates x and y. Thus, the algorithms proposed in numerical models [66, 72, 73] allow simulating the time evolution of the temperature field taking two mechanisms into account: forced convection and molecular thermal conductivity, which is important in the presence of stagnation regions on the beam path.

As an example, we present the results in [42] on numerical calculations of the effects of thermal self-action of a high-power focused laser beam in an absorbing atmosphere. Figure 3 illustrates a comparison of the results of a numerical simulation of Gaussian beam focusing without correction and with the correction based on the PC algorithm in conditions of nonstationary thermal beam defocusing. The darker shading in the figure corresponds to a higher radiation power density.

The use of the developed algorithms and programs provides modeling of the operation of OES as a whole. Such phenomena can be described as nonstationary thermal self-action under which the refractive index of the medium varies owing to heating by the absorbed laser radiation energy. The proposed algorithms are used for simulation of the time evolution of the temperature field with two mechanisms taken into account: forced convection (with an arbitrary wind velocity direction) and molecular thermal conductivity, which is important in the presence of stagnation regions on the path of laser radiation.

4.3.2 Application of parallel calculations technique. More than 30 years have passed since the pioneering work on computer studies of physical wave optics was published. The results of the studies of those years were included in monographs [17,

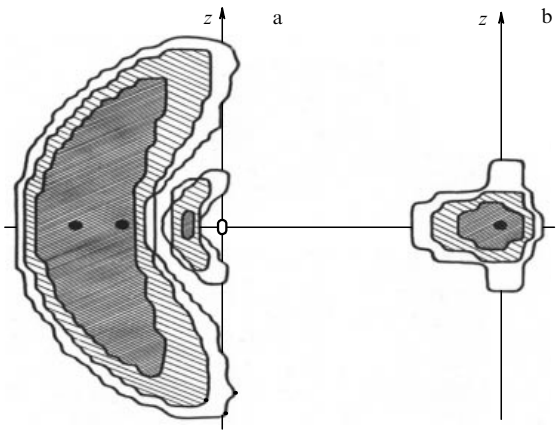

Figure 3. Adaptive correction of thermal effects for a Gaussian focused beam. a — intensity distribution in a focal spot without correction, b — with phase correction.

65, 100, 101]. Over these years, the methods of numerical simulation of wave processes have become widespread, mainly owing to advances in the development of computational processors, which evolved by the empirical Moore's law: doubling the power every two years [102]. As a result, researchers almost annually had an additional opportunity of examining fine physical phenomena, including nonlinear ones, by solving equations by numerical methods on multidimensional meshes with a large number of dimensions and mesh nodes. In recent years, however, Moore's law has apparently become inapplicable, because processor engineering is now progressing towards creation of multinuclear processors and processor clusters. In such computational systems, a further efficiency increase is associated with carrying out parallel computations. In application to AO problems, the growth in the number of calculations is caused by both a sharp increase in the measuring matrix size and the necessity of numerical transformations (multiplication, transposition, and inversion operations) of large matrices and by simulation of AO system operation, in particular, simulation of atmospheric turbulence in a wide range of scales [103]. For realization of the corresponding algorithms, technologies of parallel programming, such as OpenMP and CUDA [104, 105], are being intensely developed. They allow obtaining multiple acceleration of calculations in problems permitting operation parallelization.

The problems that permit parallelization of operations certainly include numerical simulation of AO systems and the creation of high-speed elements of AO systems, in particular, wavefront sensors, as well as numerical solutions of wave-optics scalar equations. But the existing algorithms of the solution of these equations imply successive programming and are designed to be carried out by one processor. To be applied in multinuclear processor systems and graphics accelerators, these algorithms should be modified, with regard to both the problem to be solved and the configuration of the computational equipment.

The homogeneous parabolic equation for the scalar complex amplitude $U(x, y, z)$, which describes the process of monochromatic optical wave propagation along the z axis in the paraxial approximation in a medium without refractive index variations, has the form (20). The analytic solution of this equation by the Fourier method is well known. The algorithm for deriving a particular solution for the field in an arbitrary plane given the field in the initial plane involves the two-dimensional $N \times M$ digital Fourier transform (TFT), which is standardly calculated by the FFT algorithm. The number of operations in the two-dimensional FFT is proportional to $N \times M \times \log_2(N \times M)$, and therefore, for large M and N, the calculation time can be considerable. Although the FFT algorithm has been repeatedly improved by different authors since the moment of its appearance, the most noticeable increase in speed was reached for parallel versions of this algorithm. The modern library Intel Math Kernel Library (MKL) is a set of linear algebra functions, FFT, and vector mathematics functions. It contains several different FFT algorithm realizations having different productivity and precision of computations. The library functions are versions of the FFT algorithm optimized purposefully for microprocessors compatible with Intel microprocessors. Parallelism is attained owing to multithreading, when separate nuclei work simultaneously with separate streams. In parallelizing the FFT algorithm on the central processor, the technique of multistream programming is applied,

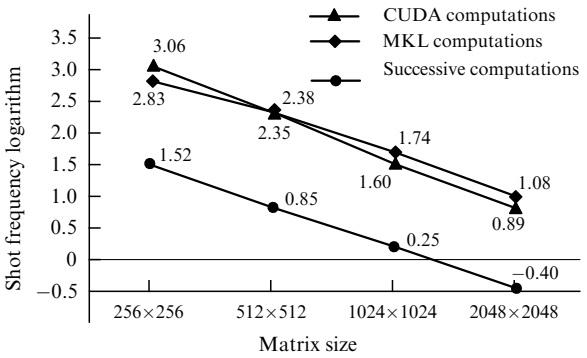

Figure 4. The number of solutions of a diffraction problem per second (frame rate) depending on the matrix size.

realized in MKL, as is the OpenMP technique for unfolding multidimensional cycles. In all cases, the problem is divided into subproblems that are simultaneously computable elementary transformations of a smaller-size matrix. All the algorithms use separable memory to speed up the computation process.

The efficiencies of three approaches were compared in [106]: standard successive and two parallel approaches, OpenMP for multinuclear processors of the Intel Company and CUDA for graphics accelerators of the NVIDIA Company. The performance of all the three algorithms was compared in the following hardware configuration: the Intel Core 17-860 processor, the XFX GTX-285 graphics card, and the Gigabyte P55A-UD4 system board. The number of video display-board processors was 220, and the number of computational streams of the processor could vary from 1 to 8. Figure 4 presents a plot of the matrix-size dependence of the number of solutions of the two-dimensional diffraction problem per second (frame rate) in a logarithmic scale. We note that with increasing the matrix size, the advantage in performance of the CUDA Toolkit algorithm becomes more and more obvious. The plots convincingly show a considerable (tens of times) increase in performance in passing from the standard successive algorithm to parallel ones.

Passing from successive to parallel programming certainly requires great effort on the part of software developers. In order that modifying the already written and debugged programs be as easy as possible, the basic heavy computation algorithms are realized in the form of dynamic link libraries, DLLs, with a subsequent inclusion of calls of the necessary functions to the original code. Such a technique allows minimizing the work on code modification and thus speeding up the inclusion of parallel programming methods in scientific investigations and computer simulations. Graphics accelerators give an advantage in performance over multinuclear processors in the most processor-heavy problems and are economically more justified.

4.3.3 Development of the spectral phase method for dynamic turbulence simulation. Advances in the development of computer technology and electronics have made it possible, in adaptive optics in particular, to simulate complex components and entire systems operating in the dynamic regime. For the atmospheric applications of AO systems, dynamic models of atmospheric turbulence evolving in time are also needed. The authors of [107] generalized the known spectral phase method [65] by generalizing the Taylor hypothesis of turbulence 'freezing' using a recursive algorithm. The author

of [108] proposed a further extension of the spectral phase method to simulate time-varying two-dimensional random fields with a known time spectrum. The method is based on the model of moving-average autoregression described by a discrete difference equation. To simulate the time evolution of a two-dimensional field, it was necessary to specify a functional relation of two-dimensional arrays of random numbers $g(l,m)=f(t)$ for discrete instants of time $t_n = nT_D$, where T_D is the discretization time interval. For this, a first-order autoregression model was used that is described by the finite-difference equation

$$\begin{aligned} f(nT_D) &= a_1 f\big((n-1)\,T_D\big) + z(nT_D)\,, \\ z(nT_D) &= b_1 r\big((n-1)\,T_D\big) + r(nT_D)\,. \end{aligned} \tag{23}$$

At the nodes of the two-dimensional mesh $g(l,m)$, model (23) generates the independent processes of evolution of random initial field values, which are stationary in time. The obtained model can be applied in computer simulation of time-variable random processes and fields. It can be realized using parallel algorithms.

5. Application of adaptive optics systems in astronomy

It is a historical fact that AO systems were first applied in astronomy. At the turn of the millennium, the modern advances in optics and electronics resulted in the appearance of a new generation of astronomical telescopes with the image quality close to the diffraction one. The use of a thin (continuous or compound) light-gathering mirror as the principal one has allowed reducing the weight and size of the telescope mounting and tower and thus significantly decreasing the expenditures on its construction. The tendency of designing increasingly large instruments has become most evident over the last two decades. Telescopes with a mirror larger than six meters (MMT, two Magellan telescopes), and instruments with a mirror 8 to 10 m in diameter (Keck I & Keck II, VLT, SUBARU, GEMINI, North & South, LBT, SALT, HET, (Hobby & Eberly), GTC) became customary in observational practice.

Larger-scale projects are currently being implemented: the Giant Magellan telescope (GMT), which is a packing of 7 mirrors 8.4 m each, and a 30 m telescope (TMT). The necessity of building new large telescopes is due to problems that require limit sensitivity of the instruments for registering radiation from the weakest space objects.

5.1 Why does astronomy need adaptive optics?

The main problem in astronomical observations using ground-based instruments is Earth's atmosphere, more precisely, random refractive index irregularities due to turbulent motion in the atmosphere. The telescope efficiency, understood as the capability of revealing dim point-like objects, is limited by the influence of Earth's atmosphere. The effect of atmospheric turbulence also decreases the potentially high angular resolution of a telescope, estimated as the ratio of the radiation wavelength to the aperture diameter. For work with an extra-atmospheric object in a turbulent atmosphere, the angular resolution of the telescope is given by the ratio of the radiation wavelength to the atmospheric coherence radius r_0, whose value is determined by an integral value of the structural characteristic of atmospheric turbulence along the optical wave path [12, 17, 109–111]. For the best observatories in the world, including those in Chile, the Hawaiian Islands, the Canary Islands, and Uzbekistan (Majdanak Mountain), the typical value of the coherence radius r_0 exceeds 10 cm in the visible range. Thus, present-day ground-based astronomical instruments have an actual angular resolution during operation in the atmosphere given by a hundredth to a thousandth of the diffraction limit, whose value is practically independent of the aperture size and the wavelength and is about one angular second. For this reason, large telescopes can fully realize their efficiency only with the help of AO systems, which have practically become an inalienable element of the modern astronomical telescope.

5.2 Application of partial correction in astronomy

Adaptive optics is now widely used in some of the most advanced observatories, providing elimination of atmospheric effects on the image quality. The characteristic feature of adaptive systems is that measurements, correction, and control are performed simultaneously. In its simplest form, for wavefront tilt correction, the AO system involves the so-called tip-tilt mirrors that stabilize the position of star 'jittering' because of atmospheric oscillations.

The next stage in the development of AO systems for astronomy was the appearance of AO elements — mirrors with a small number of degrees of freedom (actuators). This was the starting point for the use of AO systems enabling astronomical instruments to at least partially correct the images. For the design of AO systems, the initial data on the atmosphere are needed in order to formulate the requirements on future AO systems. For an estimation of the requirements for the technical characteristics of an AO system, several parameters of atmospheric turbulence that determine the image have been introduced [10, 17, 112–116].

This is, first and foremost, the coherence radius r_0, which is calculated for a plane optical wave that has passed through the entire atmospheric depth, by the computational formula [8, 10]

$$r_0 \approx \left(k^2 \cos^{-1}\Theta \int_{H_0}^{\infty} \mathrm{d}\xi C_n^2(\xi)\right)^{-5/3}, \tag{24}$$

where Θ is the zenith angle of the direction to the investigated object, H_0 is the telescope elevation above sea level, $k = 2\pi/\lambda$, and λ is the radiation wavelength.

The parameter r_0 can be calculated based on the model of vertical evolution of the structural parameter of the refractive index of turbulence $C_n^2(\xi)$ or is directly measured on the telescope itself with special equipment [110, 116–122]. This parameter determines the size of the coherent part of the wave and, thus, the necessary size of the subaperture in the wavefront sensor. Formula (24) implies that this atmosphere coherence radius is proportional to the radiation wavelength $\lambda^{6/5}$, i.e., with increasing the wavelength, the coherence radius also increases. The ratio of the telescope aperture size to the coherence radius gives the numerical value of the number of the degrees of freedom of the optical field within the instrument [39, 48, 123].

The parameter second in importance is the admissible time delay τ_0 of the signal in the correction feedback loop, which ensures an efficient adaptive correction. This admissible time delay τ_0 can be evaluated based on the results in [13, 14, 17, 65, 123] as the ratio of the wave coherence radius r_0 to the characteristic wave velocity v (or, more precisely, the rate

of phase distortion evolution), $\tau_0 \approx r_0/v$. Estimates show that the admissible time lag τ_0 under average conditions for astronomical observations must not normally exceed $10^{-3}-10^{-2}$ s. The inverse of this admissible time delay is called the Greenwood frequency [13, 14]. It is precisely the minimum frequency that an adaptive system must reach, and preferably exceed.

The next important parameter determining the image of an adaptive system is the angle of system isoplanatism — a solid angle within which the adaptive system can efficiently correct phase distortions [45, 113–115]. It determines the maximum possible value of angular detuning of the direction to the investigated (observed) object from the direction to the reference star and is defined as the ratio of the atmosphere coherence radius r_0 to the effective depth h_ξ of Earth's atmosphere [7, 8, 46]:

$$\Theta_0 \approx \frac{r_0 \cos^{-1} \Theta}{h_\xi} . \qquad (25)$$

And, finally, another parameter is the outer scale of atmospheric turbulence. This scale determines the variance of phase fluctuations [17, 115, 124] and the value of the Strehl parameter S. This parameter becomes especially important for extremely large OESs, in particular, for astronomical telescopes with the receiving aperture size exceeding 10 m.

These four parameters of atmospheric turbulence can be calculated from the measurement data on atmospheric turbulence structure in the region of optical experiments. They allow estimating the subaperture size, the necessary number of wave-front sensor subapertures into which the entire telescope aperture is divided, the required number of control elements in the correcting mirror, its dynamic range, the frequency at which the WFS fixing camera should work, the frequency band of active mirror operation, the necessary operation speed of the computational device, etc. On the basis of these parameters, we can also calculate the maximum admissible telescope characteristics [65, 109] obtained as a result of the application of an adaptive system, in particular, the attainable level of the Strehl parameter S and the form of a distribution of the average formed image, the so-called point smearing function (PSF).

The Strehl parameter S — the ratio of the energy on the axis of the telescope during its operation through the atmosphere to its energy on the axis during the operation in the vacuum — determines the minimum stellar magnitude of an investigated space object that can be registered using this telescope. The Strehl parameter calculation is based on the knowledge of the vertical profiles of structural parameters of the atmospheric refractive index and the outer scale of turbulence [65, 124]. In the absence of correction under average conditions of observation through large telescopes, the Strehl parameter is approximately 0.001 and can be even smaller. This means that the efficiency of large telescopes without adaptive correction makes up thousandths from the standpoint of the possibility of detecting weak space objects.

The aperture size in modern telescopes is dozens of times greater than the atmospheric coherence radius in the visible range. For a complete correction [47–50] of turbulent distortions in such telescopes, an adaptive system would be required with hundreds of correction channels. The complexity and cost of AO devices rapidly increases with increasing requirements for their spatial resolution.

For this reason, many projects of adaptive system design for large telescopes have made provision for the stage of working out the technological solutions for a relatively small number of corrector degrees of freedom, so-called partial phase correction. Such systems can give an almost complete compensation of turbulent distortions in the IR range and only a partial compensation in the visible range. Complete correction is typically understood as that in which the Strehl ratio S is above 0.5. Considerable gain can also be obtained with partial correction. For example, if the Strehl ratio without correction was 0.01 and after correction it was 0.1, the image recording time can be reduced by an order of magnitude. Under adaptive correction in astronomy, the levels of 0.4 to 0.7 are practically attainable for the visible wavelength range.

5.3 Efficiency of the application of adaptive optics systems in astronomy

The size of the main mirror of a modern astronomical instrument is known to be of the order of 10 m. Because of the atmosphere, the actual angular resolution is D/r_0 times smaller, i.e., 1/20 to 1/100 of the diffraction limit, and it is practically independent of the aperture size and the wavelength, being about 1–2 angular seconds (D is the telescope diameter).

A typical optical scheme of adaptive telescopes is presented in Fig. 5. The wavefront distorted by turbulent inhomogeneities is reflected from the primary (main), secondary, and other telescope mirrors and goes into a beam splitter. Part of the energy of the received optical radiation is directed to the imaging photographic camera and the rest of the energy goes to the WFS, which measures the residual aberrations and, using a computer, forms signals for an actuator of dynamically controlled (correcting random tilts) and active deformable mirrors. In the early 1990s, about the same setups were used by most researchers for an analysis of the capacity of partial phase correction in large telescopes [3–6, 17–19, 24, 43, 46, 47].

In 1993–1994, a setup similar to that presented in Fig. 5 was chosen for the design of an AO system [33] of the project of the Russian compound 10 m adaptive telescope ACT-10 [31], implemented at the request of the Russian Ministry of Science and Engineering. With the example of this project, we show how the choice of this scheme and the analysis of AO system efficiency for a large astronomical telescope are carried out. In the project, the ACT-10 telescope had a 91-element primary main mirror (approximately 10 m in size), which turned out to be too slow for a real-time compensation of turbulent distortions. Therefore, a system of correction using two active mirrors was introduced into its optical system. The world experience in the development of such systems was also generalized, and the resultant efficiency of partial phase correction was examined on the basis of a simulation program of a numerical dynamic model of atmospheric adaptive systems [65–68]. This program was based on classical models of the atmosphere itself — turbulence, refraction, and absorption [8, 65, 112, 125–129] — and on the model of adaptive system components: active optical elements, sensors of wavefront distortions, and algorithms of adaptive system operation. Such a computer program underlay simulation of the whole optical system of the telescope, beginning with the errors in its primary mirror alignment. The main focus in the simulation was the calculation of the telescope angular resolution (on the basis of PSF calculations) and the Strehl parameter.

Simulation of AO systems allows considering the important aspects of imaging in a telescope, namely, the capability

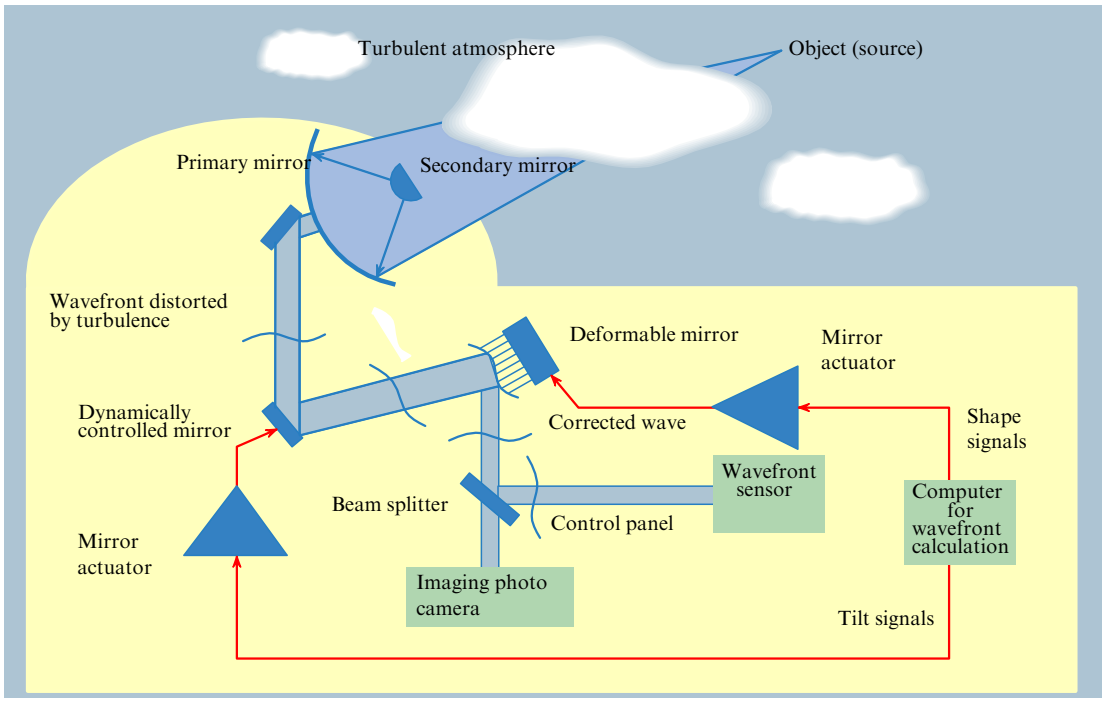

Figure 5. (Color online) Structural schematic of the astronomical telescope with an AO system for distortion correction.

of PSF width minimization for the atmosphere–telescope system by selecting the optimum wavelength and the estimation of PSF parameters during adaptive system operation in the partial correction mode. The simulation gave results regarding the capability of partial phase correction of the image using an adaptive mirror. Different atmospheric turbulence levels, different types of active mirrors (compound, flexible, and mode type), and different wavefront measuring devices were studied.

The numerical experiment was set up as follows. Turbulent distortions were simulated with a given coherence radius value r_0 in (24). Corrector control was determined on the basis of minimization of the integral quadratic error in correction (16). The size of the calculation was 128×128; averaging was done over 100 instances of random distortions corresponding to the Kolmogorov spectrum of atmospheric turbulence [7, 17, 65, 66]. Figure 6 demonstrates the results of calculations of the Strehl parameter S and PSF in the telescope, the turbulence level being defined as the ratio of the telescope diameter to the coherence radius ($D/r_0 = 10$, 20, 30). The parameter α characterizing the angular coordinates of the image normalized to its diffraction size λ/D was used as the argument in Figs 6 and 7. The variable parameter of the problem was also the number N of corrected modes (Zernike polynomials) varying in the range 3–28, which corresponded to correction of aberrations with radial polynomials of degrees from 1 to 5 (in the figures, the number of modes N increases downward as 3, 6, 10, 15, 21, 28).

According to calculations based on the Noll theory [48, 49], for example, the modal corrector with the number of corrected modes $N = 78$ is necessary for a complete correction of distortions for $D/r_0 = 20$. However, it was shown that even if the simplest corrector with $N = 10$ is used, the first diffraction rings can already be distinguished in the central

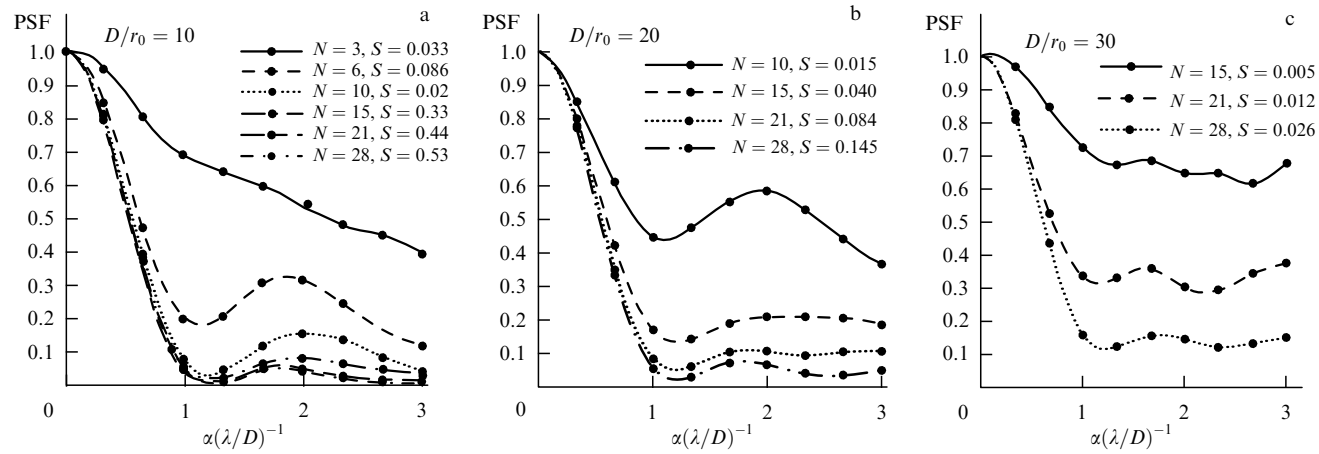

Figure 6. Results of PSF calculations with a modal corrector in the telescope. N parameter values are presented that correspond to the number of Zernike polynomials corrected by an adaptive system. The calculated PSF values are normalized to their axial value; values of the attained Strehl parameter S are also given.

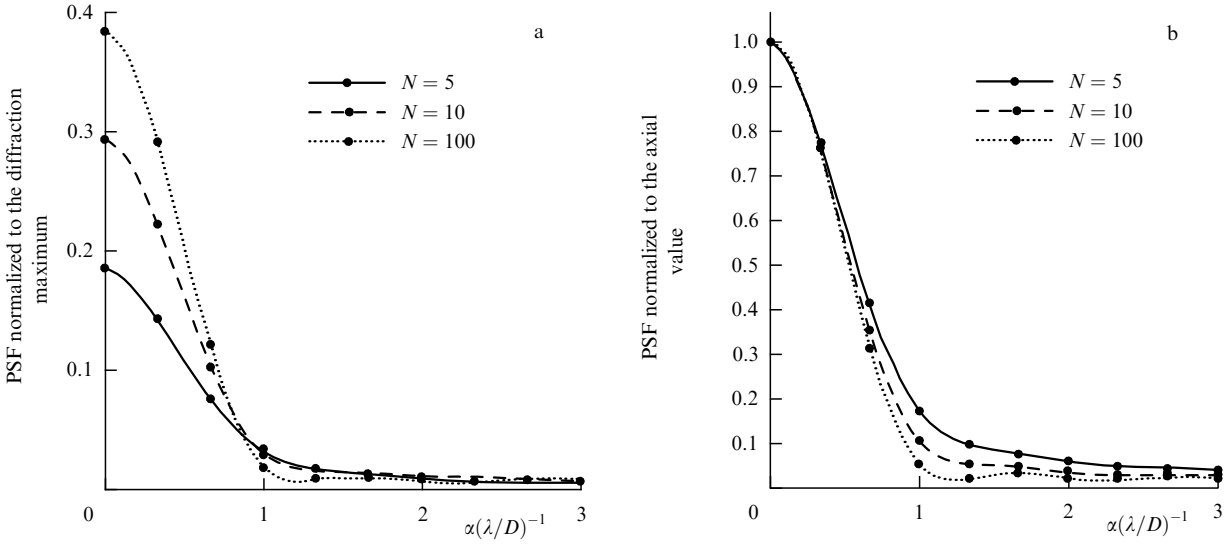

Figure 7. Results of modeling an adaptive telescope with a Shack–Hartmann sensor. The parameter N is the average statistical number of photons on a subaperture during one exposition.

part of PSF of images. The intensity of the central PSF petal is 66 times lower than in a diffraction-restricted system ($S = 0.015 \approx 1/66$), and the partially corrected PSF itself seems to consist of two components, one of which has a width close to the turbulent PSF width, and the other has a diffraction-restricted angular size. As a result of numerical experiments, it was found in [65] that upon compensation of lower aberrations, only the spatial spectrum of wavefront distortions changes radically. Noncorrected small-scale aberrations lead to energy redistribution of the corrected PSF to the far 'wings' (compared to the turbulent PSF with the same dispersion of phase distortions). It turns out that the PSF width differs from the diffraction width only slightly. This allows performing astronomical measurements related to the measurement of angular positions of objects with an accuracy approaching the diffraction accuracy, even in the course of a sufficiently 'poor' (in the Strehl parameter) correction.

As was shown in [27, 28, 33, 65], the residual distortions in an adaptive telescope can be due not only to the imperfection of the correcting device but also to the measurement errors. The wavefront sensor, the same as the corrector, almost always has a finite space–time resolution. Furthermore, an important factor for astronomical applications is the low-level brightness of the reference source used in the sensor operation. The reference source (star) brightness determines the intensity of the radiation quantum (photon) flux and the level of quantum noise. The Shack–Hartmann sensor was investigated as the most widespread in astronomical applications. The spatial resolution for this sensor is determined by the subaperture size, and the temporal resolution is determined by the time of signal accumulation. The product of the subaperture area, the accumulation time, and the reference radiation intensity defines the number Fn of photoelectrons at the sensor output. This number is the parameter determining the signal-to-noise ratio. In the numerical experiment, the adaptive system model, including the Shack–Hartmann sensor with a 10×10 subaperture matrix, was used to reconstruct the map of aberrations; the modal algorithm of reconstructions was used and the coefficients of 28 aberrations were calculated. It was assumed that an ideal corrector exactly reproduces all aberrations, and the telescope aperture has the diameter $D/r_0 = 10$, i.e., the sensor subaperture size is equal to the coherence radius.

Figure 7 shows the PSF obtained in the numerical experiment discussed above. The average statistical number N of photons per sensor subaperture in one measurement cycle varied in the range 3–100. The figure presents the results of PSF calculations for the photon numbers $N = 5, 10, 100$. It turned out that for $N = 100$, the Strehl parameter is equal to 0.38. This value is close to the result in [65] obtained for the modal corrector with the same number of corrected aberrations with the use of an ideal sensor model: $S = 0.53$. The difference is explained by a finite sensor resolution and a small noise error. For $N = 5$, the axial PSF value decreases by approximately two times, and the Strehl parameter is equal to 0.19. However, a comparison of PSF normalized to the axial value shows that the PSF width changed only slightly, and the contrast is equal to 10 even with such a noise level. A further decrease in the reference wave intensity leads to a fast increase in dispersion of the residual phase distortions and to a decrease in the parameter S. Figure 6 illustrates the dependences of these quantities on N. For $N = 3$, the S value decreases to 0.06, which is, however, almost twice as large as the value 0.033 obtained when tilts alone were corrected.

We note that almost all the existing large telescopes have passed such a stage of simulation of the partial phase correction application. Currently, many large telescopes (see Table 1) ensure a high operation efficiency owing exclusively to the use of AO systems. Moreover, because the largest modern telescopes [Keck I & Keck II, HET (Hobby & Eberly), and SALT] were fabricated using the technology of a compound principal mirror, their efficient operation necessitated concordance and active maintenance of the principal mirror shape [130–134]. We emphasize that this serious additional problem has not yet been completely solved [133]. Somewhat later, the VLT, SUBARU, and GEMINI North & South telescopes appeared with continuous thin active mirrors. They are fabricated by agglomeration of thin profile elements with a consequent grinding and polishing of the whole mirror using a special system for active maintenance of its shape.

Table 1. Modern telescopes and AO systems.

Name of telescope, what country it belongs to, and **where it is mounted**	Main mirror size, m Minimum stellar size of object	Parameters of WFS operating by the laser reference star		Presence of a wavefront tilt correction system, the base it is built on
		Sensor type	Number of subapertures	
Gemini-N USA, Canada, England, Argentina, Brazil, Chile **Hawaii**	8.1 18.5	Shack–Hartmann (S–H) sensor	12 × 12 matrix	STRAP system is used to eliminate tilt fluctuations using avalanche photodiodes (APDs); the system is designed in ESL (European Southern Laboratory) and at the Microgate Company
Keck I USA **Hawaii (Mauna Kea obs.)**	10 19	S–H	20 × 20	STRAP system on APDs (avalanche photodiodes)
Subaru Japan **Hawaii (Mauna Kea obs.)**	8.2 18	Curvature sensor (CS)	188	STRAP system on 16 APDs
VLT European Union **Chile (Paranal obs.)**	4 × 8.2 17	S–H, CS	14 × 14 or 7 × 7	STRAP system on APDs
Gemini-S USA, Canada, Chile, UK, Argentina, Brazil **Chile**	8.1 18.5	5 S–H sensors	16 × 16	STRAP sysmem on 3 APDs
Keck II USA **Hawaii (Mauna Kea obs.)**	10 19	S–H	10 × 10	STRAP system on APDs
MMT USA **USA, Arizona (Mount Hopkins obs.)**	6.5 18	S–H	60	CCD chamber with brightness amplifier
SOAR RSA **Africa**	4.1 18	S–H	10 × 10	2 × 4 APDs

We note that currently, in view of the creation of industrial samples of AO elements, the analysis of phase correction efficiency remains topical first and foremost because the introduction of AO systems to astronomy has become a common practice. This is especially evident in the analysis of the literature. For example, at the International Symposium on Astronomy (September 2012, Amsterdam, The Netherlands), advances in the development of AO systems for astronomical telescopes [111] were summarized [130, 131].

The data on the largest telescopes and the AO systems set up in them are presented in Table 1. The world optical community has now begun creating AO systems for telescopes with extremely large apertures (more than 20 m). This will call for further development of the elemental base for AO systems. In particular, in report [68], the following estimations were made: for the use of one deformable mirror in an AO system for 8 m class telescopes, approximately 200 actuators are necessary, while a 40 m class telescope requires about 4700 actuators. Such an increase in the number of control elements presents additional difficulties for all telescope systems. Even larger projects have now started, namely, the Giant Magellan Telescope (GMT) consisting of seven 8.4 m mirrors, and the 30 m telescope (TMT). The advances of recent decades in telescope construction give a real basis even for such projects as the European Extremely Large Telescope (E-ELT) with a mirror 38–42 m in diameter, the 50 m telescope EURO-50 [133], and the 100 m overwhelmingly large (OWL) telescope [132]. The application of adaptive systems is virtually the only way to provide efficient operation of such astronomical systems.

5.4 Development of adaptive optics systems for solar telescopes

Currently, solar telescopes with high spatial resolution are also indispensable for the study of physical processes in small objects on the Sun. Observations of the Sun on scales smaller than 70 km are believed to be necessary today. To fix processes on such scales, the angular resolution of the telescope should be better than 0.1 angular seconds [135–149]. The study of phenomena such as solar corona heating, solar activity, and variations of solar luminosity affecting

Earth's climate require observations of the microstructure of magnetic fields of the solar atmosphere with an angular resolution better than 0.05 angular seconds. For construction of theoretical models of the solar atmosphere, parameters are needed that can be obtained by analyzing the behavior of even smaller spatial scales of the solar atmosphere.

Adaptive optics systems for solar telescopes are technically more complicated than stellar systems. This is because diurnal turbulence is more rigid than nocturnal, and also because it changes strongly with time. Moreover, the wavefront sensor must operate with radiation in the visible range with the use of low-contrast, extended, time-variable objects, such as solar granulation. A typical value of the coherence radius r_0 for diurnal turbulence is no larger than 10 cm (at a wavelength of 0.55 μm), even in the best places of observation and with a typical telescope altitude 20–40 m above Earth. In addition, the coherence radius r_0 [10] characterizing the strength of atmospheric turbulence fluctuates strongly on short time scales (seconds) and often decreases to several centimeters. Hence, in spite of the comparatively small input apertures of solar telescopes, solar AO systems require a larger number of more rapid elements of correction than stellar ones. The WFS used for stellar AO systems cannot be employed for solar ones, because the Sun is an extended object, and objects that can be regarded as reference for nocturnal systems are inapplicable here. In the AO systems designed for solar telescopes, a Hartmann correlation sensor [143–147] is typically used, for which extended structures in images of the solar disc surface, i.e., solar spots, pores, and solar granulation, are objects of observation. We note that the solar granulation picture is rather difficult to use in tracking and measuring systems, because such a granulation picture has a low contrast and varies on time scales of the order of several minutes.

The first experiments with AO systems [46] were carried out by J Hardy in 1979 using the solar VTT (Vacuum Tower Telescope) at the Sacramento Peak Observatory, USA. A shearing interferometer was then used in the experiment as a WFS. It was assumed that the system would be able to work with both bright stars and solar spots. Actually, the AO system demonstrated an improvement in the star image quality, but it practically failed to improve the solar spot image.

The first full-fledged AO system [143, 144] was designed by the Lockheed Company in 1992–1993 for the DST (Richard B Dunn Solar Telescope), which is included in the composition of Sacramento Peak Observatory, USA. This system was based on a 19-element compound mirror and a Shack–Hartmann wavefront sensor that involved a simple analogue system with a quadrant detector for shear measurement. We note that the Shack–Hartmann sensor differs from the traditional Hartmann sensor in that its small holes in the diaphragm are replaced by microlenses, which increases light accumulation. The first AO system was restricted to contrast objects of monitoring: solar spots and pores. The breakthrough in solar AO systems was due to the development of the correlation Shack–Hartmann sensor [135] and its introduction into a low-order AO system for the telescope. The correlation sensor exploits the same principle as was used in tilt correction systems (tip-tilt) in processing the 'correlation monitoring' device [135, 144–147].

At the same time, in spite of the efforts made, the Roddier curvature sensor [55] did not find application in solar AO systems. Currently, practically all solar AO systems use the correlation Shack–Hartmann sensor. Several operating AO systems on world solar telescopes are known at present [136–144].

The latest Swedish solar telescope (NSST) — a 97-cm vacuum telescope operating at the observatory on La Palma island — uses a deformable mirror as a corrector, placed beyond the vacuum system of the solar telescope [143, 144]. A separate correlation tracker is used to measure the wavefront tilt. The WFS is constructed on the basis of a lens matrix with a hexagonal packing according to the design of the correlation Shack–Hartmann sensor. The size of an individual subaperture is 13.8 cm. A Dalsa CA D6 streak camera (made in Canada) is used, which 'reads' 955 shots a second. The data are processed by two specialized Athlon computers. The system includes a deformable bimorph mirror of the AOPTICS Inc. Company, which has 37 actuators (control elements) and ensures phase correction with expansion up to 60 Zernike modes. The real correction frequency band in a closed circuit of the whole system is not greater than 45 Hz. The large aperture (97 cm) of the NSST telescope in combination with the 37-element AO system provides the highest resolution in images of the Sun.

The adaptive system was designed at the Potsdam Astrophysical Institute (Institut fur Sonnenphysic and Astrophysikalisches Institut, Potsdam, Germany) [138–140] and was placed on the 70 cm solar vacuum telescope VTT on Tenerife island. In its design and setup, the system is very similar to that for NSST. It involves a Hartmann correlation sensor with 37 subapertures (each 10 cm in size) with a hexagonal arrangement. The field of vision of the subaperture is $12'' \times 12''$. The 35-element bimorph deformable mirror has an aperture of 50 mm. The system corrects the image up to the value $D/r_0 > 10$. The principal processor is a Sun Fire V880. The system enables the Strehl parameter to be increased to 0.3 for the angle of vision of the order of $1''$, the frequency band of the system being of the order of 50 Hz.

At NSO (North Solar Observatory) and the Institute of Technology NJIT, New Jersey, USA, two (more or less identical) high-order AO systems were set up, which are now operating in the 76 cm telescopes Dunn Solar Telescope (DST) and Big Bear Solar Observatory (BBSO). The systems employ a 97-element deformable mirror. The composition of these AO systems for higher-mode correction was established after the very successful work of the AO system for lower-mode correction on the DST. The systems use a Shack–Hartmann correlation sensor and parallel processing by commercial microprocessors that provide high-speed computations and data measurements.

A new solar telescope, GREGOR, with a 1.5 m tracking mirror was rather recently put into operation. The telescope was mounted on Tenerife island (Spain) by the German consortium Kiepenheuer Institut Potsdam, Institut fur Astrophysik Göttingen, and a number of their partners. A still larger 4-meter solar telescope (Advanced Technology Solar Telescope, ATST), which can only operate with a high-power AO system [144], is now being designed in the USA. For high-accuracy measurements of the Sun, narrow-band observations (< 20 mÅ) and a high spatial resolution are needed. This, in turn, requires long exposures during observations, because even the Sun becomes a weak source with such spectral and spatial resolutions.

An important stage in the development of solar AO systems was the creation of wavefront correlation sensors

Table 2. Active correction systems in solar telescopes.

Country	USA	France–Italy	Spain	China	Russia (LSVT)
Years of operation	1989	1995	1995	2001	2001 – 2005
Mirror diameter, cm	76	90	98	43	76
Reference signal	Solar spots, granulation pattern	Granulation pattern	Granulation pattern	Solar spots	Solar spots, granulation pattern
Camera operation frequency, Hz	417	582	1350	419	164 – 245
Field of vision, ang. sec.	10 × 10	2 × 2 – 12 × 12	14 × 14	5 × 5 – 20 × 20	33 × 33
Frequency band, Hz	25 in the open loop	60 in the closed loop at a level of 3 dB	100 in the open loop	84 in the open loop; in the closed loop, band 30 at a level of 3 dB	120 in the open loop
Attained image quality (root-mean-square deviation)	0.023″	at least 0.2″	0.05″	0.14″	0.7″

permitting the use of solar granulation as an object of monitoring. Inclusion of AO with a correlation sensor [143–149] in the composition of operating solar telescopes located in places most advantageous in the astronomical climate improves the image contrast of solar granulation, but the diffraction resolution can only be reached under exceptionally good conditions of vision (for a coherence radius > 20 cm). An improvement in the granulation pattern quality on solar telescopes operating under worse viewing conditions remains a fairly complicated task. Table 2 gives comparisons of several correction systems for solar telescopes.

5.5 Design of an adaptive optics system for the LSVT solar telescopes

Certain experience exists in Russia for developing AO systems for solar telescopes. For example, in 2001 at the Zuev Institute of Atmospheric Optics, SD RAS, the first tests [145] were carried out of the AO system with a correlation sensor on the Large Solar Vacuum Telescope (LSVT) of the Baikal astrophysical observatory of the Institute of Solar–Terrestrial Physics, SD RAS. The LSVT is mounted on the Baikal lakeshore at the altitude 645 m above sea level; it has a 1-meter tracking mirror. Under medium conditions of LSVT observation, the Fried radius was estimated to be 40–55 mm. The AO system used images of sufficiently contrasting solar spots as tracking objects. In 2003, after an improvement of the image recording system through a change of the video camera, the AO system showed good results when an image region with a small solar pore whose contrast was below 8% was used as a tracking object.

As an illustration of the adaptive system operation, Figure 8 presents the results obtained in the stabilization of the position of a part of a solar surface image (framed in the left part of the figure). The tracking object was the image of a solar spot with a size of 9 angular seconds at a level of 0.5 of the luminosity modulation depth. The image contrast was 8%. The adaptive system operation was estimated on the basis of the efficiency of suppression of image jitter spectral components, $|S(f)|^2_{\rm er}/|S(f)|^2_{\rm c}$, where $|S(f)|^2_{\rm c}$ and $|S(f)|^2_{\rm er}$ are spectral power densities of uncorrected image displacement signals and signals of residual image displacements in the tracking mode (see the right part of Fig. 8). The work of 2003 was aimed at working through the model of the system, among other things, for the many-mirror adaptive system control. The model consisted of a high-speed video camera, hardware for image input to the computer, and algorithms of image analysis. The model was tested on the LSVT during an

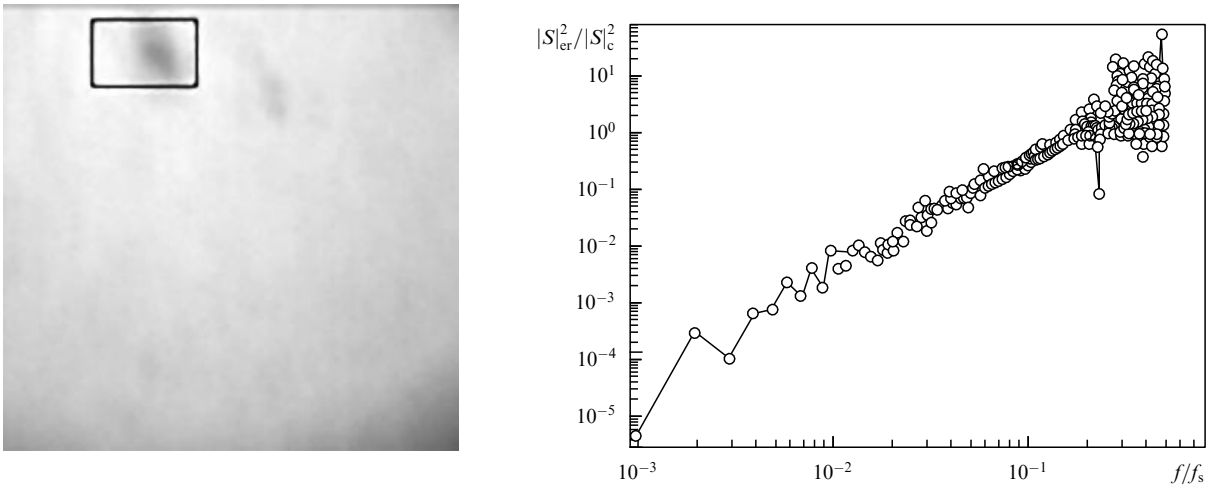

Figure 8. Part of the image and frequency dependence of the image jitter suppression efficiency.

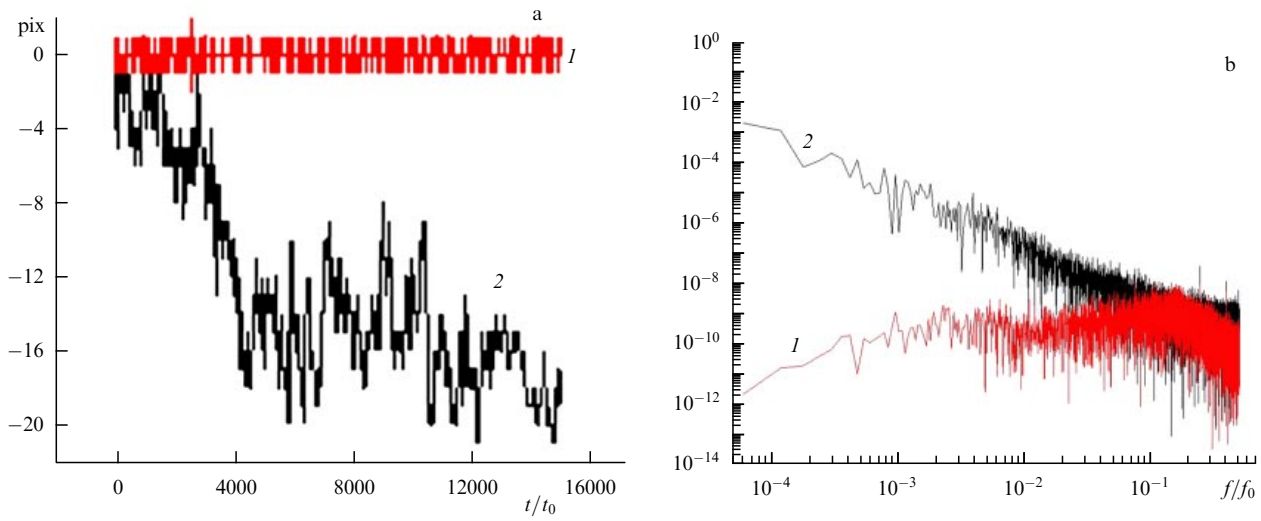

Figure 9. (Color online) (a) Signals of image displacement and (b) their power spectra for closed (curves 1) and open (curves 2) loops of the AO system control.

expedition in the environs of Lake Baikal. The algorithm for measuring the displacement of a part of the image in the telescope focus implemented the correlation methods of measurements.

Figure 9 presents the results of operating an AO system with a correlation sensor based on the DALSTAR camera (128×128-pixel matrix, A-to-D converter). The transmission band of the AO system with a closed control loop was estimated during the WFS operation for a solar pore (contrast 13%) in the LSVT. The analysis window had 96×96 pixels, the readout frequency was $f_0 = 245$ Hz ($t_0 = 1/245$ s). To obtain the spectra, 98 s instances were used that were recorded in the measurement and tracking modes successfully with the interval of several seconds. The coefficient of suppression of the root-mean-square value of the fluctuation level calculated by the data of measurements was 29–36 times.

In 2004, a modified correlation tracking algorithm for WFS was designed and was tested in measurements of solar granulation image displacement. The correctness of displacement measurements by the modified correlation sensor was verified by a comparison with measurements of displacements by a traditional correlation sensor of image pieces for which the traditional correlation algorithm is applicable.

The employed algorithm traces large scales (a smeared image) and gives a large error when the filtering function singles out small scales (the small image structure seldom shows up in the course of measurement) [146, 147]. The use of the modified algorithm of correlation sensor operation permits recording the displacement of low-contrast image pieces. Figure 10 gives an example of the operation of an AO system with the granulation pattern of the visible solar surface. The average contrast of the granulation pattern image did not exceed 2%. A comparison of fragments a, b, and c in Fig. 10 convincingly demonstrates the high efficiency of the Angara AO system.

Thus, we can state that along with the solar telescope system of the US National Solar Observatory (NSO) and the correction system for solar telescopes in the Canary Islands, the Angara model for the LSVT [149] designed with the participation of IAO SB RAS and ISTP SB RAS is now one of the most advanced prototypes of an adaptive system for large-aperture solar telescopes.

In solar AO systems, two controllable mirrors are normally used: one for control of general wavefront tilts and the other for second-order and higher-order aberration correction. The application in an AO system of one controlled mirror with a construction allowing the combination of both functions has certain advantages, first and foremost a decrease in the number of optical elements, because only one output pupil of the telescope is formed, and a decrease in the optical path length in the AO system. As a result, wavefront aberrations introduced by optical elements and pavilion turbulence decrease. For an AO system of the LSVT, a controllable mirror is necessary, which was developed with allowance for the specificity of LSVT construction and the astronomical climate of the telescope location site. In the existing AO scheme, the range of tip angles of the controlled mirror should not be less than $\pm(1.5-2)$ angular minutes and the time of setting should be at least 5 ms.

The 2006–2007 LSVT tests of the Angara AO system with a modified correlation sensor [148, 149] showed a sufficiently high efficiency of the system in which parts of the granulation pattern with a contrast of 2–3% were used as traced objects. Not only does an adaptive system increase the percentage of high-quality images but, which is of paramount importance, the telescope assumes a new quality in further modification and an extension of the feasibility of realizing new ways of solar observations.

5.6 Artificial reference sources in adaptive optics systems and methods of their creation in astronomy

AO system operation is based on obtaining, one way or another, information on phase distortions introduced by a turbulent atmosphere into the spatial field structure. This information can certainly be obtained by analyzing the radiation wavefront from some optical celestial source. Some problems arise in choosing such a reference source. For good operation of the wavefront sensor, a rather large number of photons are needed, but large telescopes deal with exceedingly weak space objects. For this reason, the investigated object itself cannot be regarded as a reference source. Therefore, neighboring (rather close) brighter stars are used

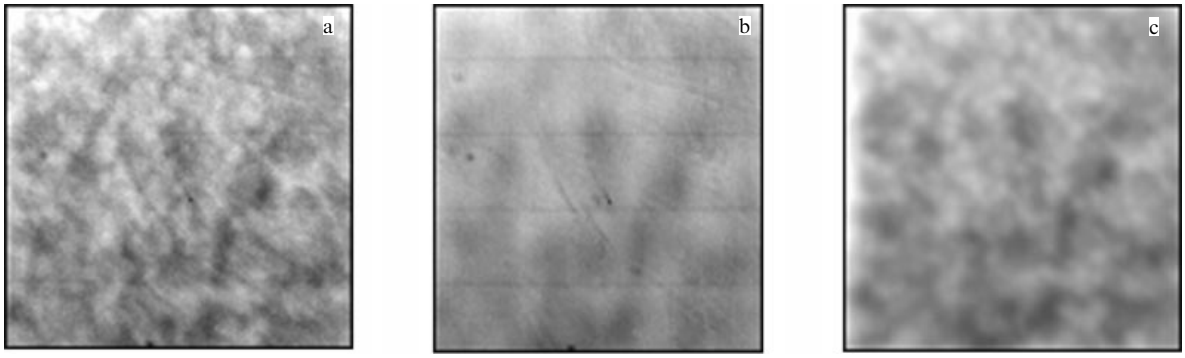

Figure 10. Illustration of the operation of the Angara system with a modified WFS (37 apertures); a — separate image shot with an exposure of 5 ms; b — averaged image for the time of 1 s without correction, c — averaged image for the time of 1 s with correction.

in AO systems. For efficient image correction, a reference source should be a brighter star, close to the investigated object, with a glow of at least 10^m. This can only be realized in conditions of a sufficiently close angular disposition of a natural bright star and the investigated object. Calculations in [45, 46] show that an admissible angular mismatch between the directions to the reference star and to the investigated object must not exceed 15–20 angular seconds. As a result, most of the celestial regions turn out to be unfit for observations with AO systems, because it is impossible to find a sufficiently bright natural reference star [150].

Two solutions exist to overcome the above-described restrictions. The first is to work at longer (infrared) waves for which the turbulence effects manifest themselves much more weakly, the wavefront distortions occur more slowly, and more time is available for photon accumulation; then not very bright stars can be used as references. Furthermore, the isoplanatic angle in (25) becomes larger with increasing the wavelength, and therefore the region where efficient correction is feasible also increases. As a result, natural reference stars become suitable for infrared observations in larger celestial areas than in the visible spectral regions. However, from the standpoint of astronomical observations, the visible wavelength range is still of great scientific interest.

The second approach consists in forming an artificial reference signal source in the atmospheric region of the radiation propagation channel, i.e., between the astronomical object and the telescope objective, based on laser radiation backscattering in the atmosphere and called a laser guide star. The idea of using artificial laser guide stars (LGSs), also called laser beacons, appeared in adaptive optics in the late 1970s [44, 45, 151–155]. We emphasize that all the American studies on LGSs were classified, and it was only in 1992 that the first open publication appeared [74]. It was at that time that all the basic principles underlying the present-day concept of adaptive OESs were formulated. According to that concept, the reference source is the key element of the optoelectronic scheme, which is used for obtaining information on the distribution of irregularities of the refractive index of the medium in the radiation propagation channel. The OES structure as a whole depends largely on the way the reference wave is formed. If the adaptive system is based on the reciprocity principle, the most efficient system is one using an independent reference source of radiation propagating in the direction opposite to the corrected radiation direction.

The fact that LGSs are formed on the basis of the backscattering signal imposes serious restrictions on their application in real systems. We note that as far back as approximately the mid-1970s, researchers and engineers working on creating optical systems of atmospheric vision and probing realized the importance of the specificities of reflected wave fluctuations. In contrast to transmitting OESs, the effect due to the double passage of the optical path is always present in optical probing systems. The probing radiation passes through optical inhomogeneities twice, during forward and backward propagation.

A relatively complete review of this problem can be found, e.g., in [17, 156–158]. The works summarize the results of research on the effects of fluctuations of the refractive index of the atmosphere in optical wave propagation in conditions when a wave passes twice through the same atmospheric region. Such a situation occurs for laser radiation reflected from an object or for waves scattered backward by atmospheric aerosol. In this case, the optical wave fluctuations are determined by a considerable correlation between fluctuations in incident and reflected waves passing through the same inhomogeneities in a turbulent atmosphere. This may lead to qualitatively new properties of fluctuations compared to the effects of forward propagation, in particular, to amplification of inverse scattering of intensity fluctuations, far-field correlations in the reflected wave, and other effects [17, 156–158]. The priority of Russian researchers in this area was confirmed at the International Conference on Wave Propagation in Random Media (Seattle, USA, 1992) [158].

The first results on LGS application were obtained in the USA [155]. The practical introduction of AO systems with LGSs in large telescopes not only permitted obtaining new results in astronomy [159–162] but also revealed fundamental restrictions on their application. The efficiency of the corresponding AO systems with LGSs is mainly limited by the focus and angular anisoplanatism, as well as by the impossibility of correcting the global wavefront tilt based on measurement data from an artificial reference source [150, 154, 155]. In spite of the large number of studies [163–171] seeking ways to solve the above-mentioned problems, they now remain topical.

It therefore seems reasonable to continue research in this area and develop new approaches to the formation and application of an artificial reference wave source, to the algorithms of operation, and to obtaining information from such a source. We stress that these problems are closely related to a number of theoretical issues that have not yet been solved satisfactorily. For example, to date, no proper analytic expressions exist that would allow the calculation of

the effect of focus anisoplanatism under AO correction with LGSs and, therefore, the synthesis of the AO system on the basis of real data on the intensity and altitude distribution of turbulence at the point of telescope location [172–177]. We also note the phenomenon of angular isoplanatism in AO systems, which has not been comprehensively studied so far, because in practice a partial or mode correction [176] of atmospheric fluctuations occurs.

It is known that an artificial reference source can be formed on the basis of (1) Rayleigh backscattering of optical radiation or the elastic scattering of light by atmospheric aerosol at altitudes of 8 to 20 km; (2) resonance scattering (fluorescence) by atoms of some metals, in particular, sodium atoms in the mesosphere at altitudes of 85 to 95 km. In the former case, the laser guide stars are referred to as Rayleigh LGSs and in the latter case, as sodium LGSs [74, 155]. Depending on the type of star being formed, the requirements for the laser source change radically. To form a Rayleigh star, rather powerful short-wave laser radiation is needed. To create a sodium LGS, laser radiation must have a narrow spectral band (~ 3 GHz) and be tuned precisely to the sodium line, which is caused by selectivity of absorption. A certain emitter power is needed because of a fairly low level at which the saturation of sodium layers in the atmosphere sets in. Systems for creating sodium LGSs are now in continuous operation in several large astronomical telescopes [111, 130, 131, 172–174], but no complete agreement has yet been reached concerning selection of the optimum time and space parameters and laser radiation power for LGS formation. These problems are directly related to the physics of interaction between laser radiation and sodium atoms of the mesosphere. The sodium layer parameters (the total number of atoms, the average altitude, and the profile) show seasonal variations and vary within days, hours, and even minutes, and sporadic layers occur unexpectedly and then vanish within several hours. A fundamental requirement is a laser source wavelength in the range of the doublet D_1 (589, 594 nm) and D_2 (590.0 nm) of the sodium absorption spectrum. We note that other mesospheric metals (besides sodium), e.g., iron, potassium, and calcium, can practically be used. Several laser techniques now exist that are capable of emission at this wavelength with the power up to 50 W; they are at different levels of scientific and technological development [130, 131, 172, 173].

More than ten projects of adaptive systems of large ground-based astronomical telescopes [130–133] have been implemented or are being designed in the world in the last decade. Almost each large observatory now has or is working out AO systems with LGSs. Such a wide implementation calls for investigations of the methods of adaptive correction of atmospheric distortions for the purpose of their development. These studies are becoming especially topical owing to the tendency of creating increasingly large ground-based telescopes. LGS systems for astronomy are also being developed intensely and, as a consequence, a large number of papers have been published recently devoted to theoretical and experimental studies in this area. Practically introducing AO systems with LGSs into large telescopes yielded new scientific results in astronomy [111, 130, 131], including the use of the laser reference source technique [175–177].

5.7 Multiconjugate adaptive system

Multiconjugate adaptive optics (MCAO) deal with a further development of the AO system concept. The MCAO system is aimed at turbulence correction using more than one deformable mirror [178–180]. Each such deformable mirror is optically conjugated with a definite distance from the telescope in the atmosphere. The main advantage of MCAO consists in increasing the field of vision of a corrected image. Control signals for these several mirrors are received not from one but from several WFSs, each of which uses its own reference star in measurements. The information from several WFS is simultaneously processed by a computer reconstructor to restore the three-dimensional wavefront perturbation, the same as is done in medical tomography, where the three-dimensional object structure is determined from observations at different angles. In this case, the quality of distortion correction is better than with only one reference star. The continually increasing interest in the development of methods of three-dimensional turbulence reconstruction and their application in MCAO is directly connected to the prospects of turbulence correction in large and (in the future) superlarge telescopes in the entire visible and infrared ranges [131, 132].

6. Application of adaptive optics systems for the formation of laser radiation beams

We emphasize that the range of problems that have been successfully solved recently using laser systems has widened considerably. Modern OESs, including AO systems, are now finding an increasingly extensive practical application. Historically, AO systems were first used in astronomy only. In recent years, adaptive optics have also been employed, for example, in ground-based systems imaging Earth's artificial satellites and other space objects; other efficient applications of AO systems, including the use in medicine, are now reported increasingly often. The applicability limits of adaptive optics for problems of modern technology are expected to widen in the nearest future. Contemporary adaptive optics are capable of perpetrating a revolution in industrial and medical technologies. It is possible to significantly improve the technical and operational characteristics and parameters of OESs for technological purposes (welding, cutting, drilling metal and superhard materials, glass cutting, laser scalpels, optical systems in ophthalmology) using coherent signal processing by introducing adaptive optical elements and systems.

6.1 Optimization of laser beam formation

Along with turbulent distortions, the thermal self-action (blooming) of high-power laser beams is a serious factor limiting laser energy concentration on the object [66–92]. In some situations, in particular, in the use of IR-range lasers, the thermal self-action is practically the only obstacle to reaching a high intensity level on the target. This factor is also important for a wide application of AO systems, and therefore different methods are employed for an efficient energy transfer of optical radiation beams. These methods are relatively simple — power optimization, distribution of intensity, focal length [181], and the time regime of radiation — and are also more complicated, involving a priori (programmed) phase correction, the algorithms of phase conjugation, and wavefront reversal.

Thermal self-action is known to be a substantially nonlinear effect. A consequence of this is a nonlinear dependence of the parameters of intensity distribution on the target on the initial beam power. As a rule, an optimum power exists for

which a chosen criterion attains an extreme value. After power optimization, the next stage is the choice of the initial intensity distribution in the beam cross section. It is known that different types of laser resonators can yield different intensity distributions at the output of the active medium. For the single-mode generation regime, the Gaussian intensity distribution is typical, and for the multimode regime, a more uniform intensity distribution in the beam cross section is described by hyper-Gaussian and super-Gaussian beam models [17, 65, 98–101, 182]. Another specificity of the intensity distribution can be the gap in the beam center [183, 184] due either to a peculiarity of the resonator and laser generation regime or to the shading of the central part of the beam by a secondary mirror of the forming telescope. Thermal blooming of a scanning beam was also considered in [17, 65, 185], where a uniform (Gaussian type) intensity distribution was shown to give better results than a Gaussian beam.

The power optimization of different focused beams was calculated in [65]. To estimate a possible gain 'from above', the self-action on the phase screen located in the plane of the radiating aperture was considered. The intensity distribution in the focal plane was determined in the Fraunhofer diffraction approximation, i.e., in the far diffraction region. Figure 11 illustrates the dependences of the dimensionless power of focused laser radiation in a circle with a size equal to the effective angular size of the undistorted focused Gaussian beam, $R = 0.64\lambda/D$, where $D = 2a_0$ and a_0 is the original size of the focused beam.

In Fig. 11, the dimensionless total power $P' = P/P_0$ transferred by a laser beam is shown along the x axis. The normalization was done in accordance with [65] to the quantity

$$P_0 = \frac{\rho C_p V_\perp a_0}{\alpha k n'_T L}\,, \tag{26}$$

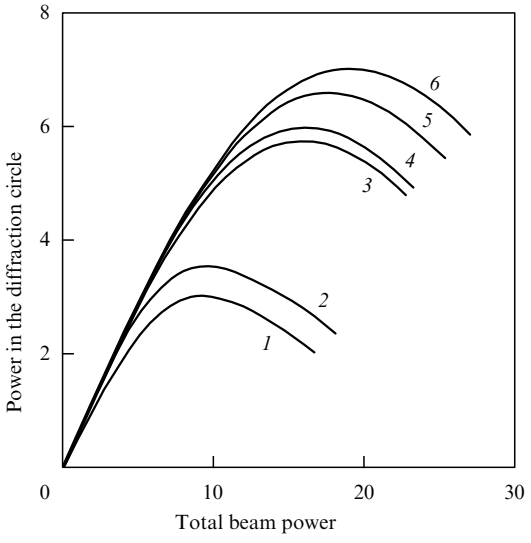

Figure 11. Dependence of the power in a circle of the diffraction size $R = 0.64\lambda/D$ on the total beam power (curves of power optimization for beams without correction for a constant wind direction). Beam types: *1* — truncated Gaussian, *2* — unrestricted Gaussian, *3* — hyper-Gaussian directed at 45° to the wind, *4* — wide Gaussian, *5* — super-Gaussian, *6* — hyper-Gaussian directed from the side to the wind.

where L is the length of the nonlinear region represented by a phase screen, i.e., the part of the path with the highest absorption, α is the energy absorption coefficient in the medium, ρC_p is the product of the bulk density of the medium and its thermal capacity, and $V_\perp$ is the magnitude of the transverse component of the velocity vector of the medium (wind).

Figure 11 shows that non-Gaussian (super-Gaussian, hyper-Gaussian) beams give a 3- to 5-fold gain over Gaussian beams. Obviously, the distinction between beams with different intensity distributions has two reasons: first, a different effective beam size, which also gives better results in the absence of nonlinear distortions, and, second, a different structure of aberrations occurring in them during propagation in a nonlinear absorbing medium.

6.2 A priori phase correction

Problems exist in which the so-called a priori phase correction can be implemented. They include the reduction in the effect of thermal self-action caused by radiation energy absorption and a powerful radiation beam along vertical paths. Thermal self-action along a vertical path is represented by the situation where phase correction can be highly efficient because nonlinear phase distortions are mainly concentrated in a small (relative to the whole pathlength) region near the radiating aperture, and the wave parameter of the effective length of this region is much less than unity for broad beams normally used for radiation transport onto the object located at a high altitude or even beyond the atmosphere.

Such a correction can be used, e.g., to eliminate the effect of thermal heating of active elements in a system generating high-power radiation in solid-state laser systems. A priori (or programmed) phase correction (APC) is based on the information on the parameters of the medium entering the heat transfer equation. If they are known, then, knowing the intensity distribution in the beam cross section, we can calculate the thermal lens structure in the channel of optical beam propagation. The APC efficiency is limited by three main groups of factors: first, the inaccuracy of a priori information on the parameters of the atmospheric path and the beam affecting the formation of optical inhomogeneities in the beam channel; second, the non-optimality of the used algorithm of the construction of phase corrections; third, a finite spatial resolution of the correcting element of the adaptive system, restricting the possibility of exact formation of the necessary phase profile. The most significant components of a priori information about the state of the atmosphere are the altitude profile of the wind velocity vector and less variable factors such as the profiles of the refractive index of the atmosphere and its temperature. The a priori information that is inaccessible in principle is the instantaneous state of turbulent inhomogeneities, which restricts the range of the most efficient APC application in both the visible and near IR ranges.

The known methods for constructing phase correction [185–187] can be presented in the order of increasing complexity as three groups.

(1) Phase correction, defined as a predistortion equal to minus the integral phase distortion in a nonlinear medium, calculated as the integral along the path:

$$\varphi_c(\boldsymbol{\rho}) = \frac{2\pi}{\lambda}\int \tilde{n}(\boldsymbol{\rho}, z)\,\mathrm{d}z\,, \quad \tilde{n}(\boldsymbol{\rho}, z) = n(\boldsymbol{\rho}, z) - n_0\,. \tag{27}$$

The refractive index irregularities can be obtained from the solution of the thermodynamic part of the self-action problem derived on the basis of either the beam intensity distribution in the radiating aperture plane [185, 186] or the three-dimensional intensity distribution corresponding to the diffraction approximation in the description of beam propagation [187] or in some other approximation.

(2) Phase correction determined from the wavefront calculation for some reference radiation propagating along a high-power beam channel in the oncoming direction [187] relative to a high-power laser beam. Such an approximation is essentially the phase conjugation method, with the exception that in this case, instead of a real reference source, its mathematical (numerical) analogue is used, because the distortions of the phase profile of the reference beam are calculated numerically. In contrast to the efficiency of the ordinary phase-conjugate AO, the capability of this method, like the efficiency of any other APC method, depends on the accuracy of the used a priori information.

(3) Phase correction determined on the basis of optimization of expansion coefficients in a certain basis of functions [188], for example, in the basis of Zernike polynomials or in the basis of phase corrector response functions. It is not the actual energy concentration on the object, but its value calculated by solving the self-action problem based on the available a priori information that is maximized.

Method 1 is the simplest to carry out; phase correction is determined in an unambiguous and natural way, and this method can be expected to be the least sensitive to errors in the a priori information. However, its efficiency may turn out to be lower than that of methods 2 and 3 if the accuracy of a priori information is high.

We consider the dependence of the APC efficiency on the configuration and the number of the corrector degrees of freedom. This underlies the determination of the upper bound of correction efficiency with the use of the currently available technology for implementing APC [189]. To exclude the influence of other factors on the correction efficiency, we represent a nonlinear medium as a thin phase screen located in the radiating aperture plane. Phase correction is then determined as the quantity equal to the nonlinear phase increment [65, 187, 190, 191]:

$$\varphi(\boldsymbol{\rho}) = -\varphi_{\mathrm{N}}(\boldsymbol{\rho})\,. \tag{28}$$

Corrector control is then determined from the minimization condition of the integral quadratic error of approximation:

$$\sigma^2 = \iint \mathrm{d}^2\rho\big(\varphi_{\mathrm{K}}(\boldsymbol{\rho}) - \varphi(\boldsymbol{\rho})\big)^2 \to \sigma^2_{\min}\,. \tag{29}$$

Here, $\varphi_{\mathrm{N}}(\boldsymbol{\rho})$ is the nonlinear phase increment and $\varphi_{\mathrm{K}}(\boldsymbol{\rho})$ is the correcting phase.

Figure 12 demonstrates the computational results of APC operation done with a modal corrector used for a Gaussian beam [65]. The x axis is the dimensionless power of formed radiation in the circle whose size is equal to the effective angular size $R = 0.64\lambda/D$ of an undistorted focused Gaussian beam. The figure shows that simple adaptive systems (curves *2* and *3*) that only control linear and quadratic aberrations allow about a twofold increase (compared with curve *1*) in the energy concentration on the object. The y axis is the dimensionless total energy transferred by a laser beam.

Thus, a rather significant increase in the energy concentration on the object can be reached for a comparatively small

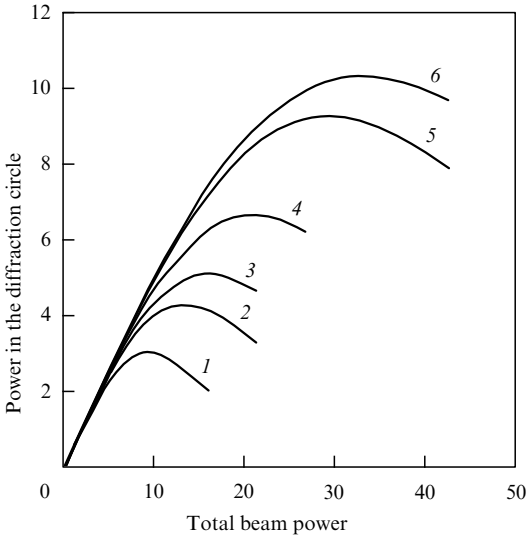

Figure 12. APC efficiency with the use of a modal corrector for a Gaussian beam (power optimization curves for a constant wind direction); without correction (*1*), with correction of tilt (*2*), and defocusing (*3*), and astigmatism (*4*), and coma (*5*), and spherical aberration (*6*).

number (10 to 20) of corrector degrees of freedom, which is explained by the predominance of lower (large-scale) aberrations in the thermal lens structure. However, these results [65] were obtained under the assumption that nonlinear distortions are concentrated in the radiating aperture plane. The thermal lens actually has an extensive character, which violates the additivity of correcting pre-distortions and nonlinear wavefront distortions, and complete compensation cannot be reached even with an infinite spatial resolution of the corrector. In such a situation, the phase conjugation algorithm is applied.

6.3 Using the phase conjugation algorithm for correction of the effects of thermal radiation self-action

The idea underlying the application of the PC algorithm is known to be based on the reciprocity principle [7, 16, 35, 65] of electromagnetic wave field propagation. In application to the considered problem of wave beam propagation, this can be most simply illustrated by the example of reversibility of the parabolic wave equation for the slow component of the complex amplitude of electromagnetic oscillations. It was shown previously that the reciprocity principle is also valid in an optically inhomogeneous medium, e.g., in propagation through atmospheric turbulence [7, 16]. The efficiency of the PC algorithm for correction of thermal self-action effects can be guaranteed if the phase distortions due to thermal heating of the atmosphere are small within the AO system actuation time Δt. The AO system actuation time Δt is understood as the time necessary for the calculation and formation of the correcting phase using an active deformable mirror. The necessary condition for the AO system actuation time Δt was formulated in [65, 190–192]: it must be less than the characteristic time of thermal 'lens' formation

$$\tau = \left(\frac{\lambda}{L}\right)\frac{10^6}{I}\,. \tag{30}$$

Formula (30) uses the quantities introduced in [65, 191]: the dimensionless intensity I is the intensity normalized to the

quantity $I_0 = \rho C_p V_\perp / 2\alpha k^2 (\partial N/\partial T)\, a_0^2$ and the dimensionless time τ is the time normalized to the heat transfer time $\tau_v = a_0/V_\perp$, where α is the absorption coefficient of the medium, a_0 is the effective size of the beam in the cross section, $V_\perp$ is the transverse component of wind velocity, and n is the refractive index of the medium. We note that the notation is the same as that used in formula (26).

Adaptive optics systems in which the actuation time Δt is less than the time τ_v were called 'fast' [190–192], and in contrast to them, systems with the actuation time $\Delta t > \tau_v$ were called 'slow' [193–195]. Although some optical devices based on nonlinear interactions of optical waves are capable of realizing WFR (to a limited accuracy) [39–42], in practice they more frequently do not go beyond phase control. The question of how good the phase-conjugate AO is from the standpoint of applicability can be answered by thorough research, e.g., similar to that done in [65]. The authors of [189–195] certainly asked themselves such a question. In addition, they were interested in how the increase in the transferred power affects the correction quality and whether the increase in this power under conditions of nonlinear interaction between the beam and the medium leads to the appearance of specific effects, including different kinds of instabilities.

Herrmann [184, 189] was apparently the first to report on the possibility of an unstable regime occurring upon phase correction. The numerical analysis carried out in [65, 191, 192] showed that the main problem of a successful PC algorithm operation is the development of instability upon thermal self-action of a focused beam, for example, on a homogeneous horizontal pass. The search for ways of 'canceling' the instability and increasing the efficiency of adaptive phase correction in such a situation has begun. On the basis of a simplified mathematical model of nonlinear propagation, it was shown in [189] that beginning with a certain threshold power, the application of phase conjugation induces an unlimited growth of the corrected beam divergence. It was also mentioned that a small-scale instability was observed in a numerical experiment. The mechanism of the development of small-scale instability was examined in detail in Refs [186, 190]. Such instability is apparently typical of the situation where nonlinear (and, possibly, turbulent) distortions are concentrated within a short part of a path whose length is much less than the diffraction beam length. This is typical of vertical atmospheric paths. Horizontal paths are characterized by a vibration-type instability [37, 191], which is associated in [192] with the occurrence of wavefront dislocations in the reference beam.

The adaptive focusing of a high-power radiation beam in a homogeneous absorbing medium has been considered. Such a medium has no random inhomogeneities, and all its parameters determining thermal self-action remain invariable along the entire path. We suppose that the initial beam is focused to a distance f. From the focal plane of this beam (with the coordinate $z = f$), an incoming reference beam propagates along the axis without self-action. The boundary conditions for this reference beam correspond to WFR of a diffraction-limited high-power beam. In the radiating aperture plane, the AO system performs phase correction with the result that at each instant of time, the phase distribution of the corrected high-power beam corresponds to the phase distribution in the reference beam. The dimensionless peak intensity $I_{\max}/I_0$ and the power in an annulus corresponding to the effective radius of a diffraction-limited focused Gaussian beam were registered in the focal plane. Calculations show that with increasing the power above a certain threshold, the corrected beam parameters exhibit the known oscillations [65, 191]. To understand the mechanism of the occurrence of oscillations, we investigate the behavior of the dimensionless coordinate $z_{\max}/f$ of the corrected beam waist. For this, we register the waist position determined as the distance between the radiating aperture plane and the plane in which the peak intensity in the beam cross section reaches its maximum value. Figure 13 shows the dynamics of the waist position and the peak intensity value in its cross section for the power for which the system exhibits oscillations.

At the initial instant, the waist is located near the focal plane, as follows from the theory of focused Gaussian beam diffraction. Then the waist is displaced towards the radiating aperture, which is explained by a defocusing correction introduced by a developing thermal lens. The reference beam passing through the thermal lens formed as a result of self-action of a high-power corrected beam experiences defocusing. Due to the application of the PC algorithm, this defocusing is transformed into an additional focusing of the corrected beam, which leads to waist displacement towards the AO system aperture and to the corresponding decrease in the focal distance of the system.

The diffraction-limited beam width decreases in proportion to the focal length, and the intensity has a quadratic

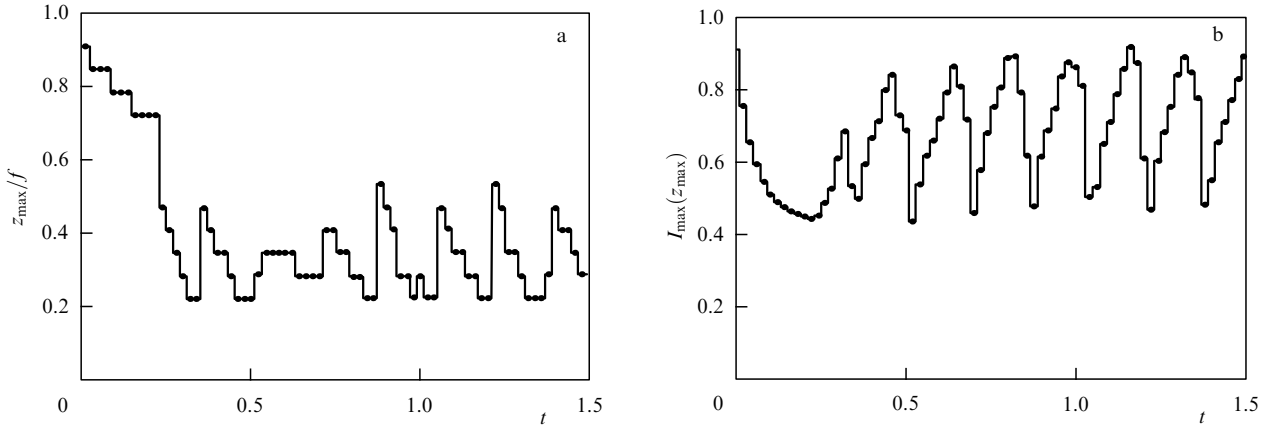

Figure 13. Dynamics of (a) the waist position and (b) the peak intensity value in its cross section for the initial value $I_0 = 24$. The intensity is normalized to the diffraction-limited intensity value in the beam focus. On the x axis is the (dimensionless) time normalized to the heat transfer time $a_0/V_\perp$.

dependence. Hence, a decrease in the focal length leads to a considerable intensity increase in the waist. An increase in intensity leads to the corresponding increase in the temperature gradient in the thermal lens, which results in a further increase in the reference beam defocusing and the corrected beam focusing.

Thus, positive feedback is formed in the optical loop of the adaptive system, which can be represented as the following chain: occurrence of a thermal lens — reference wave defocusing — high-power beam focusing — waist displacement towards the radiating aperture — intensity increase in the waist — thermal lens amplification. However, no unlimited 'signal' increase is observed in this chain, and therefore factors restricting the waist displacement and leading to the attainment of saturation by such a nonlinear feedback system exist. Obviously, several factors are acting here simultaneously.

1. The AO system tries to compensate the defocusing effect of the thermal lens. The waist displacement depends on the distance between the radiating aperture of the AO system and the portion of the path where the thermal lens is concentrated, i.e., the waist position at the previous iteration. The closer this portion is to the AO aperture, the smaller the waist displacement because, when passing through this portion, the excess focusing is compensated by the thermal lens.

2. As the waist shifts and the effective beam size decreases in this cross section, the effective transverse size of the thermal lens also decreases. At the same time, the reference beam size does not decrease in the same measure. For this reason, the thermal lens only affects the central part of the reference radiation and, accordingly, only the central part of the corrected beam is subjected to additional focusing.

3. The general defocusing only prevails at the initial stage of thermal lens formation. Beginning with the time instant $t > (2-3)\, a/V_\perp$, defocusing prevails in the direction perpendicular to the wind direction. The corresponding corrected beam focusing along this axis leads to a beam size decrease in only one direction, and the intensity in the waist decreases in proportion to the first rather than second power of the corresponding focusing parameter.

We note that in the description of adaptive correction of thermal defocusing effects, two limit cases were introduced in [191]: 'slow' adaptive systems with the actuation time $\Delta t \gg \tau_v$, where $\tau_v = a_0/V_\perp$ and the thermal regime is described by the stationary heat transfer equation, and 'fast' AO systems for which $\Delta t < \tau_v$ and the corresponding material equation has the form of nonstationary transfer equation (22). It was shown in [191] that the slow adaptive correction [188, 193–195] operating according to the PC algorithm of the reference wave rapidly loses efficiency with increasing the beam intensity, whereas fast systems [17] can long remain effective.

The reason for the appearance of the oscillatory instability in specific behavior of the reference wavefront was studied in [191, 192]. It is known that upon sufficiently strong distortions, the wavefront topology can acquire a qualitatively new character [196]. The wavefront dislocations that occur on the intersection lines of sign reversal of the real and imaginary parts of the complex amplitude make it into a multisheeted surface, and projecting such a surface onto a two-dimensional cross section gives a phase distribution with lines of discontinuities by 2π joining points with dislocations wound in opposite directions. It is logical to assume that the qualitatively new character of the reference wavefront topology can lead to a qualitatively new regime of AO system operation, i.e., self-oscillations. The topology of the reference beam wavefront has been investigated. For this, on each iteration of fast phase conjugation, the reference beam field was tested for the presence of dislocations, their coordinates being fixed. The detection of dislocations was based on the known fact that the line integral of the phase gradient $\mathbf{g}$,

$$\oint \mathbf{g}\, \mathrm{d}^2 l = 2\pi(N_+ + N_-)\,, \tag{31}$$

is proportional to the sum of the number of positive N_+ (i.e., wound in the positive direction) and negative N_- topological charges [196]. The smallest loop in numerical simulation is a square with four neighboring mesh nodes at its vertices. Because the integral along the segment joining two vertices is equal to the phase difference between these two points, the line integral can be calculated as

$$\Sigma = \Delta_1 + \Delta_2 + \Delta_3 + \Delta_4\,, \tag{32}$$

where $\Delta = \arg(UU^*)$ is the corresponding phase difference of the optical field U. The occurrence of dislocation was considered registered if $|\Sigma| > \pi$. A dislocation determined in such a way was assigned the coordinates of the loop center.

In the experiments in [192], it was revealed that for a power corresponding to the threshold of the onset of the self-oscillation regime, two dislocations of opposite signs occur in the reference beam. The dislocations move in the wind vector direction. An analysis of the dynamics of dislocation motion, the time-dependent behavior of waist parameters, and the focal spot showed similar periodicity of all three processes. This obviously means that these oscillations are closely related to the appearance of dislocations in the reference beam. A comparison of the dynamics of all the processes gives grounds for the following interpretation of the oscillatory regime of an AO system. The displacement of a high-power beam waist and the corresponding intensity increase in it cause the appearance of a strong local thermal lens. When distortions in the reference beam become sufficiently strong and it exhibits dislocations, information on the thermal lens contained in the phase of reference radiation is distorted so much that the optical feedback loop is 'unlocked'. Further development of the processes in an AO system apparently proceeds as follows. The local thermal lens positioned in the cross section where the beam waist was located moves in the wind direction in accordance with the mechanism of stimulated heat transfer. This corresponds to the propagation of reference beam dislocations in the same direction observed in the AO system aperture plane. After the local thermal lens extends beyond the reference beam effective cross section and the corresponding wavefront dislocations appear beyond the limits of the system aperture, the phase optical feedback is restored, which leads to a new cycle of focusing increase.

It can be readily seen that the PC algorithm, as opposed to the WFR algorithm, does not actually use information on amplitude distortions in the course of control. Therefore, the more phase distortions change into amplitude ones, the lower the efficiency of the PC algorithm. When the amplitude profile distortions reach the extent that the intensity vanishes at some points, a qualitatively new situation arises. If the difference between the algorithms of adaptive correction of WFR and PC is characterized [65, 192] by the intensity ratio

of corrected-to-reference beams at each point of the AO system aperture, then, upon the occurrence of dislocations, this parameter tends to infinity at the points of their occurrence. We seem to be dealing here with the mechanism of violation of the phase optical feedback underlying the operation of the considered AO system, the violation being so substantial that the focusing not only stops increasing but also begins rapidly decreasing, which is seen from the rapid waist displacement towards the focal plane.

In one of the first papers [189] devoted to this problem, it was pointed out that beginning with a certain threshold power value, the use of the algorithm causes an increase in the divergence of the corrected beam, which obstructs a considerable increase in the light field concentration in the plane of observation. Along with the divergence, an oscillatory type instability (i.e., oscillations of the radiation parameters) is observed [190–192]. The mechanism of oscillation development is described in [192]. The authors believe that the development of a self-oscillating regime is explained by the feedback loop opening in an adaptive system. A 'strong' defocusing lens on the path leads to the loop discontinuity and a decrease in the field concentration on the focusing object. With time, the local thermal lens moves in the wind direction, and after it oversteps the beam limits, the feedback is restored, and the radiation parameters in the observation plane increase. A more detailed analysis of the process of control by the PC algorithm suggests that under the conditions considered here, it is impossible to speak of feedback breaking. The cause of oscillations is obviously a violation of the optical reversibility principle underlying the phase conjugation algorithm.

6.4 Phase correction under strong fluctuations

In Section 6.3, we considered the characteristics of phase correction upon high dispersion of residual phase fluctuations. However, we assumed that the intensity fluctuations were absent. In this section, we discuss another limit case, that of strong intensity fluctuations. We assume that the adaptive system has an unlimited space–time resolution with respect to phase distortion correction.

Phase distortions occurring on propagation through an optically inhomogeneous medium are known to transform, with a further wave propagation, into modulation of the spatial intensity distribution. When the modulation is deep enough, zero-intensity points can emerge. If a wave is described in terms of a complex amplitude U, such points are formed at the intersection of lines where its real and imaginary parts are equal to zero. If in crossing these lines the quantities $\mathrm{Re}\,U$ and $\mathrm{Im}\,U$ change sign from positive to negative, such intersection points are points of wavefront dislocations [196]. Important from the standpoint of adaptive phase correction is the fact that the continuity of the two-dimensional phase distribution is broken with the occurrence of dislocations [197].

With the emergence of discontinuities, the error in the wavefront approximation by an adaptive mirror increases significantly. The application of special correctors does not generally have an effect either, because with correction of turbulent distortions, dislocations occur at arbitrary random points of the aperture. The algorithms for the formation of a map of reference wave aberrations presently used in the majority of WFSs yield a continuous function of transverse coordinates at the output; hence, they virtually filter the vortex part of the measurement vector [192].

Numerical experiments performed in [65, 192] showed the effects of intensity and dislocation fluctuations on the correction of turbulent distortions. In this context, two questions were formulated: how much does the loss of amplitude information affect the phase correction efficiency and how much does the loss of information contained in the vortex part of phase measurements lower the adaptation efficiency? The numerical experiments were carried out for the PC algorithm.

A plane reference wave propagates in the direction opposite to the corrected radiation. In the original plane, an adaptive system measures reference radiation distortions and, in accordance with the PC algorithm, corrects the emitted wave. This problem involves four numerical parameters: the propagation pathlength L, the beam aperture diameter D, the radiation wavelength λ, and the turbulence intensity C_n^2. According to the Gurvich similarity theory [8], the problem of plane wave propagation in a turbulent atmosphere can only be characterized by two scales. The coherence radius r_0 can be chosen as the transverse scale, and the diffraction length at the coherence radius, $L_T = kr_0^2$, can be chosen as the longitudinal scale. Then the considered problem is characterized by a normalized pathlength L/L_T and a normalized aperture diameter D/r_0. The scintillation index of the plane wave [35] for the Kolmogorov power-law spectrum of turbulence [8] is $\beta_{\mathrm{R}}^2 = 2.9(L/L_T)^{5/6}$.

Two versions of the phase measurement algorithm have been considered. In the first version, an ideal adaptive system instantaneously and accurately reproduces the reference wave phase on the entire cross section plane, including singular points (dislocations) of the wavefront. In the second version, only the phase component is corrected that corresponds to the potential part of the wavefront local tilt vector. The results of numerical experiments [192] are presented in Fig. 14, showing the dependence of the Strehl ratio S on the scintillation index $\beta_{\mathrm{R}}^2 = 2.9(L/L_T)^{5/6}$ calculated by Rytov's formula for two schemes of adaptive correction. The aperture diameter D normalized to the coherence radius r_0 took the values $D/r_0 = 10$, 20, and 30. The figure therefore demonstrates two families of three curves.

In the case of (complete) phase correction by the PC algorithm (the upper curves in Fig. 14), it turned out that for all intended purposes, the Strehl parameter S values depend

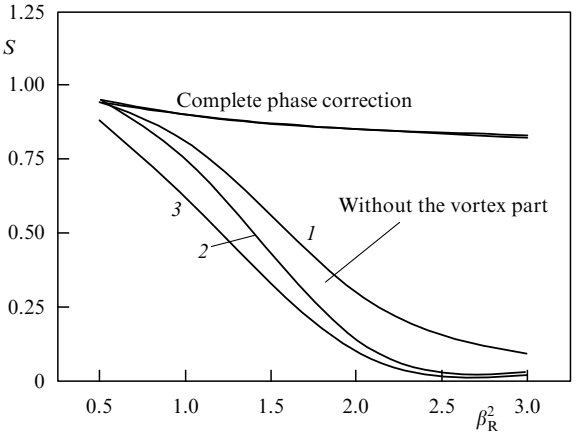

Figure 14. Dependence of the Strehl parameter S on the scintillation index $\beta_{\mathrm{R}}^2 = 2.9(L/L_T)^{5/6}$ in an AO system operating according to the PC algorithm. $D/r_0 = 10$ (*1*), 20 (*2*), 30 (*3*).

neither on the normalized aperture diameter nor on the pathlength. The difference between the parameter S and the diffraction-limited value, equal to unity, is small in practice. This agrees with the idea that the leading role in image distortion is played by phase fluctuations, and the role of amplitude fluctuations is insignificant. In this case, the fluctuations are completely corrected. If only the smooth ('screw-free') part of the phase is compensated, the correction efficiency decreases rather significantly with increasing the scintillation index (the lower curves). A reduction in the Strehl parameter by half is reached already for the values of $\beta_R^2 = 2.9(L/L_T)^{5/6}$ approximately equal to 1–1.5. A further increase in intensity fluctuations leads to the mean intensity tending to an uncorrected value. The correction efficiency decreases by an order of magnitude at $\beta_R^2 = 2-3$. This means that such phase correction loses efficiency when the path reaches the diffraction length on the coherence radius. The correction efficiency in the scheme of an ideal PC algorithm is already not indifferent to the value of intensity fluctuations. However, the dependence is not so strong as might be expected. For $\beta_R^2 = 3$, the Strehl parameter decreases to 0.8 and is virtually independent of the aperture diameter.

The numerical results were confirmed by the experiment carried out at the Lincoln Laboratory, USA, with an atmospheric path 5.5 km long [198] (Fig. 15). The AO system included a Hartmann sensor and a deformable mirror, and the PC algorithm was used to focus the laser beam. It is pertinent to mention that the parameter $\sigma_{\chi_R}^2$ shown in Fig. 15 is approximately equal to the scintillation index β_R^2 introduced in [8]. The solid line in the figure corresponds to the result of calculation [192], the black triangles being the experimental data from the Lincoln Laboratory. The vertical segments show the spread of the experimental data.

Because the experiment was carried out with a fixed pathlength, the change in the parameter $\sigma_{\chi_R}^2$ could only be the result of variation of the turbulence level along the path. The increase in the turbulent fluctuation intensity led simultaneously to an increase in the dispersion of the fluctuation intensity $\sigma_{\chi_R}^2$ and to a decrease in the coherence radius r_0. The decrease in the coherence radius r_0 in itself causes a decrease in the correction efficiency for a fixed space–time resolution of the adaptive system. A comparison of the Russian and American results (see Fig. 15) showed that the results of numerical calculations [192] and the data of a natural experiment [198] agree well with each other.

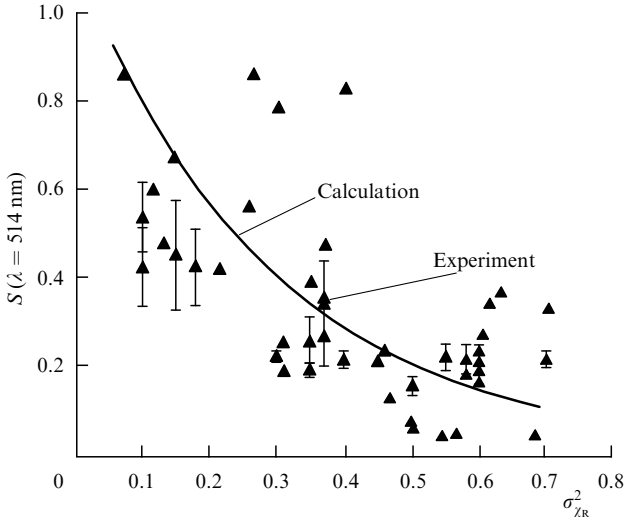

Figure 15. Comparison of calculated and experimental dependences of the Strehl parameter S on the variance of fluctuations of the spherical wave amplitude logarithm $\sigma_{\chi_R}^2$.

6.5 Amplitude–phase control based on linear systems

Application of AO for distortion correction in the course of laser beam formation in a turbulent medium was further developed in connection with the application of double-reflector corrections. This was associated with the attempt to use two active mirrors to reproduce amplitude–phase control and, in fact, reconstruct the reversed wavefront. Approaches to the application of adaptive systems in which several active mirrors correct spatially separated inhomogeneities were known earlier [178–180, 199].

A new approach to the amplitude–phase control using several active controllable mirrors has been proposed [200–204]. It is based on creating a required amplitude–phase profile with an adaptive system including at least two mirrors separated by a fixed-length spacing in which an optical wave propagates without distortions. The first mirror acts on a laser beam to generate some changes in the beam phase. In the course of propagation in free space, these phase variations cause variations in the beam amplitude. Next, the second mirror is located. In the plane of the second mirror, amplitude fluctuations in the beam distribution already appear, caused by beam diffraction in the course of propagation, i.e., the required distribution of the light field intensity in the beam is attained. For a given intensity variation, the second mirror introduces the required phase changes. As a result, the beam with a given distribution of amplitude and phase profiles is formed. In this scheme, the main difficulty is to specify the phase profile that provides formation of the required amplitude distribution [202–204].

The compensation of turbulent distortions of coherent radiation was studied based on the developed algorithm. As a result, the efficiency of double-reflector correction was comparable to the efficiency of purely phase control (Fig. 16).

We can conclude that the proposed method [200] of amplitude–phase control does not guarantee absolute compensation of the distributed turbulent lens, but the obtained values of the energy focusing effect are higher than those obtained in a purely phase control. Thus, the possibility is shown of obtaining the amplitude–phase correction using two phase correctors.

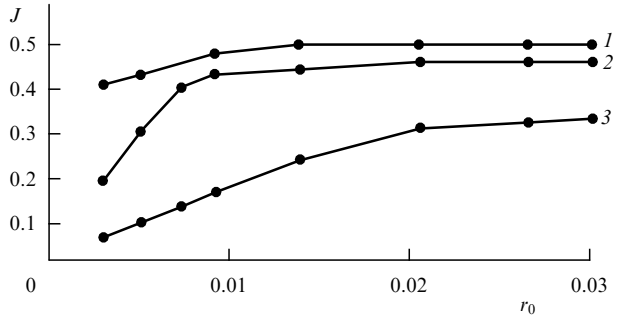

Figure 16. Dependence of the amount (fraction) of energy J within the diffraction spot on the turbulent distortion intensity. On the abscissa are the values of the coherence radius r_0 normalized to the initial beam size a. The Fresnel number of the propagation path is equal to $ka^2/L = 2$. Curves: *1* — correction by a system with two mirrors, *2* — correction based on phase conjugation, *3* — without control.

6.6 Adaptive optics systems for high-power laser systems

In recent years, in different countries in the world, interest in the studies of wavefronts of high-power pulsed solid-state laser radiation has continued to increase. This type of laser with petawatt radiation power and supershort pulses allows solving present-day problems of fundamental research related to the interaction of superstrong (exceeding interatomic) electromagnetic fields with matter. In particular, these are the latest problems of thermonuclear fusion, atomic and relativistic physics, astrophysics, and even medicine. Projects of many countries are aimed at the development of such systems, in particular, the systems National Ignition Facility (USA), Laser MegaJoule (France), Extreme Light Infrastructure (European Union), Shenguang (China), and Luch (Beam) (Russia). In recent years, such systems were being rapidly developed. Modern femtosecond titanium–sapphire lasers (800 nm) have a radiation power of several hundred terawatts and the peak intensity 10^{22} W cm^{-2} in the focused beam [205, 206].

Further development of these systems typically stems from the tendency to focus radiation onto a spot close to the diffraction limit in size, which is only possible after elimination of wavefront distortions. The use of AO for correcting lasing wavefront aberrations in static conditions helps heighten the quality of high-power pulsed laser beams used to study the interaction between laser radiation and matter (see, e.g., [207, 208]).

Examples are known of the use of AO systems for enhancing the radiation focusing quality in supershort-pulsed lasers created for fundamental research in high-energy physics. For example, in titanium–sapphire lasers (Ti : Al_2O_3) with 8 TW radiation pulses, a power density of 4×10^{19} W cm^{-2} in the focal plane was obtained, and in a neodymium laser with the 100 J pulse energy and duration of 0.6 ns, the Strehl parameter was increased from 0.1 to 0.6 owing to an AO system.

An increase in the efficiency of modern AO systems will substantially widen the range of problems to be solved in high-power laser radiation transport for the purposes of location, communication, and optical processing of information. Among modern AO system requirements [209], two aspects play an important role. The first is the achievement of the high accuracy of phase correction with allowance for the specificities of spatial distortions of the radiation wavefront, e.g., in a turbulent atmosphere. The second is the necessity of ensuring phase correction of a laser beam in dynamics, i.e., the system must have time to trace the radiation phase variations and correct them in time.

At the Institute of Laser Physics Research Russian Federal Nuclear Center — All-Russia Scientific Research Institute of Experimental Physics, very promising results were obtained on phase correction [210–213] of pulsed and continuous laser radiation by AO systems operating in a closed loop with the help of flexible deformable mirrors. Aberrations of a beam from the high-power pulsed laser setup Luch (Beam) were decreased by an order of magnitude using a standard AO system with a Shack–Hartmann-type wavefront sensor and an adaptive mirror with a 220×220 mm^2 aperture. Notably, an adaptive optical system [213] with closed feedback based on the phase conjugation algorithm and including a deformable bimorph mirror and a Shack–Hartmann-type wavefront sensor has been developed and tested.

Figure 17 presents the experimentally obtained [213] distributions of the energy density of output radiation in the far zone before and after the correction. Their analysis shows that phase correction leads to a decrease in divergence (at the level of 80% energy) by a factor of four, from 4×10^{-4} rad to 1×10^{-4} rad. We note that close values were obtained after correction using the Laser MegaJoul setup (France) [214] having an adaptive mirror with actuators of a similar geometry which were, however, smaller in number (39). The WFS had 64×64 subapertures.

An application of AO systems is known [213] where the adaptive mirror is controlled not by wavefront measurements but by seeking the extremum of the selected objective function with the help of a stochastic parallel gradient algorithm [215]. The use of microcontrollers in the control units allows reaching the bandwidth of 5 kHz and demonstrating the dynamic phase correction of tilts and higher wavefront aberrations due to turbulence.

6.7 Application of adaptive optics in military laser projects

Since the very first day that the laser was created, projects have come forth aimed at its use for military purposes. In the 1980s, work on the design of prospective ground-based, airborne, and cosmic laser weapon systems was intensely developed. The constructed laser systems are simultaneously systems of protection from tactical missiles and systems to knock out ballistic missiles on the active part of their flight trajectories. The possible operative range of these systems is 50 to 500 km. A qualitative distinction in the task of hitting ballistic missiles, for instance, using airborne carriers is the presence of a very extended atmospheric region for laser beam propagation. Clearly, laser beam passage through the atmosphere along such an extended path is limited by cloudiness,

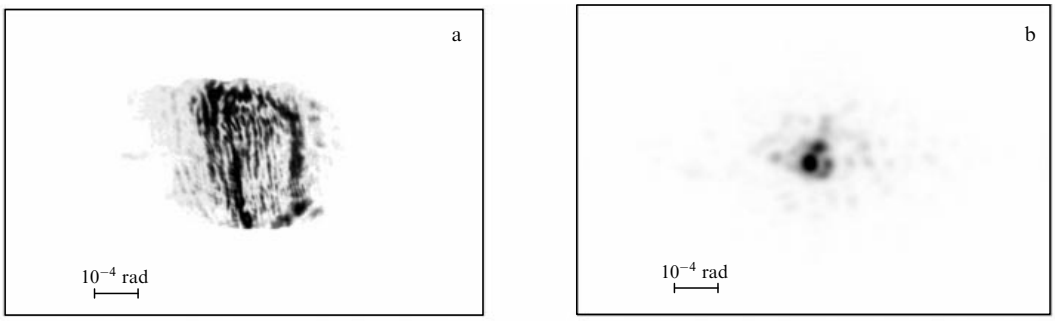

Figure 17. Distributions of the output radiation energy density in the far region (a) without correction and (b) as a result of correction.

atmospheric refraction, and turbulence. Undoubtedly, this leads designers of such systems to use AO elements in their composition.

About 10 years ago, military research [216, 217] pointed to the advantage of the use for military purposes of precisely chemical lasers, because the weapon should be mobile, and chemical fuels contain more energy per kg of weight than electric batteries. As an example, we can mention the American Airborne Laser program and the American–Israeli Nautilus project, which represent a new concept of a regional BMD system.

The Nautilus project was aimed at hitting missiles and projectiles using laser radiation. When tested at the White Sands rocket installation, the American–Israeli tactical high-energy laser based on an HF–DF (deuterium–fluoride) laser radiation source was placed on five trailers.

The most ambitious project today is the American Airborne Laser exploiting a megawatt-class laser positioned aboard an airplane to counter enemy ballistic missiles. This project in its current version has been in development since 1996. The main contractor is the Boeing Company, which, in designing the aerocarrier, significantly modified the cargo version of a Boeing 747-400F. The Northrop Grumman Corporation is responsible for developing the laser itself. The allotment for laser development has already reached 6.7 billion dollars. After the bench tests had been completed in 2004, the air tests began. In the Airborne Laser project, a chemical iodine–oxygen laser is used. Several reagents are simultaneously fed into the reaction chamber. At first, liquid hydrogen peroxide is sprayed in the chamber, and then potassium hydroxide and gaseous chlorine are added. The reagent interaction generates extremely active singlet delta-oxygen, which, when interacting with gaseous iodine, ionizes it. Returning to the normal state, the iodine atom emits a photon with a wavelength of 1.315 μm.

The aim of the project is to design a system capable of transporting such a power density of laser radiation to a remote target that would quickly heat the target to a high temperature. Along with the main laser, the system contains many auxiliary systems, from infrared sensors recording missile launches to several relatively low-power solid-state lasers for 'impact'-beam aiming, i.e., for the creation of a reference source on the target and determination of the atmospheric parameters. The airborne system includes an adaptive system, an ATR system of hunt, tracking, and designation of the target. Altogether, four lasers will be used in the airborne system, namely, HEL, a high-energy (megawatt class) chemical iodine–oxygen laser; TILL, an erbium glass (kilowatt class) laser for target illumination through a nose output opening; BILL, a neodymium glass laser for receiving signals from the atmosphere for creation of a reference source; and an ARS (CO_2) laser with a power of about 200 W for obtaining information on the distance and direction. The control system has six infrared measuring devices and tracking sensors; operation in the passive regime and operation within a sphere of 360 degrees are possible, in particular, for starting-rocket flame detection.

The creators of this system implied that such a laser weapon system must operate in the absence of cloudiness on the radiation path. Therefore, in order not to deal with clouds seriously obstructing the radiation, the laser weapon should be placed at an altitude of 12–15 km. Then, at the middle and high latitudes, clouds would be practically absent; but for subequatorial regions, clouds can be encountered up to altitudes of 20 km. The Boeing-747 airplane, which is chosen as a carrier, is certified for flights at altitudes up to 13.7 km. The B-52 bomber (which was earlier planned to be used as the carrier of such a system) can fly a little higher, and supersonic TU-144 airplanes, The Concord, and the U-2 reconnaissance aircraft can fly steadily up to altitudes of 20 km.

To control the atmospheric turbulence effects in the Airborne Laser system, an adaptive phase correction by the PC algorithm was planned using the signal reflected from the target as a reference. The progress achieved in this field to date is quite modest. Several systems of active and adaptive correction are known to have been constructed [216, 217]. The first adaptive system involves a deformable mirror with 69 actuators, a Hartmann WFS in the form of a 9×9 matrix of subapertures. The second adaptive system, BCDM, includes a deformable mirror with 256 actuators, a WFS in the form of an 18×18 element matrix, and a silicon photo receiver. The WFS must work at two wavelengths, 1.064 μm and 1.315 μm, the active mirror ensuring reconstruction in the range of ± 4 wavelengths.

It is known that in the USA, in the period from 1999 to 2003, the experimental program ABL-ACT (Air-borne Laser Advanced Concepts Test-Bed) was being implemented with the goal to work out the algorithms of operation of an adaptive system for transporting the energy of a high-power laser to a target in the atmosphere at a distance of up to 50 km. The points of transmission and reception of optical radiation were positioned on two mountain peaks — Salinas Peak and North Oscura — at the elevation of nearly 2000 m. At scientific conferences in the period from 1999 to 2001 [218, 219], it was reported that at these peaks, a special test bench had been arranged for ground-based development of detailed salient features of AO system operation for ABL. Because the effects of 'strong' fluctuations were expected on extensive atmospheric paths, investigations were started on the application of amplitude–phase correction. This was stimulated first and foremost by the work of Russian authors [192, 200, 202], and later such studies appeared in the USA [201]. The authors of [218] clearly declared that the new concept of AO application for the ABL system is connected with the use of two active mirrors for amplitude- and phase-distortion correction. The specificity of the whole ABL system is that its angle of isoplanatism described by formula (25) is less than the diffraction limit. Experiments according to the ABL-ACT program were first of all aimed at developing an adaptive system for atmospheric turbulence compensation. The task of the experiments was to analyze the possibilities of the system with respect to adaptive radiation focusing for three purposes: propagation to an immobile target, propagation of radiation to an airplane (a slowly moving target), and propagation of radiation to a missile (a rapidly moving target).

The ultimate image of the AO system in this program is a telescope with a 0.75 m mirror to illuminate a target located at one end of the path. At the opposite end of the atmospheric path is a tracking system designed on the basis of a 1.4 m telescope, and a radiating-laser-diode system is used as a reference source (beacon). Also mounted on the North Oscura peak is a gauge of dispersion of intensity fluctuations. Because of strong fluctuations on a path longer than 50 km, it was decided to create a new adaptive system, designed by the Optical Science Company (USA). It contains (according to the open press) a deformable mirror with 349 actuators (produced by the Xinetics Company, USA), a

Hartmann-type wavefront sensor with 16×16 apertures. Matching telescopes were fabricated by the Contraves Company, USA. Work on dynamic targets was started in 2000. Upon moving to work with a movable target, the requirements for the rate of the adaptive control system operation became much more strict.

In the calculations, the authors of [218, 219] proceeded from the fact that the radiation coherence radius was about 15 cm, the rms deviation of intensity fluctuations was 0.5, and the minimum AO system operation rate was more than 1000 Hz. Cameras with CCD matrices 128×128 pixels in size were used to design a wavefront sensor with 16×16 subapertures. The cameras were manufactured at the Lincoln Laboratory, USA. At the first stage, for work with a stationary target, the data acquisition frequency was 2.5 kHz and for work with a variable target, the data acquisition frequency was above 10 kHz. The new deformable mirror was manufactured by the Xinetics Company and had 349 actuators, while the computer used for calculations processed 2500 shots a second. The WFS operated according to the Hartmann scheme on the receiving 70 cm aperture. The authors note the importance of designing a phase reconstruction algorithm to be used in conditions of strong intensity fluctuations, i.e., with the occurrence of intensity zeros in the distribution.

The US Air Force also uses an iodine–oxygen laser in a project for the design of a tactical laser to be used aboard a C-130 transport airplane or on a large helicopter. A certain shortcoming of chemically pumped lasers is the toxicity of the applied reagents. For this reason, solid-state lasers are now somewhat more preferable and can in the near future meet the technical requirements at the level of the megawatt class of generated power. Already now, these lasers are ready to be a viable alternative to gas lasers in the 100 kW class. Moreover, the use of solid-state lasers leads to what military engineers call a 'deep artillery cellar', that is, the ability to go on sending laser pulses (i.e., to shoot) during longer periods of time. Two projects of solid-state lasers are now being worked on in USA. They are, first, a solid-state laser with a high-temperature active body being developed at the Livermore National Laboratory, USA, which is based on the slab-laser technology already used in industry. The designers note that a large unstable resonator with a single (separate) aperture is technologically sufficient to be used in carriers. As an alternative to this laser, being considered now is a lattice [220] of optical mode-locked lasers with output combined coherently into a single beam. The US Air Force distinguishes this particular approach for a military bomber designed by the Lockheed Martin Corporation. An obvious advantage of such mode-locked lasers consists in the use of extremely simple optics, high-efficiency pumping, single-mode yield, and simple technical solutions concerning optical fiber cooling.

6.8 Application of adaptive optics systems in medicine

Correcting laser radiation aberrations is urgent not only in laser physics and industrial technologies. For example, in ophthalmology, obtaining high-quality image resolutions on the retina is impossible without correction of optical aberrations of the patient's eye [221–224]. Therefore, contemporary fundus cameras are supplied with AO systems that compensate aberrations of the eye.

A fast and accurate measurement of eye aberrations enabled their correction by various phase modulators. The static correction of eye aberrations was first done in 1997 [221]; it was demonstrated that AO is capable of compensating eye aberrations virtually to the level of the diffraction limit. A flexible bimorph mirror capable of compensating both lower- and higher-order aberrations was used as a corrector. Correction of small-scale aberrations was shown to guarantee an unprecedented resolution of the eyeground, which was inaccessible with traditional correction methods such as glasses and contact lenses. Statistical correction was further realized by other types of phase correctors, such as phase plates [222] and liquid-crystal modulators [223]. However, for a more efficient correction, it was necessary to make a real-time aberration compensation, which was first done in 2001 [224]. A membrane mirror was used to correct aberrations. Eye aberrations were measured by a Shack–Hartmann wavefront sensor, and then the information on aberrations went to a computer used to calculate the control orders for the membrane mirror. The achieved level of aberration correction was unprecedented: the residual correction error did not exceed 0.1 μm. The successful application of bimorph mirrors for dynamic compensation of eye aberrations was demonstrated in 2002 [225]. The method of the isoplanatism zone extension was first applied for correction of axial and extra-axial aberrations of the human eye and for the first time these methods were shown to be capable of extending the region of high-quality imaging of the retina twofold [226, 227].

7. Conclusion

The construction of large modern OESs is known to be a rather long process, which customarily proceeds in the absence of comprehensive information on peculiarities of the medium of optical radiation propagation. But the latest OESs are fairly expensive because the corresponding calculations and evaluations of the efficiency of application of different kinds of algorithms and programs realized using modern AO techniques are required at the initial stage of their design, and, in addition, their construction lasts many years, and hence the main parameters of the system are necessarily modified. This dictates the construction of such systems with allowance for a possible change in their main parameters [228] at different stages of design and fabrication. The possibility of a flexible variation of the parameters of an optical system is currently one of the main requirements of modern engineering of optoelectronic equipment, and AO systems suggest such a possibility. This is first of all because the radical change in the main parameters of an optical system can only be provided by changing the algorithm of the AO system operation. On the way to creating optical systems, the unavoidable stages are system design and determination of the feasibility of their application in a real atmosphere. Each element of an optical system should be preliminarily calculated, and therefore not only the parameters of the adaptive optics but also the system as a whole often have to be calculated.

Both the theory and the AO systems themselves are being constantly developed. The problems of the formation of particular parameters and correction of laser radiation aberrations can be solved by different methods: using amplitude masks, holographic and diffraction elements, etc. However, all the abovementioned methods depend similarly on particular beam parameters in the presence of noises and aberrations in the optical system. Hence, the application of flexible mirrors whose parameters can be fitted to the varied

experimental conditions is the most universal from that standpoint.

In recent years, methods of laser radiation parameter control based on intracavity systems exploiting flexible active mirrors on the basis of hybrid algorithms allowing effective control over focusing, power, peak intensity, and the form of laser radiation field distribution have been developed rather intensely. The proposed methods of the extracavity hybrid algorithm of bimorph corrector control can be effectively used to correct aberrations and to form defined distributions of intensity of single-mode and multimode (in transverse indices) laser radiation in a given plane.

A new aspect of the problem, for example, is the generation and compensation of vortex optical beams by controlled phase elements allowing the formation of such beams [229, 230], for example, for laser communication systems and for compensation of their negative effect in problems of atmospheric optics.

We emphasize that in connection with widening the applicability limits of AO systems, topical issues of well-known journals are regularly published: a topical issue of the journal *Applied Optics* appeared in 1998 [231], and an issue of the journal *Avtometriya* [232] was devoted to the development of the elemental base of AO.

This work was supported in part by a grant from the program of joint research of NAS of Ukraine, SB RAS, and FTP Personnel of the Russian Ministry of Education and Science (contract 8877).

The author is grateful to the researchers of the Laboratory of Coherent and Adaptive Optics of the Zuev Institute of Atmospheric Optics, Siberian Branch, Russian Academy of Sciences for comprehensive help and support. The author regrets that because of the limited space of the review, he could not present some important and interesting results; he agrees in advance with a possible reader opinion that the way of submitting information and the style of presentation of the subject largely reflect the scientific interests of the author himself.

References

1. Babcock H W *Publ. Astron. Soc. Pacific* **65** 229 (1953)
2. Linnik V P *Opt. Spektrosk.* **57** 401 (1957)
3. Tyson R K *Principles of Adaptive Optics* (Boston: Academic Press, 1991)
4. Hardy J W *Proc. IEEE* **66** 651 (1978)
5. Hardy J W, Feinlieb J, Wyant J C, in *Proc. Topical Meeting* (Boulder, CO: Univ. of Colorado, 1974)
6. Merkle F et al. *Messenger* **58** 1 (1989)
7. Tatarskii V I *Rasprostranenie Voln v Turbulentnoi Atmosfere* (Wave Propagation in a Turbulent Atmosphere) (Moscow: Nauka, 1967)
8. Gurvich A S et al. *Lazernoe Izluchenie v Turbulentnoi Atmosfere* (Laser Radiation in Turbulent Atmosphere) (Moscow: Nauka, 1976)
9. Strohbehn J W (Ed.) *Laser Beam Propagation in the Atmosphere* (Berlin: Springer-Verlag, 1978)
10. Fried D L *J. Opt. Soc. Am.* **56** 1380 (1966)
11. Labeyrie A *Astron. Astrophys.* **6** 85 (1970)
12. Fried D L *J. Opt. Soc. Am.* **55** 1427 (1965)
13. Greenwood D P *J. Opt. Soc. Am.* **67** 390 (1977)
14. Greenwood D P, Fried D L *J. Opt. Soc. Am.* **66** 193 (1976)
15. Tatarskii V I *Radiophys. Quantum Electron.* **24** 590 (1981); *Izv. Vyssh. Uchebn. Zaved. Radiofiz.* **24** 861 (1981)
16. Lukin V P, Charnotskii M I *Sov. Phys. J.* **28** 894 (1985); *Izv. Vyssh. Uchebn. Zaved. Fiz.* **28** (11) 51 (1985)
17. Lukin V P *Atmospheric Adaptive Optics* (Bellingham, Wash.: SPIE, 1995); Translated from Russian: *Atmosfernaya Adaptivnaya Optika* (Novosibirsk: Nauka, 1986)
18. *J. Opt. Soc. Am.* **67** (3) (1977), Special issue on adaptive optics
19. *J. Opt. Soc. Am. A* **11** (2) (1994), Special issue on adaptive optics
20. Vorontsov M A, Shmal'gauzen V I *Printsipy Adaptivnoi Optiki* (Principles of Adaptive Optics) (Moscow: Nauka, 1985)
21. Vorontsov M A, Koryabin A V, Shmal'gauzen V I *Upravlyaemye Opticheskie Sistemy* (Controlled Optical Systems) (Moscow: Nauka, 1988)
22. Luk'yanov D P, Kornienko A A, Rudnitskii B E *Opticheskie Adaptivnye Sistemy* (Optical Adaptive Systems) (Moscow: Radio i Svyaz', 1989)
23. Taranenko V G, Shanin O I *Adaptivnaya Optika* (Adaptive Optics) (Moscow: Radio i Svyaz', 1990)
24. Kurmaeva A Kh, Shevchenko V S (Exec. Ed.) *Atmosfernaya Nestabil'nost' i Adaptivnyi Teleskop* (Atmospheric Instability and Adaptive Telescope) (Leningrad: Nauka, 1988)
25. *Sov. Phys. J.* **28** (11) (1985), Topical issue "Atmospheric adaptive optics"; *Izv. Vyssh. Uchebn. Zaved. Fiz.* **28** (11) (1985), Tematicheskii vypusk "Atmosfernaya adaptivnaya optika"
26. *Atmospheric Opt.* **3** (12) (1990), Topical issue "Atmospheric adaptive optics"; *Opt. Atmos.* **3** (12) (1990), Tematicheskii vypusk "Atmosfernaya adaptivnaya optika"
27. *Atmospheric Opt.* **4** 855 (1991), Topical issue "Atmospheric adaptive optics"; *Opt. Atmos.* **4** (12) (1991), Tematicheskii vypusk "Atmosfernaya adaptivnaya optika"
28. *Atmospheric Opt.* **5** (12) (1992), Topical issue "Atmospheric adaptive optics"; *Opt. Atmos.* **5** (12) (1992), Tematicheskii vypusk "Atmosfernaya adaptivnaya optika"
29. *Atmospheric Opt.* **6** (12) (1993), Topical issue "Atmospheric adaptive optics"; *Opt. Atmos.* **6** (12) (1993), Tematicheskii vypusk "Atmosfernaya adaptivnaya optika"
30. *Atmospheric Ocean. Opt.* **8** 151 (1995), Topical issue "Atmospheric adaptive optics"; *Opt. Atmos. Okeana* **8** 172 (1995), Tematicheskii vypusk "Atmosfernaya adaptivnaya optika"
31. Belkin N D, Kasperskii V B, Sychev V V *J. Opt. Technol.* **61** 175 (1994); *Opt. Zh.* **61** (3) 5 (1994)
32. Es'kov D N et al. *J. Opt. Technol.* **62** 669 (1995); *Opt. Zh.* **62** (10) 13 (1995)
33. Lukin V P, Fortes B V *Opt. Atmos. Okeana* **9** 1492 (1996)
34. Sychev V V *Adaptivnye Opticheskie Sistemy v Krupnogabaritnom Teleskopostroenii* (Adaptive Optical Systems in Bulky Telescope-building) (Staryi Oskol: Ltd. 'TNT' 2005)
35. Rytov S M, Kravtsov Yu A, Tatarskii V I *Principles of Statistical Radiophysics* Vol. 3 *Elements of Random Fields* (Berlin: Springer-Verlag, 1989); Translated from Russian: *Vvedenie v Statisticheskuyu Radiofiziku* Pt. 2 *Sluchainye Polya* (Introduction to Statistical Radio Physics. Pt. 2 Random Fields) (Moscow: Nauka, 1978)
36. Lukin V P, Charnotskii M I *Sov. J. Quantum Electron.* **12** 602 (1982); *Kvantovaya Elektron.* **9** 952 (1982)
37. Bespalov V I (Exec. Ed.) *Obrashchenie Volnovogo Fronta Opticheskogo Izlucheniya v Nelineinykh Sredakh* (Optical Radiation Wavefront Reversal in Nonlinear Media) (Gorky: IPF, 1979)
38. Bespalov V I (Exec. Ed.) *Obrashchenie Volnovogo Fronta Izlucheniya v Nelineinykh Sredakh* (Optical Radiation Wavefront Reversal in Nonlinear Media) (Gorky: IPF, 1982)
39. Zel'dovich B Ya, Pilipetsky N F, Shkunov V V *Principles of Phase Conjugation* (Berlin: Springer-Verlag, 1985); Translated from Russian: *Obrashchenie Volnovogo Fronta* (Wavefront Reversal) (Moscow: Nauka, 1985)
40. Bespalov V I, Pasmanik G A *Nonlinear Optics and Adaptive Laser Systems* (Commack, NY: Nova Sci. Publ., 1994); Translated from Russian: *Nelineinaya Optika i Adaptivnye Lazernye Sistemy* (Moscow: Nauka, 1986)
41. Dmitriev V G *Nelineinaya Optika i Obrashchenie Volnovogo Fronta* (Nonlinear Optics and Wavefront Reversal) (Moscow: Fizmatlit, 2003)
42. Zuev V E, Konyaev P A, Lukin V P *Sov. Phys. J.* **28** 859 (1985); *Izv. Vyssh. Uchebn. Zaved. Fiz.* **28** (11) 6 (1985)
43. Bakut P A et al. *Zarubezh. Radioelektron.* (11) 3 (1978)
44. Lukin V P *Sov. J. Quantum Electron.* **11** 1311 (1981); *Kvantovaya Elektron.* **8** 2145 (1981)
45. Lukin V P, Matyukhin V F *Sov. J. Quantum Electron.* **13** 1604 (1983); *Kvantovaya Elektron.* **10** 2465 (1983)

46. Hardy J W *Adaptive Optics for Astronomical Telescopes* (New York: Oxford Univ. Press, 1998)
47. Muller R A, Buffington A *J. Opt. Soc. Am.* **64** 1200 (1974)
48. Noll R J *J. Opt. Soc. Am.* **66** 207 (1976)
49. Noll R J *J. Opt. Soc. Am.* **68** 139 (1978)
50. Valley G C, Wandzura S M *J. Opt. Soc. Am.* **69** 712 (1979)
51. Wang J Y, Markey J K *J. Opt. Soc. Am.* **68** 78 (1978)
52. Wang J Y, Silva D E *Appl. Opt.* **19** 1510 (1980)
53. Geary J M *Introduction to Wavefront Sensors* (Tutorial Texts in Optical Engineering, Vol. TT 18) (Bellingham, Wash.: SPIE Opt. Eng. Press, 1995)
54. Botygina N N, Emaleev O N, Konyaev P A, Lukin V P *Measurement Sci. Rev.* **10** (3) 101 (2010)
55. Roddier F *Appl. Opt.* **27** 1223 (1988)
56. Ragazzoni R *J. Mod. Opt.* **43** 289 (1996)
57. Védrenne N et al. *J. Opt. Soc. Am. A* **24** 2980 (2007)
58. Gonsalves R A *Opt. Eng.* **21** 829 (1982)
59. Hudgin R H *J. Opt. Soc. Am.* **67** 375 (1977)
60. Fried D L *J. Opt. Soc. Am.* **67** 370 (1977)
61. Cubalchini R *J. Opt. Soc. Am.* **69** 972 (1979)
62. Herrmann J *J. Opt. Soc. Am.* **71** 989 (1981)
63. Takajo H, Takahashi T *J. Opt. Soc. Am. A* **5** 1818 (1988)
64. Takajo H, Takahashi T *J. Opt. Soc. Am. A* **5** 416 (1988)
65. Lukin V P, Fortes B V *Adaptive Beaming and Imaging in the Turbulent Atmosphere* (Bellingham, Wash.: SPIE Press, 2002); Translated from Russian: *Adaptivnoe Formirovanie Puchkov i Izobrazhenii v Atmosfere* (Novosibirsk: Izd. SO RAN, 1999)
66. Lukin V P, Kanev F Yu, Konyaev P A, Fortes B V *Opt. Atmos. Okeana* **8** 409 (1995)
67. Kudryashov A V, Tikhonov V A, Shmal'gauzen V I *Opt. Atmos.* **1** (3) 61 (1988)
68. Madec P-Y *Proc. SPIE* **8447** 844705 (2012)
69. Alikhanov A N et al. *Lazerno-opticheskie Sistemy i Tekhnologii* (Laser Optical Systems and Technologies) (Moscow: FSUE SPA 'Astrofizika', 2009)
70. Loktev M, Soloviev O, Vdovin G *Adaptive Optics Guide* (Delft, The Netherlands: OKO Technologies, 2008)
71. Cornelissen S, SPIE Newsroom, 19 December (2011)
72. Vorob'ev V V *Radiotekh. Elektron.* **11** 2334 (1981)
73. Kandidov V P, Larionova I V, Popov V P *Opt. Atmos.* **2** 836 (1989)
74. *Adaptive Optics Lincoln Laboratory J.* **5** (1) (1992), Special issue
75. Zarubin P V *Quantum Electron.* **32** 1048 (2002); *Kvantovaya Elektron.* **32** 1048 (2002)
76. Gebhardt F G *Appl. Opt.* **15** 1479 (1976)
77. Gebhardt F G, Smith D C *Appl. Opt.* **11** 244 (1972)
78. Gebhardt F, Smith D C *IEEE J. Quantum Electron.* **7** 63 (1971)
79. Bradley L C, Herrmann J *J. Opt. Soc. Am.* **61** 668 (1971)
80. Ulrich P B, Hayes J N, Aitken A H *J. Opt. Soc. Am.* **62** 298 (1972)
81. Bradley L C, Herrmann J *Appl. Opt.* **13** 331 (1974)
82. Lukin V P *Sov. J. Quantum Electron.* **7** 522 (1977); *Kvantovaya Elektron.* **4** 923 (1977)
83. Fleck J A, Morris J R, Feit M D *Appl. Phys.* **10** 129 (1976)
84. Agrovskii B S et al. *Sov. J. Quantum Electron.* **8** 765 (1978); *Kvantovaya Elektron.* **5** 1341 (1978)
85. Konyaev P A, in *Tezisy Dokladov V Vsesoyuz. Simpoziuma po Rasprostraneniyu Lazernogo Izlucheniya v Atmosfere* (Theses of Proc. of the Vth All-Union Symp. on Laser Radiation Propagation in Atmosphere) (Tomsk: IOA SO AN SSSR, 1979)
86. Konyaev P A, in *Tezisy Dokladov VII Vsesoyuz. Simpoziuma po Rasprostraneniyu Lazernogo Izlucheniya v Atmosfere* (Theses of Proc. of the Vth All-Union Symp. on Laser Radiation Propagation in Atmosphere) (Tomsk: IOA SO AN SSSR, 1983)
87. Vorontsov M A, Chesnokov S S *Radiophys. Quantum Electron.* **22** 917 (1979); *Izv. Vyssh. Uchebn. Zaved. Radiofiz.* **22** 1318 (1979)
88. Vysloukh V A, Egorov K D, Kandidov V P *Radiophys. Quantum Electron.* **22** 299 (1979); *Izv. Vyssh. Uchebn. Zaved. Radiofiz.* **22** 434 (1979;
89. Konyaev P A, Lukin V P *Sov. Phys. J.* **26** 173 (1983); *Izv. Vyssh. Uchebn. Zaved. Fiz.* **9** (2) 79 (1983)
90. Buckley R *J. Atmos. Terr. Phys.* **37** 1431 (1975)
91. Kandidov V P, Ledenev V I *Radiophys. Quantum Electron.* **24** 301 (1981); *Izv. Vyssh. Uchebn. Zaved. Radiofiz.* **24** 438 (1981)
92. Martin J M, Flatte S M *Appl. Opt.* **27** 2111 (1988)
93. Bykov V V *Tsifrovoe Modelirovanie v Statisticheskoi Radiotekhnike* (Digital Simulation in Statistical Radio Engineering) (Moscow: Sovetskoe Radio, 1971)
94. Collins S A (Jr), Duncan D D *J. Opt. Soc. Am.* **65** 1218 (1975)
95. Duncan D D, Collins S A (Jr) *J. Opt. Soc. Am.* **65** 1232 (1975)
96. Telpukhovskii I E, Chesnokov S S *Opt. Atmos.* **4** 1294 (1991)
97. Fortes B V, Lukin V P *Proc. SPIE* **1668** 477 (1992)
98. Lukin V P et al. *J. Opt. Soc. Am. A* **11** (2) 903 (1994)
99. Konyaev P A, PhD Thesis of Physical and Mathematical Sciences (Tomsk: Tomsk State Univ., 1984)
100. Vorob'ev V V *Teplovoe Samovozdeistvie Lazernogo Puchka v Atmosfere*: *Teoriya i Model'nyi Eksperiment* (Thermal Self-action of a Laser Beam in Atmosphere: Theory and Model Experiment) (Moscow: Nauka, 1987)
101. Kandidov V P *Phys. Usp.* **39** 1243 (1996); *Usp. Fiz. Nauk* **166** 1309 (1996)
102. Moore G E *Proc. SPIE* **2437** 2 (1995)
103. Bolbasova L A, Konyaev P A, Lukin V P, in *Real Time Control for Adaptive Optics, Intern. Workshop, ESO, Garching, Germany, December 4–5, 2012*
104. Boreskov A V *Osnovy Raboty s Tekhnologiei CUDA* (Basic Elements of Work with CUDA Technology) (Moscow: DMK Press, 2010)
105. Troung T et al. *Proc. SPIE* **7015** 701531 (2008)
106. Konyaev P A, Tartakovskii E A, Filimonov G A *Atmos. Ocean. Opt.* **24** 425 (2011); *Opt. Atmos. Okeana* **24** 359 (2011)
107. Dudorov V V, Kolosov V V, Filimonov G A *Izv. Tomskogo Politekh. Univ.* **309** (8) 85 (2006)
108. Konyaev P A *Opt. Atmos. Okeana* **25** 948 (2012)
109. Daukantas P *Opt. Photon. News* **18** (9) 28 (2007)
110. Shcheglov P V *Problemy Opticheskoi Astronomii* (Problems of Optical Astronomy) (Moscow: Nauka, 1980)
111. Davies R, Kasper M *Annu. Rev. Astron. Astrophys.* **50** 305 (2012)
112. Lukin V P, Mayer N N, Fortes B V *Atmos. Ocean Opt.* **5** 941 (1992); *Opt. Atmos.* **5** 1241 (1992)
113. Vitrichenko E A, Voitsekhovich V V, Mishchenko M I "Otsenka uglovogo polya zreniya adaptivnogo teleskopa" ("Estimation of the angular field of vision of an adaptive telescope"), Preprint No. 790 (Moscow: Space Research Institute of the USSR Academy of Sciences, 1983)
114. Vitrichenko E A, Mishchenko M I "Otsenka radiusa polya izoplanatizma adaptivnykh sistem po kriteriyu Mareshalya' ("Estimation of isoplanatism field radius in adaptive systems by the Marechal criterion"), Preprint No. 810 (Moscow: Space Research Institute of the USSR Academy of Sciences, 1983)
115. Lukin V P *Opt. Atmos. Okeana* **5** 1294 (1992)
116. Vernin J, Azouit M *J. Opt.* **14** 131 (1983)
117. Wilson R W *Mon. Not. R. Astron. Soc.* **337** 103 (2002)
118. Tokovinin A et al. *Mon. Not. R. Astron. Soc.* **343** 891 (2003)
119. Antoshkin L V et al. *Opt. Atmos.* **2** 621 (1989)
120. Sarazin M, Roddier F *Astron. Astrophys.* **227** 294 (1990)
121. Martin F et al. *Astron. Astrophys.* **336** L49 (1998)
122. Nosov V V et al. *Proc. SPIE* **7296** 82 (2008)
123. Lukin V P *J. Opt. Soc. Am. A* **27** A216 (2010)
124. Lukin V P, Pokasov V V *Appl. Opt.* **20** 121 (1981)
125. Good R E et al. *Proc. SPIE* **928** 165 (1988)
126. McKechnie T S *J. Opt. Soc. Am. A* **9** 1937 (1992)
127. Lukin V P *Opt. Atmos. Okeana* **5** 354 (1992)
128. Lukin V P *Opt. Atmos. Okeana* **6** 1102 (1993)
129. Voitsekhovich V V, Cuevas S *J. Opt. Soc. Am. A* **12** 2523 (1995)
130. Kasper M *Proc. SPIE* **8447** 8447OB (2012)
131. Wizinowich P *Proc. SPIE* **8447** 8447OD (2012)
132. Shustov B M *Zemlya Vselennaya* (5) 3 (2006)
133. Ardeberg A, Andersen T *EURO50*: *A European 50M Adaptive Optics Extremely Large Telescope* (Berlin: Springer, 2006)
134. Roddier F "Effects of atmospheric turbulence in astronomy", in *Progress in Optics* Vol. 19 (Ed. E Wolf) (Amsterdam: Elsevier, 1981) p. 281
135. Michau V, Rousset G, Fontanella J C, in *Proc. of the Workshop on Real Time and Post Facto Solar Image Correction, NSO Sacramento Peak, USA, 15–18 September 1992*
136. Ricort G et al. *Solar Phys.* **69** 223 (1981)

137. Rutten R J, Hammersclag R H, Bettonvil F C M, in *Proc. THEMIS Forum "Science with THEMIS", France, Observatoire de Paris at Meudon, 1997*
138. von der Luehe O *Adv. Space Res.* **11** 275 (1991)
139. Acton D S, Smithson R C *Appl. Opt.* **31** 3161 (1992)
140. von der Luhe O et al. *Astron. Astrophys.* **224** 351 (1989)
141. Scharmera B G et al. *Proc. SPIE* **4853** 370 (2002)
142. Didkovsky L V et al. *Proc. SPIE* **4853** 630 (2002)
143. Rimmele T R *Proc. SPIE* **5490** 549004 (2004)
144. Rimmele T R et al. *Proc. SPIE* **5901** 5901 (2005)
145. Antoshkin L V et al. *Opt. Atmos. Okeana* **15** 1027 (2002)
146. Lukin V P et al. *J. Opt. Technol.* **73** 197 (2006); *Opt. Zh.* **73** (3) 55 (2006)
147. Lukin V P et al. *Proc. SPIE* **6272** 62725I (2006)
148. Lukin V P et al. *Solnechno-Zemnaya Fiz.* (12) 74 (2008)
149. Lukin V P et al. *Proc. SPIE* **8447** 84476E (2012)
150. Clare R M, Ellerbroek B L *J. Opt. Soc. Am. A* **23** 418 (2006)
151. Lukin V P *Quantum Electronics* **10** 727 (1980); *Kvantovaya Elektron.* **7** 1270 (1980)
152. Foy R , Labeyrie A *Astron. Astrophys.* **152** L29 (1985)
153. Tallon M, Foy R *Astron. Astrophys.* **235** 549 (1990)
154. Lukin V P, in *Proc. of the ICO-16 Satellite Conf. on Active and Adaptive Optics* (ESO Conf. and Workshop Proc., No. 48) (1993) p. 521
155. Fugate R Q *Opt. Photon. News* **4** (6) 14 (1993)
156. Banakh V A, Mironov V L *Lidar in a Turbulent Atmosphere* (Boston: Artech House, 1987); Translated from Russian: *Lokatsionnoe Rasprostranenie Lazernogo Izlucheniya v Turbulentnoi Atmosfere* (Novosibirsk: Nauka, 1986)
157. Orlov V M et al. *Elementy Teorii Svetorasseyaniya i Opticheskaya Lokatsiya* (Elements of the Light Scattering Theory and Optical Location) (Novosibirsk: Nauka, 1982)
158. Tatarskii V I, Ishimaru A, Zavorotny V U (Eds) *Wave Propagation in Random Media* (*Scintillations*), *Intern. Conf., Univ. of Washington, Seattle, USA, 1992* (Bellingham, Wash.: SPIE, 1993)
159. Gavel D *Proc. SPIE* **7015** 70150J (2008)
160. Hankla A K et al. *Proc. SPIE* **6272** 62721G (2006)
161. Thompson L, Gardner C *Nature* **328** 229 (1987)
162. Bonaccini D et al., in *Workshop on Laser Technology and Systems for Astronomy, 2006*
163. Fried D L *J. Opt. Soc. Am. A* **12** 939 (1995)
164. Foy R et al. *Astron. Astrophys. Suppl.* **111** 569 (1995)
165. Ragazzoni R *Astron. Astrophys.* **305** L13 (1996)
166. Lukin V P *Adaptive Opt. Tech. Digest Ser.* **13** 35 (1996)
167. Lukin V P *Opt. Atmos. Okeana* **8** 301 (1995)
168. Belen'kii M S *Proc. SPIE* **2471** 289 (1995)
169. Lukin V P, Fortes B V *Opt. Atmos. Okeana* **10** 34 (1997)
170. Milonni P W, Fugate R Q, Telle J M *J. Opt. Soc. Am. A* **15** 217 (1998)
171. Ragazzoni R, Marchetti E, Valente G *Nature* **403** 54 (2000)
172. Gavel D et al. *Proc. SPIE* **7015** 701511 (2008)
173. Roberts E, Bouchez A H, Angione J *Proc. SPIE* **7015** 70152S (2008)
174. Yutaka H, Hideki T, Olivier G *Proc. SPIE* **7015** 701510 (2008)
175. Femania B *J. Opt. Soc. Am. A* **22** 2719 (2005)
176. Bol'basova L A, Lukin V P *Proc. SPIE* **6747** 67470M (2007)
177. Bol'basova L A, Lukin V P, Nosov V V *Opt. Spectrosc.* **107** 993 (2009); *Opt. Spektrosk.* **107** 833 (2009)
178. Milton N M, Lloyd-Hart M, Baranec C *Proc. SPIE* **7015** 701522 (2008)
179. Rabien S et al. *Proc. SPIE* **7015** 701515 (2008)
180. Clénet Y et al. *Proc. SPIE* **7015** 701529 (2008)
181. Kolosov V V, Sysoev S I *Opt. Atmos.* **3** 83 (1990)
182. Wallace J, Pasciak J *J. Opt. Soc. Am.* **65** 1257 (1975)
183. Bradley L C, Herrmann J *Appl. Opt.* **13** 331 (1974)
184. Herrmann J *J. Opt. Soc. Am.* **65** 1212 (1975)
185. Dunphy J R, Smith D C *J. Opt. Soc. Am.* **67** 295 (1977)
186. Karr T J *Proc. SPIE* **1060** 120 (1989)
187. Akhmanov S A et al. *Radiophys. Quantum Electron.* **23** 1 (1980); *Izv. Vyssh. Uchebn. Zaved. Radiofiz.* **23** 1 (1980)
188. Vasil'ev F P, Vorontsov M A, Litvinova O A *USSR Comput. Math. Math. Phys.* **19** 272 (1979); *Zh. Vychisl. Matem. Matem. Fiz.* **19** 1053 (1979)
189. Herrmann J *J. Opt. Soc. Am.* **67** 290 (1977)
190. Konyaev P A *Opt. Atmos. Okeana* **5** 1261 (1992)
191. Konyaev P A, Lukin V P, Mironov V L *Izv. Akad. Nauk SSSR. Ser. Fiz.* **49** 536 (1985)
192. Lukin V P, Fortes B V *Opt. Atmos. Okeana* **8** 435 (1995)
193. Vorontsov M A *Sov. J. Quantum Electron.* **9** 1221 (1979); *Kvantovaya Elektron.* **6** 2078 (1979)
194. Vorontsov M A, Chesnokov S S *Radiophys. Quantum Electron.* **22** 917 (1979); *Izv. Vyssh. Uchebn. Zaved. Radiofiz.* **22** 1318 (1979)
195. Vysloukh, V A, Egorov K D, Kandidov V P *Radiophys. Quantum Electron.* **22** 299 (1979); *Izv. Vyssh. Uchebn. Zaved. Radiofiz.* **22** 434 (1979)
196. Baranova N B, Zel'dovich B Ya *Sov. Phys. JETP* **53** 925 (1981); *Zh. Eksp. Teor. Fiz.* **80** 1789 (1981)
197. Fried D L, Vaughn J L *Appl. Opt.* **31** 2865 (1992)
198. Primmerman C A et al. *Appl. Opt.* **34** 2081 (1995)
199. Vysotina N V et al. *Sov. Phys. J.* **28** 887 (1985); *Izv. Vyssh. Uchebn. Zaved. Fiz.* **28** (11) 42 (1985)
200. Kanev F Yu, Lukin V P *Opt. Atmos.* **4** 1273 (1991)
201. Roggermann M C, Lee J L *Appl. Opt.* **37** 4577 (1998)
202. Kanev F Y, Lukin V P, Makenova N A *Proc. SPIE* **5026** 127 (2002)
203. Kanev F Y, Lukin V P, Lavrinova L N *Proc. SPIE* **4341** 135 (2000)
204. Kanev F Yu, Lukin V P *Adaptivnaya Optika. Chislennye i Eksperimental'nye Issledovaniya* (Adaptive Optics. Numerical and Experimental Studies) (Tomsk: Izd. Inst. Optiki Atmosfery SO RAN, 2005)
205. Bahk S-W G, Rousseau P, Planchon T A *Opt. Lett.* **29** 24 (2004)
206. Grosset-Grange C et al. *Proc. SPIE.* **6584** 658403 (2007)
207. Aleksandrov A G et al. *Quantum Electron.* **40** 321 (2010); *Kvantovaya Elektron.* **40** 321 (2010)
208. Aleksandrov A G et al. *Avtometriya* **48** (2) 52 (2011)
209. Atuchin V V et al. *Proc. SPIE* **5481** 43 (2004)
210. Starikov F A et al., Technical Program of EOS Annual Meeting 4-3188-22 (2010) p. 80
211. Starikov F A et al. *Opt. Lett.* **34** 2264 (2009)
212. Garanin S G et al. *Quantum Electron.* **37** 691 (2007); *Kvantovaya Elektron.* **37** 691 (2007)
213. Garanin S G et al. *Optoelectron. Instrum. Data Proces.* **48** (2) 134 (2012); *Avtometriya* **48** (2) 30 (2012)
214. Grosset-Grange C et al. *Proc. SPIE* **6584** 658403 (2007)
215. Vorontsov M et al. *Appl. Opt.* **48** A47 (2009)
216. Duffner R W *Airborne Laser. Bullets of Light* (New York: Plenum Trade, 1997)
217. Steiner T D, Merritt P H *Proc. SPIE* **3706** 3 (1999)
218. Steiner T D, Butts R R *Proc. SPIE* **3706** 180 (1999)
219. "Air Force Shoots For Laser Ballistic Missile Terminator" *National Defense* **81** (522) 23 (1996)
220. Chadwell P A *National Defense* **64** 56 (1979)
221. Semchishen V, Mirokhen M, Sailer T *Refraktsionnaya Khirurgiya Oftal'mologiya* **3** (1) 5 (2003)
222. Artal P *J. Refract. Surg.* **16** (5) 560 (2000)
223. Koh Set al. *Am. J. Ophthalmol.* **134** 115 (2002)
224. Barbero S et al. *J. Refract. Surg.* **18** (3) 263 (2002)
225. Maeda N et al. *Ophthalmology* **109** (11) 1996 (2002)
226. Larichev A V et al. *Sov. J. Quantum Electron.* **32** 902 (2002); *Kvantovaya Elektron.* **32** 902 (2002)
227. Kudryashov A et al. *Proc. SPIE* **6113** 61130D (2006)
228. Galetskii S O et al. *J. Opt. Technol.* **73** 491 (2006); *Opt. Zh.* **73** (7) 79 (2006)
229. Durnin J, Miceli J J (Jr.), Eberly J H *Phys. Rev. Lett.* **58** 1499 (1987)
230. Lukin V P, Konyaev P A, Sennikov V A *Appl. Opt.* **51** (10) C84 (2012)
231. *Appl. Opt.* **37** (1998) Special issue "Adaptive Optics"
232. *Avtometriya* **48** (2) (2012), Tematicheskii vypusk "Opticheskie informatsionnye tekhnologii" (Topical issue "Optical and information technologies")